A CRITICAL REVIEW OF THE MECHANICS OF METAL ROLLING; ITS APPLICATION TO THE DESIGN OF HOT STRIP MILLS.

A MAJOR TECHNICAL REPORT

IN THE

FACULTY OF ENGINEERING

BY

KUMAR K. MUKERJEE

Presented in partial fulfilment of the requirements for the Degree of MASTER OF ENGINEERING

at

Sir George Williams University

Montreal, Canada

April 1973

ACKNOWLEDGEMENT

The author wishes to express his gratitude and indebtedness to his faculty advisor, Dr. M.O.M. Osman for the valuable discussions and guidance received during the preparation of this study.

Grateful appreciation is also accorded to the Management of Sidbec-Dosco Ltd., for permission to carry out tests on their Hot-Strip Rolling Mill at Contrecoeur, Québec, for verification of one of the Rolling Theories contained in this work.

ABSTRACT

In this investigation it has been attempted to present in a broad spectrum, the complex interaction, nature and influence of the many factors that basically affect the mechanical forming of metals during the rolling process. The basic physical phenomena, that occur within the arc of contact between the metal and the cylindrical rolls causing deformation of metal through plastic yielding, are complex and have been the subject of extensive research and experimentation for the past several decades.

The first two chapters of this work describe the fundamental terms and concepts used in rolling parlance and present some of the theoretical analyses for their prediction and explanation. The behaviour of metal under plastic yielding conditions of hot and cold rolling has been discussed, leading to the introduction of the concepts of roll force and torque.

Chapter 3 is devoted to the presentation of some of the more popular and general theories of flat rolling which, in their approach, attempt to explain the force inter-relationships existing within the roll gap and, from the analysis of these, deduce expressions for the specific roll force required for the deformation. To be of practical use, in the design of rolling mills, it is necessary for a theory

of rolling to be reasonably accurate in its analysis while, simultaneously, to be capable of presenting formulae and graphs which can be used with convenience and rapidity for design calculations. Accordingly, a method has been selected from the theories presented and its validity has been tested and reviewed by means of measurements taken from a production mill.

There are, however, many factors and phenomena in the rolling process which have not been satisfactorily analysed and incorporated in the popular rolling theories, and recommendations are made in the concluding chapter, for topics of further research and experimentation.

TABLE OF CONTENTS

	Page
ACKNOWLEDGEMENT	i
ABSTRACT	ii
TABLE OF CONTENTS	iv
INDEX TO FIGURES AND TABLES	vii
LIST OF PRINCIPAL SYMBOLS USED	xiii
CHAPTER 1	1
INTRODUCTION	1
1.1 Background	1
1.2 Scope of the investigation	3
1.3 Parameters influencing the formulation of rolling theory	3
CHAPTER 2	7
BASIC CONCEPTS IN THE ROLLING PROCESS	7
2.1 Geometrical relations	7
2.2 Inter-relationship between Draught, Elongation and Spread in Hot Rolling	10
2.3 Friction, Bite, Neutral Angle and Forward Slip	17
2.4 Flow of metal in rolling	36
2.5 Plastic deformation in Rolling, factors affecting yield stress	42
2.5.1 Criteria for plastic yielding	42
2.5.2 Yield stress in hot rolling	48

		Page
2.5.3	Mean strain rate in rolling	58
2.5.4	Effect of temperature on yield stress	60
2.5.5	Yield stress in cold rolling	62
2.6	Specific roll pressure, rolling load and torque	67
2.6.1	Calculation of rolling load in hot rolling	76
2.6.2	Calculation of torque in hot rolling	77
CHAPTER 3		80
THEORIES OF STRIP ROLLING		80
3.1	The basic differential equation for pressure distribution in the roll gap	80
3.2	VonKarman's theory	86
3.3	Nadai's theory	89
3.4	Tselikov's theory	101
3.5	Discussion on the theories of Von Karman, Nadai and Tselikov	105
3.6	Orowan's theory	106
3.7	Discussion of Orowan's theory	121
3.8	Sims' theory	122
3.9	Cook and McCrum's development of Sims' theory	128
3.10	Discussion	131

	Page
CHAPTER 4	132
PRACTICAL APPLICATION OF ROLLING THEORY	132
4.1 Selection of a technique for calculating roll force and torque	132
4.2 Case study: Comparison of Calculated and measured values of roll force	137
4.2.1 Description of rolling setup	137
4.2.2 Experimental and calculated results	138
4.2.3 Typical calculation of roll force	144
4.2.4 Discussion of results	146
CHAPTER 5	148
CONCLUSION AND RECOMMENDATION FOR FURTHER WORK	148
5.1 Conclusion	148
5.2 Recommendation for further work	149
BIBLIOGRAPHY	151

INDEX TO FIGURES AND TABLES

Figure	Title	Page
1	Geometric relationships in rolling, Deformation in Rolling	6
2	Projected Contact Area in Rolling	11
3	Relation between β, γ, δ_w, ϵ_w and W	15
4	Distribution of forces at roll bite	18
5	Rolling at condition where $\alpha = 2\rho$	20
6	Illustration of neutral point	22
7	Forces acting between rolls and material	25
8	Ekelund's derivation of forward slip	28
9	Relation between forward slip and rolling temperature	33
10	Relation between forward slip and reduction	33
11	Effect of roll diameter on relationship between forward slip and reduction	34
12	Effect of rolling speed on the relationship between forward slip and reduction	34
13	Effect of external friction on the relationship between forward slip and reduction	35
14	Effect of strip width on the relationship between forward slip and reduction	35

Figure	Title	Page
15	Hot rolling tests on soft steel bars covered by network of grooves initially 30 mm apart	38
16	Flow of material in a composite plasticine bar rolled between wooden rolls	41
17	Inhomogeneous deformation of material between rolls. Shaded areas are non-plastic regions	41
18	Plane-Strain compression test	52
19	Plane-Strain drop test	52
20	Comparative stress-strain curves for different reductions: drop test and plastometer	57
21	Variation of resistance to deformation with temperature for 0.22% C Steel	57
22	Variation of yield stress with temperature and strain-rate	61
23	Tensile true stress-strain curves for various metals	61
24	Effect of strain-rate on yield stress in mild steel	64
25	Variation of yield stress with reduction for various steels	66
26	Influence of strain hardening on roll pressure distribution	69

Figure	Title	Page
27	Influence of coefficient of friction on resistance to deformation	70
28	Influence of roll diameter on resistance to deformation	71
29	Effect of front and back tension on roll pressure distribution	72
30	Pressure distribution along contact arc for cold rolling of copper strip without tension	74
31	Pressure distribution along contact arc for hot rolling mild steel flat bar	75
32	Resultant roll force and torque arm relative to projected arc of contact	78
33	Forces and stresses acting upon an elemental vertical section of the sheet between the rolls	82
34	Parabolic arc of contact between material and roll	88
35	Trinks' graphical solution of Von Karman's equation	90
36	Effect of front and back tension	93
37a	Pressure distribution with and without strip tension using Nadai's equations	95
37b	Pressure distribution assuming constant frictional force	99

Figure	Title	Page
37c	Pressure distribution with friction proportional to relative velocity of slip	99
38	Variation of pressure distribution by Tselikov's equations	104
39	Pressures in compressed plastic strip	108
40	Stresses between non-parallel compression plates	108
41	Orowan's treatment of equilibrium of thin segment of rolled stock	111
42	Orowan's calculation of horizontal force in the sheet between rolls	111
43	Roll pressure distribution curves calculated by Orowan, for comparison with Siebel and Lueg's experimental curves	117
44	Variation of Orowan's function H against γ_2	119
45	Orowan's criteria for calculating whether material sticks or slips	119
46	Variation of Sims' function Q_p with r	126
47	Variation of Sims' function Q_G with r	126

Figure	Title	Page
48	C_p functions from Cook and McCrum	129
49	C_g functions from Cook and McCrum	129
50	I_p functions from Cook and McCrum for low carbon steel at 1000°C	130
51	I_g functions from Cook and McCrum for low carbon steel at 1000°C	130
52	Sims' comparison between calculated load and Swedish measurements	135
53	Comparison of roll pressure curves based on Sims' theory and Orowan's theory	135
54	Roll force and speed traces from rolling test	139
55	Roll force and speed traces from rolling test	140
56	Block diagram representation of rolling setup	141
57	Variation of measured and calculated values of roll force, during rolling schedule	145

Table	Title	Page
1	Measured and calculated values of forward slip	31
2	Experimental results	142
3	Calculated results	143

LIST OF PRINCIPAL SYMBOLS USED

A_1 = Cross-sectional area of stock on entry side of rolls

A_2 = Cross-sectional area of stock on exit side of rolls

A_h = Projected horizontal area of arc of contact

a = $\frac{2fp_r}{S}$, a factor used in Orowan's theory

a_1 = Lever arm, to compute rolling torque, M_w

a_1 = Correction factor for Wusatowski's spread formula

b_1 = Width of stock on entry side of rolls

b_2 = Width of stock on exit side of rolls

b_m = Mean width of stock in roll bite

c = Chord of the arc of contact

c_1 = Correction factor for Wusatowski's spread formula

c_2 = Factor in Tselikov's spread formula

c_1 = Factor for lever arm

C_1, C_2 = Constants of integration

C_R = Modulus of rigidity

d = Correction factor for Wusatowski's spread formula

D	=	Diameter of rolls
e	=	Exponential coefficient
E	=	Young's modulus
f	=	Coefficient of friction
f_1	=	Correction factor for Wusatowski's spread formula
h_1	=	Height of stock entering rolls
h_2	=	Height of stock leaving rolls
h	=	Height of stock at any point in contact arc
h_6	=	Height of stock at neutral plane
Δh	=	Absolute draught = $h_1 - h_2$
H_E	=	Horizontal component of resultant roll force K
H_V	=	Vertical component of resultant roll force K
K	=	Resultant of radial roll force and frictional force at any point on contact arc
K_B	=	Bulk modulus
K_{wm}	=	Mean resistance to deformation along contact arc
K_f	=	$\frac{2f}{\gamma_1}$, a factor used in Nadai's theory
K_g	=	$\frac{2\tau}{\gamma_1 S}$, a constant when τ is constant, a factor used in Nadai's theory
K_h	=	$\frac{2\tau_o}{\gamma_1 S}$, a factor used in Nadai's theory

M	=	Empirical factor in Siebel's spread formula
M_w	=	Rolling torque
N	=	Speed of rolls, r.p.m.
p	=	Specific vertical roll pressure
p_r	=	Specific radial roll pressure
P	=	Vertical roll force
P_R	=	Radial roll force at any point on contact arc
q	=	Strain rate
r	=	Reduction ratio = $(h_1 - h_2)/h_1 = \Delta h/h_1$
R	=	Radius of roll
S	=	Constrained yield stress
S_o	=	Yield stress in tension
S_1, S_2 S_3	=	Principal stresses
u	=	Elastic strain energy per unit volume
v	=	Peripheral velocity of rolls
V_1	=	Velocity of stock entering rolls
V_2	=	Velocity of stock leaving rolls
V	=	Velocity of stock at any plane in contact arc
v_1	=	$\tan^{-1}Z$, a factor used in Nadai's theory,
v_2	=	$\tan^{-1}\frac{r}{1-r}$, a factor in Nadai's theory
V_δ	=	Velocity of stock at neutral point

W = Factor in Wusatowski's spread formula
$= 10^{-1.269\,\epsilon_w^{0.56}\delta_w}$

x = Horizontal distance of any vertical plane in arc of contact from vertical roll centres

y = $\frac{p_r}{S}$, a factor used in Nadai's theory

Z = Factor used in Nadai's theory = $\frac{x}{\delta_1 R}$

α = Total rolling angle of arc of contact

β = Coefficient of spread = b_2/b_1

β' = Wusatowski's corrected coefficient of spread

γ = Coefficient of draught = h_2/h_1

γ_1 = Ratio of exit thickness to roll radius = h_2/R

γ_2 = $\frac{\gamma_1}{2}$, ratio of exit thickness to roll diameter

δ = No-slip angle, i.e., rolling angle at neutral point

δ_t = Mean thickness of oil film on rolls

δ_w = Form factor in Wusatowski's spread formula

ϵ_w = Roll factor in Wusatowski's spread formula

ϕ = $f/\tan\frac{\alpha}{2}$, a factor used in Tselikov's theory

λ = Coefficient of elongation = l_2/l_1

η = Mean dynamic viscosity of rolling oil

ν = Poisson's ratio for the material

ρ = Angle of friction

θ = Rolling angle at any point in arc of contact

σ = Horizontal pressure on any section in arc of contact

σ_1 = Back tension on strip

σ_2 = Front tension on strip

τ = Tangential shear stress

τ_o = Tangential shear stress at neutral plane

ς = $\frac{\tan(\rho - \theta)}{\tan\theta}$, a constant in Tselikov's theory

CHAPTER 1

INTRODUCTION

1.1 BACKGROUND

The mechanical forming of steel and other non-ferrous metals from cast ingots, slabs and billets into various shapes and sections such as flat strip, structural sections, rounds, squares, hexagons, etc. by passage through plain or grooved cylindrical rolls, is what is referred to as the "Rolling Process". As is well known, the process of rolling, in its early rudimentary form, originated several hundred years ago, with the rolling of hot material. As often happens in an industry which has its roots in the past, knowledge of how to obtain the desired result was gained without, in most cases, the knowledge of why the metal and the equipment reacted in a particular way under a given set of conditions of rolling. However, as the state of the art had to progress and come up to the challenges posed by the rolling of new types of alloy steels, the rolling of wider plates and strip to close dimensional tolerances at higher speeds, it became increasingly necessary to re-evaluate the basis of the design, control and operating parameters influencing the rolling process.

There has been, in the last fifty years or so, a great deal of research into the mechanics of the rolling process, both by fundamental research workers not directly connected with the industry and also by those who, pressed by the need to produce increasingly higher tonnages within exacting standards of gauge and surface finish, have combined the

findings of fundamentalists with their own empirically-established conclusions, to elevate the rolling process to its present importance in the area of semi-finished and finished metal products. However, despite this progress and despite the increase in research and investment of large sums in steel rolling plants, there still remains many fundamental questions of practical importance to be answered. For example, the (21)* choice of work-roll diameters in the rolling of thin strips is a matter of vital importance. The larger the diameter of the work rolls, the greater is the rolling torque required to achieve a given rolling operation. Conversely, the smaller the work-rolls, the more difficult they are to cool, even at lower rolling speeds. There are several other factors both for and against the selection of larger or smaller roll diameters. Yet, the choice of the diameter and percent reduction reflect themselves in the overall cost of the rolling mill selected and in the number of stands required, and thus in the initial capital investment necessary to accomplish a specified rolling operation.

The need thus becomes emphasized of having a reliable and accurate method of calculation which, as the primary standard, can serve as the basis for evolution of more simplified calculations, nomograms and the like and also for the verification of other simplified and empirical methods of calculation.

* Figures in brackets refer to bibliography.

1.2 SCOPE OF THE INVESTIGATION

This work will be concerned mainly with the brief presentation of various parameters that affect the rolling process and also with some of the major theories that have been presented by recent researchers on the subject. Emphasis will be laid more on the mechanics of flat strip rolling, with a critical appraisal of the various theories available on the subject, from the point of view of suitability of use for the establishment of parameters leading to the design and choice of equipment for a specific process. A typical case-study will be made, towards the end of this paper, using one of the techniques selected for the purpose.

1.3 PARAMETERS INFLUENCING THE FORMULATION OF ROLLING THEORY:

The main objectives of rolling theory are to predict the manner of the plastic deformation, the derivation of formulae for the calculation of forces involved, the establishing of control factors of product geometry and quality, and to provide a basis for the appraisal of the operation of planned new rolling mill facilities and thus, to make it possible to compare various alternative plans on a rational basis. This sort of appraisal is essential in the choice of new equipment and procedures, and also the degree of automation and the provision of control criteria.

The main factors that influence the mechanics of rolling may be listed as given below:

1. The roll diameters.
2. Reduction in one pass.
3. The initial thickness of the stock.
4. The speed of rolling (which decides the strain-rate).
5. The front and back tensions (in the case of cold rolling).
6. The nature of friction between the rolls and the material rolled.
7. The temperature field in the material and the rolls.
8. The physical properties of the material being rolled.
9. The shape of the roll contour or roll pass in which the material is being deformed.
10. The mill behaviour under load.
11. The effect of previous treatment of the material resulting in work-hardening or other effects.
12. The elastic deformation of the rolls under load.
13. The state of anisotropy of the material.
14. The aspect ratio, or the ratio of the width of stock to the initial thickness.

These above parameters may singly or jointly, in combinations of two or more, create secondary parameters and phenomena more directly related to and commonly associated with the rolling process, such as:

15. Coefficient of draught, absolute draught and relative draught, which are established by the initial and final mean thicknesses of stock.
16. "Slip", which is characterized by the difference of the linear speed of stock and the peripheral speed of the rolls. "Neutral Angle", which is determined by the point of no slip.
17. "Spread", which is the difference in width of the exit material as compared to the ingoing stock.
18. Coefficient of elongation, which is dependant on the relative values of draught and spread.
19. "Bite", which is a function of draught, roll diameter coefficient of friction and ingoing thickness.
20. Roll Pressure, Torque, Work and Power which are influenced by the above factors.

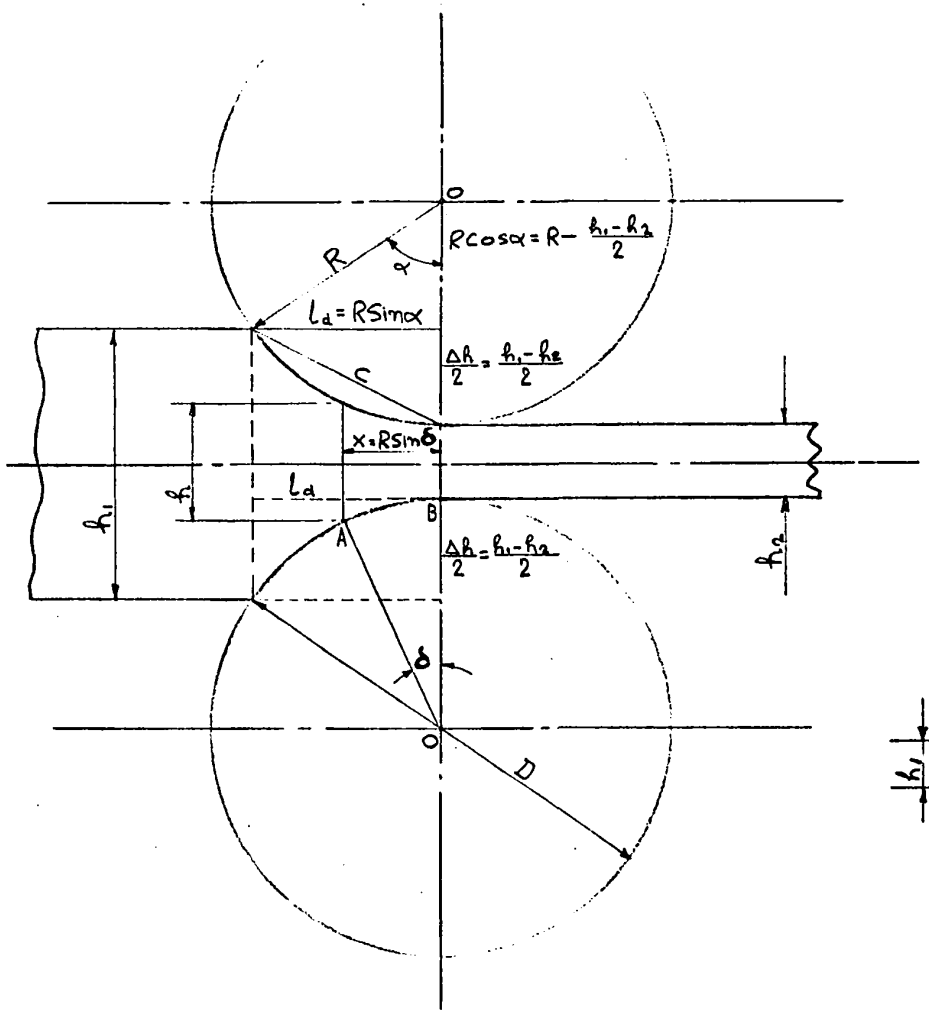

Geometrical relationships in rolling

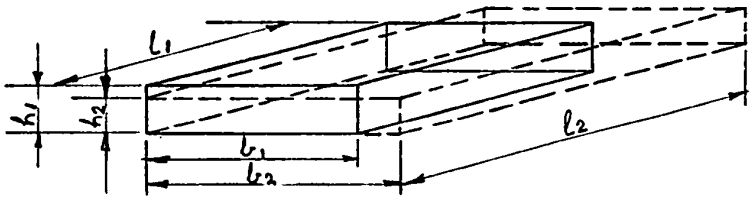

Deformation in rolling

FIGURE 1 (2)

CHAPTER 2

BASIC CONCEPTS IN THE ROLLING PROCESS

2.1 GEOMETRICAL RELATIONS

Figure 1 shows the fundamental representation of the rolling process, that of a flat, rectangular-section bar being passed through a pair of plain cylindrical rolls of equal diameter. The height (h) of the rolled stock is measured normally to the roll axis. The breadth (b) is measured parallel to the roll axis. The dimension of metal in the direction of rolling is denoted as the length (l). The dimensions may be expressed as:

h_1 = height of stock at entry

h_2 = height of stock after rolling, at exit

b_1 = breadth of stock at entry

b_2 = breadth of stock after rolling, at exit

l_1 = length of stock at entry

l_2 = length of stock after rolling, at exit

A_1 = cross-sectional area of stock at entry

A_2 = cross-sectional area of stock after rolling, at exit

X_1 = volume of stock at entry

X_2 = volume of stock after rolling, at exit.

Generally, and without much inaccuracy, it is assumed that the law of constant volume holds, i.e.:

$$X_1 = X_2 = \ldots\ldots X_n, \text{ after n passes}$$

The following geometrical relationships will follow, based on the condition of constant volume:

$$X_1 = A_1 l_1 = h_1 b_1 l_1 = X_2 = A_2 l_2 = h_2 b_2 l_2$$

From the geometrical relationships of Figure 1, we obtain the relation:

$$\frac{h_2}{h_1} \cdot \frac{b_2}{b_1} \cdot \frac{l_2}{l_1} = \gamma \cdot \beta \cdot \lambda = \text{Unity.} \qquad \ldots\ldots 2.1\text{-}1$$

where γ = Coefficient of draught

β = Coefficient of spread

λ = Coefficient of elongation

and $h_1 - h_2 = \Delta h$, is referred to as the absolute draught

Other geometrical and trigonometrical definitions and relations shown in Figure 1 are:

l_d = Projected arc of contact between rolls and metal

c = Chord of the arc of contact

h_δ = The height of bar at the neutral point, to be elaborated later

δ = The rolling angle, as defined by the roll centre, the neutral point and the point of exit of the bar from the rolls

α = The angle of bite, as defined by the roll centre, the point of entry of the bar into the rolls and the point of exit of the bar from the rolls.

From these, the following trigonometric relation can be established:

$$R \ \mathrm{Cos}\alpha = R - \frac{h_1 - h_2}{2}$$

$$\text{or:} \quad 1 - \mathrm{Cos}\,\alpha = \frac{h_1 - h_2}{2R}$$

Thus, the formula for the angle of bite is found as:

$$\mathrm{Cos}\,\alpha = 1 - \frac{h_1 - h_2}{2R} = 1 - \frac{\Delta h}{D} \quad \ldots 2.1\text{-}2$$

The projected arc of contact between the metal and the rolls is calculated from the geometrical relationship:

$$l_d^2 = R^2 - \left[R - \frac{h_1 - h_2}{2}\right]^2$$

$$\text{hence} \quad l_d = \sqrt{R^2 - \left(R - \frac{\Delta h}{2}\right)^2} = \sqrt{R\Delta h - \frac{(\Delta h)^2}{4}} \quad \ldots\ldots 2.1\text{-}3$$

When $\Delta h \leqslant 0.08\ R$, which is generally the case in actual rolling operations, we can make the following assumption involving an error of approximately 1%: (2)

$$l_d \simeq \sqrt{R.\Delta h} \qquad \ldots\ldots 2.1\text{-}4$$

This simplification also leads to another expression for the angle of bite, viz.,

$$l_d = R \sin \alpha \ ,$$

hence $$\sin \alpha = \frac{l_d}{R} = \frac{\sqrt{\Delta h R - (\Delta h)^2/4}}{R} = \frac{\sqrt{R \Delta h}}{R} = \sqrt{\frac{\Delta h}{R}}$$

When α is small and expressed in radians, one can make the assumption of:

$$\alpha \simeq \sqrt{\frac{\Delta h}{R}} \qquad \ldots\ldots 2.1\text{-}5$$

2.2 INTER-RELATIONSHIP BETWEEN DRAUGHT, ELONGATION AND SPREAD IN HOT ROLLING

As mentioned before, the increment in the width of a bar after passage through a pair of rolls, is called spread. Figure 2 shows the phenomenon of spread, as represented by the projected contact area of a narrow bar and a wide bar. In the case of hot rolling of wide bar, as with wide sheet and strip, it is found that the spread is negligibly small.

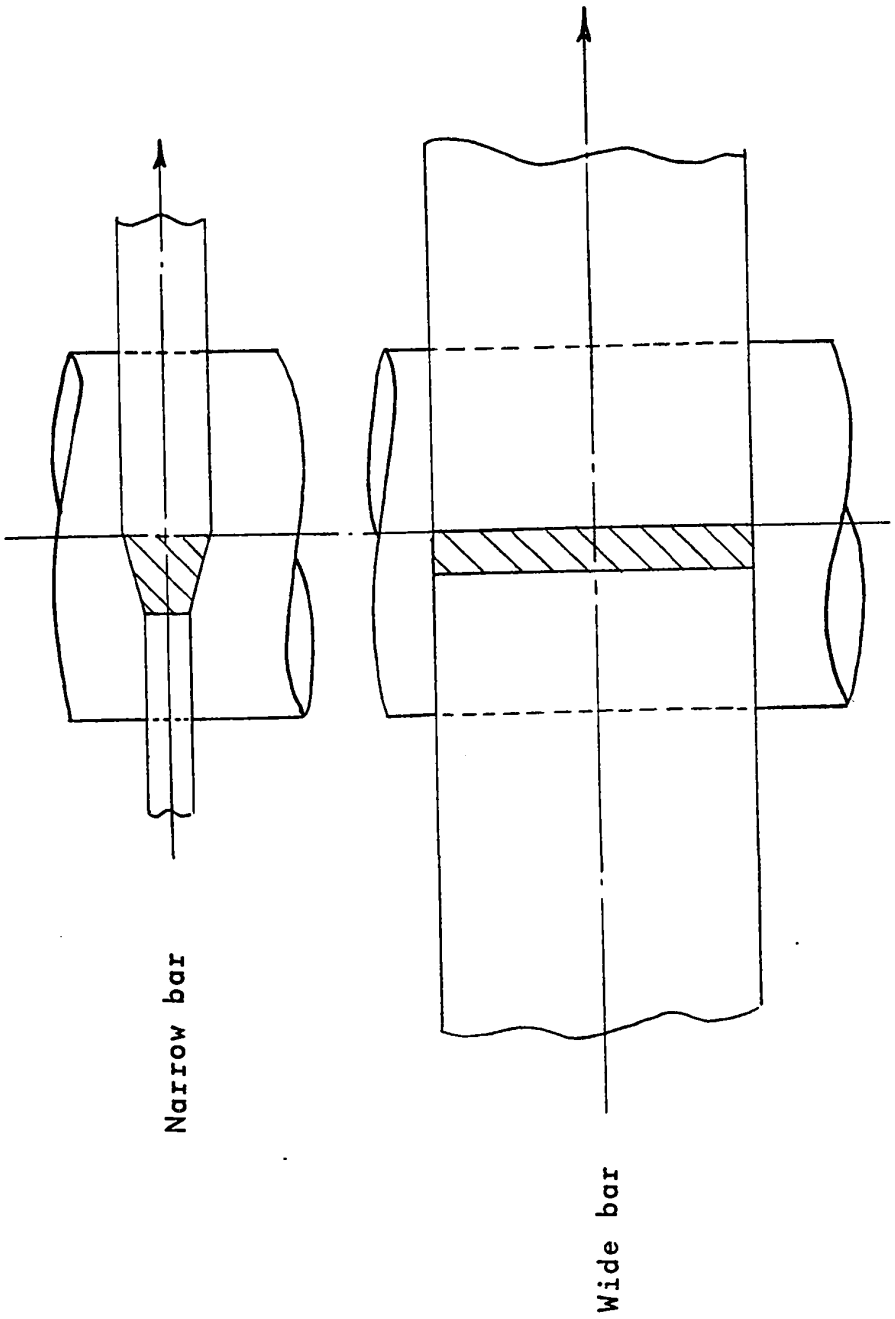

FIGURE 2 : Projected contact area in rolling (2)

This may be explained by the fact that when the metal is compressed between the cylindrical rolls, the effective total frictional resistance to metal flow in the transverse direction is much greater than that in the direction of rolling; thus, the bar is encouraged to elongate in the direction of rolling. On the other hand, in the case of a narrow bar, this resistance to flow is lower and the stock thus spreads in the lateral direction as well as elongates.

The amount of spread that a given bar will have, is (22) influenced by several parameters; such as draught, temperature, rolling speed, the entering cross-sectional contour, the manner of presenting the bar to the rolls, the shape of the roll pass (or groove), the type of steel, the ratio of bar diameter to the roll diameter, condition of roll and metal surface, etc. The importance of accurate prediction of spread under a given set of conditions cannot be over-emphasized, particularly in the rolling of structural sections and merchant bar shapes such as rounds, squares, flats, hexagons, half-rounds, etc. There have been several formulae evolved by different researchers and mill operators. For unrestricted spread in the rolling of hot metal between plain cylindrical rolls, Siebel has derived the following formula:

$$\Delta b = M \cdot \frac{\Delta h}{h_1} \cdot l_d = M \cdot \frac{\Delta h}{h_1} \cdot \sqrt{R \Delta h} \quad \text{, where} \qquad \text{.....2.2-1}$$

Δb = spread

Δh = absolute draught = $h_1 - h_2$ (16)

h_1 = ingoing thickness

R = roll radius

M = an empirical coefficient = 0.35 for steel, 0.33 for lead, 0.36 for copper and 0.45 for aluminium

Tselikov's research led to the publication of this formula (2):

$$\Delta b = C_2 \Delta h \left(2\sqrt{\frac{R}{\Delta h}} - \frac{1}{f}\right)\left(\frac{1-r}{r^2}\right)\left[(1-r)\log_e\left(\frac{1}{1-r}\right) - \left(\frac{r}{1-r}\right)\left(1-\frac{3}{2}r\right)\right] \qquad \text{.....2.2-2}$$

Here,

$C_2 = \dfrac{b_1}{\sqrt{R \cdot \Delta h}}$ and varies from 0.5 to 1.0

f = coefficient of friction between the metal and the rolls

$r = \dfrac{\Delta h}{h_1}$

Several other formulae are also available from other authors (2).

Wusatowski's investigation (22) into the phenomenon of spread take into account not only the draught on the metal and other related factors, but attempts to correlate the coefficients of draught, elongation and spread. As these three phenomena

occur simultaneously in any plastic working process, (23) including rolling, his approach may be considered to be the closest to the actual physical phenomena. From the condition of constant volume, it follows that

$$X_1 = X_2 = \ldots\ldots = X_n$$

$$\frac{h_2}{h_1} \times \frac{b_2}{b_1} \times \frac{l_2}{l_1} = 1$$

Wusatowski introduces two additional factors, to take into account the initial shape of the rolled stock and the manner in which it is introduced in the pass, viz.,

A form factor: $\delta_w = \frac{b_1}{h_1}$

and a roll factor : $\epsilon_w = \frac{h_1}{D}$

The inter-relationship between draught, spread and elongation is then found in the form

$$\beta = \gamma^{-W} \qquad \ldots\ldots 2.2\text{-}3$$

where $$-W = -10^{-1.269 \epsilon_w^{0.56} \cdot \delta_w} \qquad \ldots\ldots 2.2\text{-}4$$

From the relation $\gamma . \beta . \lambda = 1$, the expression for coefficient of elongation is obtained as

$$\lambda = \gamma^{-(1-W)} \qquad \ldots\ldots 2.2\text{-}5$$

Also, we get $$\beta = \lambda^{W/(1-W)} \qquad \ldots\ldots 2.2\text{-}6$$

The graphical relation between δ_w, ϵ_w, W, β, γ & λ are shown in Figure 3.

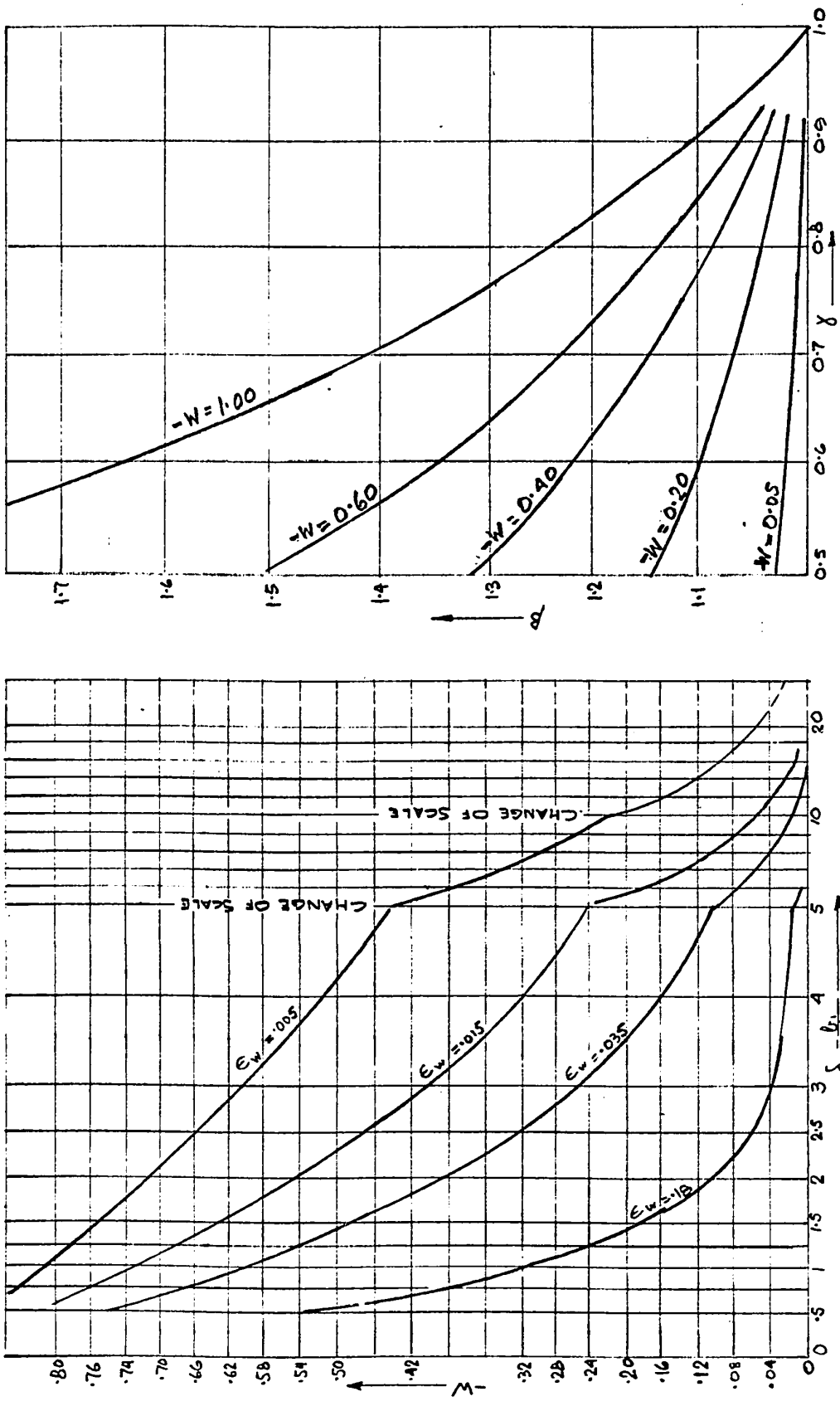

FIGURE 3 : Relation between β, γ, δ_w, ϵ_w, and W (22)

To obtain a greater accuracy in the relationship between draught, spread and elongation, additional correction factors are introduced as follows: (23)

$$\beta' = a_1 \cdot c_1 \cdot d \cdot f_1 \cdot \gamma^{-W} \qquad \text{.....2.2-7}$$

a_1 = correction factor depending on practical temperature of rolling steel

c_1 = correction factor depending on rolling speed

d = correction factor depending on grade of steel

f_1 = correction factor depending on type of rolls and their surface condition.

Formulae and experimentally determined values for the correction factors have also been established:

$a_1 = 1.005$ for $750^{\circ}C < T < 900^{\circ}C$

$= 1$ for $T \geqslant 950^{\circ}C$

$c_1 = (0.002958 + 0.00341\,\gamma)\,v + 1.07168 - 0.10431\,\gamma$,

where γ = coefficient of draught

v = rolling speed in metres/second

$f_1 = 1.020$ for cast iron and rough steel rolls

$= 1.000$ for chilled and smooth steel rolls

$= 0.98$ for ground steel rolls

d = experimentally determined values tabulated for various grades of steels, varying from 0.99741 to 1.02719

2.3 FRICTION, BITE, NEUTRAL ANGLE AND FORWARD SLIP:

With the exception of cold rolling with strip tension, it must be said that external friction, or the friction between the surface of the rolls and the material rolled, is the fundamental factor in the reduction of material by rolling; it is the force which draws the material between the rolls, and is what marks the basic distinction between rolling and drawing. Friction greatly affects the magnitude and distribution of the pressure acting between the rolls and the material, and consequently, affects the power required for the reduction of the material. It also controls the amount of reduction that is possible to take. Generally speaking, the higher the coefficient of friction, the greater is the possible draught. Depending on the conditions under which the metal is introduced into the roll gap, two situations can occur:

a) The metal is gripped by the rolls and pulled along into the roll gap.

b) The metal slips over the roll surface, is not gripped and rolling does not take place.

The two conditions, as mentioned above, are illustrated in Figure 4. The magnitude of the frictional force depends on the conditions of the surfaces in contact and increases with increasing roughness, on the relative velocity between the rolls and the roll pressure exerted. Referring to Figure 4, the following conditions may be elaborated:

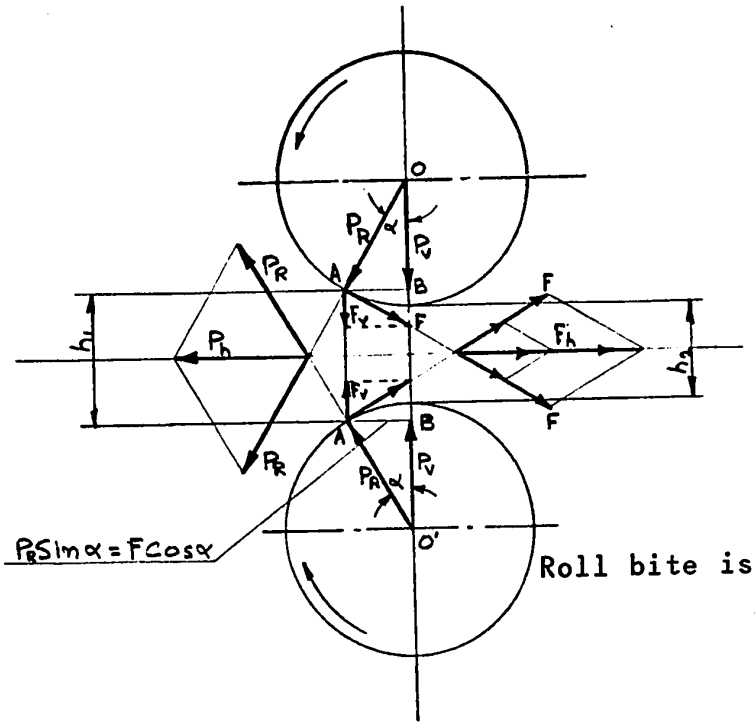

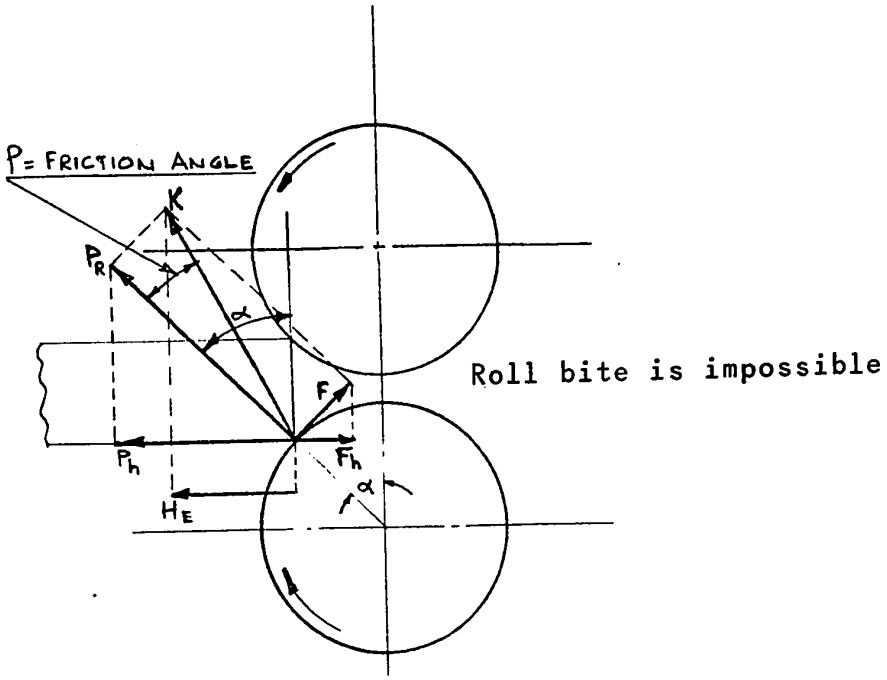

FIGURE 4 : Distribution of forces at roll bite (2)

P_R = Pressure exerted by metal on rolls = Pressure exerted by rolls on metal

F = Frictional force arising due to this roll pressure

P_v = Vertical component of roll pressure P_R tending to compress stock

P_h = Horizontal component of roll pressure P_R tending to eject stock from the rolls

F_v = Vertical component of frictional force F, tending to compress stock

F_h = Horizontal component of frictional force F, tending to draw the metal into the rolls

Now, $F = f \cdot P_R$ 2.3-1

Where f = coefficient of friction = $\tan \rho$, where ρ is the angle of friction.

Also, $P_h = - P_R \sin \alpha$ 2.3-2

$F_h = F \cos \alpha$ 2.3-3

For a condition of equilibrium, the algebraic sum of horizontal forces pulling and rejecting the metal must be equal to zero, i.e.,

$P_h + F_h = 0$ 2.3-4

or $P_R \sin \alpha = F \cos \alpha$

$= f P_R \cos \alpha$

hence $f = \frac{\sin \alpha}{\cos \alpha} = \tan \alpha$ 2.3-5

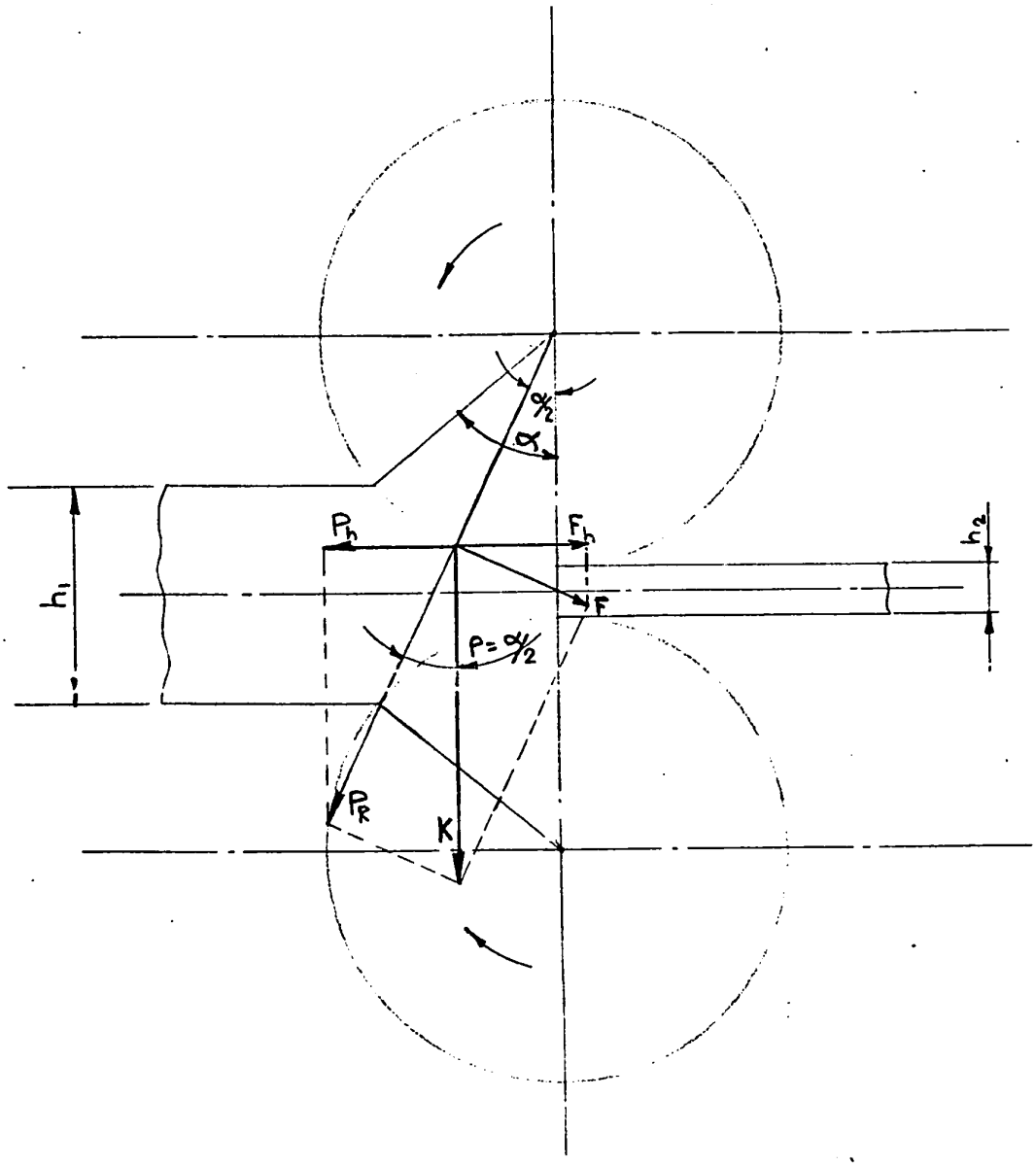

FIGURE 5 : Rolling at condition where $\alpha = 2\rho$ (5)

We thus find that, at the limiting condition, when the forces tending to pull the material into the rolls are equal to those tending to eject it, α is given by:

$$f = \tan \alpha_{max} = \tan \rho$$

hence, $\alpha_{max} = \rho$, which is the condition of the maximum angle of bite. 2.3-6

The following conclusions may be drawn from the above (2) considerations:

a) the rolls bite and rolling commences when the angle of contact at entry is less than or equal to the friction angle, ie., when $\alpha \leqslant \rho$

b) free entry and rolling takes place within the limits

$$0 < \alpha \leqslant \rho$$

c) As shown in Figure 5, the angle of the resultant roll force K moves to a position that is equal to about $\alpha/2$. Thus, it is theoretically possible, once rolling has commenced, to further reduce the roll gap and have a contact angle $= 2\rho$. Thus, after biting and filling the roll gap, free rolling can take place within the theoretical limits:

$$0 < \alpha \leqslant 2\rho$$

We now introduce the concept of the "Neutral Angle". As is apparent from the mechanism of bite, the rolled stock enters the roll gap with a speed less than the peripheral speed of the rolls. On the other hand,

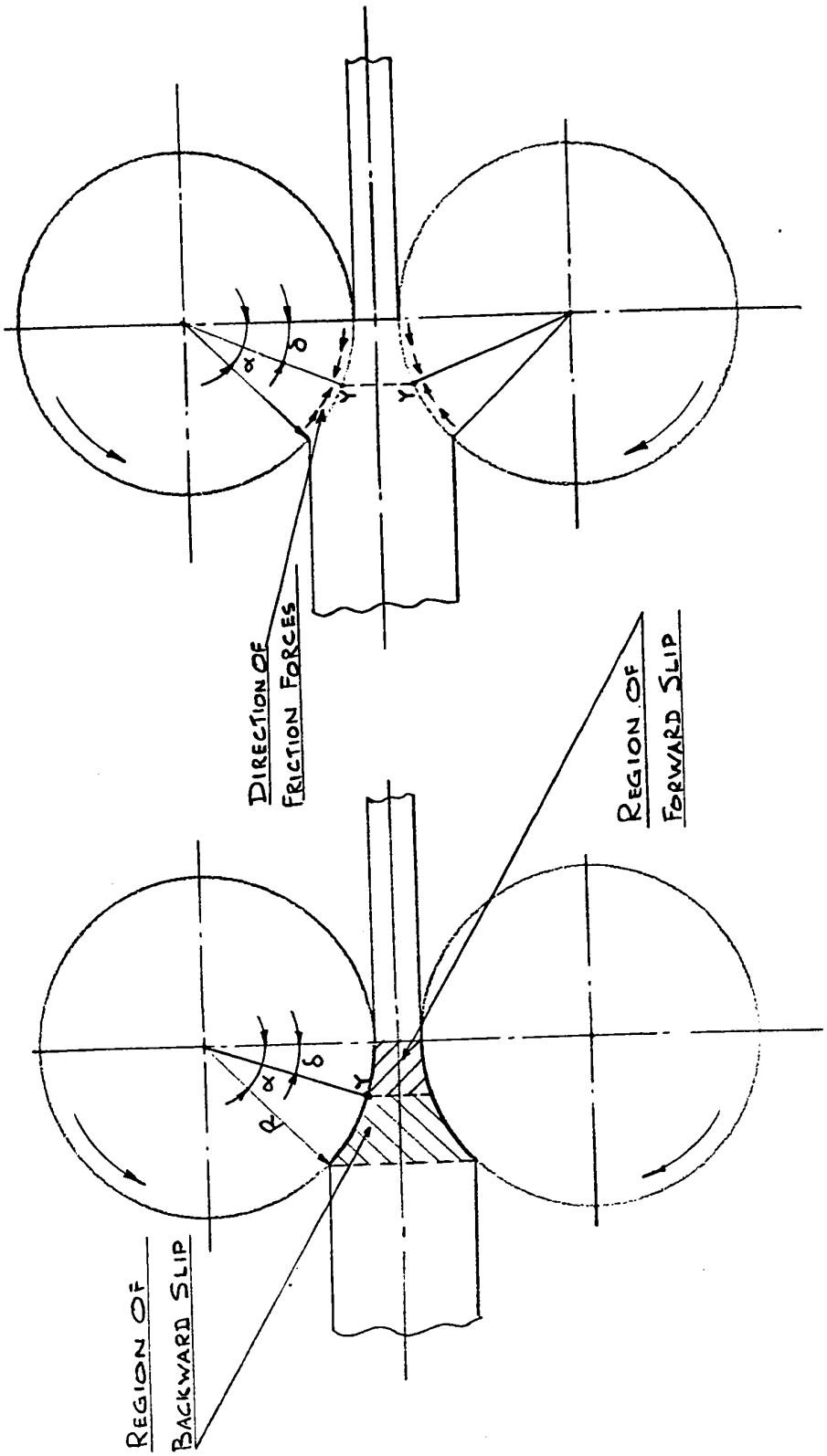

FIGURE 6 : Illustration of neutral point (2)

by means of a simple experiment, it can be shown that the exit speed of stock is greater than the peripheral speed of rolls. If transverse grooves are cut on the surface of the roll and the linear distance between these grooves is measured accurately, it will be found that the distance between ridges on the emerging rolled stock is greater than that between the grooves on the roll, i.e., the stock is leaving the rolls at a faster velocity than the peripheral speed of the rolls.

Thus, considering the velocity of the stock at entry and exit, it is concluded that there is a point somewhere in the arc of contact, where the speed of the stock is equal to the horizontal component of the peripheral speed of the rolls. This point defines the "Neutral" point or plane and also the "Neutral Angle". At the neutral plane, furthermore, the frictional forces, between the rolls and the bar, change direction. The above phenomenon is shown in Figure 6.

This postulation of the neutral point involves the assumption that plane vertical sections of the bar remain plane during rolling, that is, the rolls slip on the bar everywhere except at the neutral point and also that the radial roll pressure is constant along the arc of contact. Thus, from the point of entry to the neutral point, the peripheral speed of the rolls is greater than the bar, while from the neutral point to the point of exit, the reverse is true.

We shall later discuss, in the treatment of some theories of rolling, some considerations used to evaluate the neutral angle when the assumptions of slipping friction, homogeneous compression and plane sections are not made. If the product of the coefficient of friction and the radial roll pressure equals or exceeds the yield stress in shear of the material, then in the region of the arc of contact in which this condition holds, the surface of the bar and the roll surface will move together without slipping, and the neutral point becomes a neutral zone of "sticking". It has also been found that, in general, the radial roll pressure is not constant, but increases from the plane of entry to a maximum value somewhere along the arc of contact, and then decreases to zero towards the plane of exit.

An expression is first derived for the no-slip angle, making the simple assumptions of uniform pressure distribution and constant coefficient of friction. As seen in Figure 7, if α is the angle of contact and δ is the angle between the radius to the neutral point and the line of roll centres, then the angle δ is defined as the "no-slip" angle and is determined from the condition of equilibrium of the horizontal components for the slipping friction. This condition may be written as:

$$H_E = H_E' \qquad \text{.....2.3-7}$$

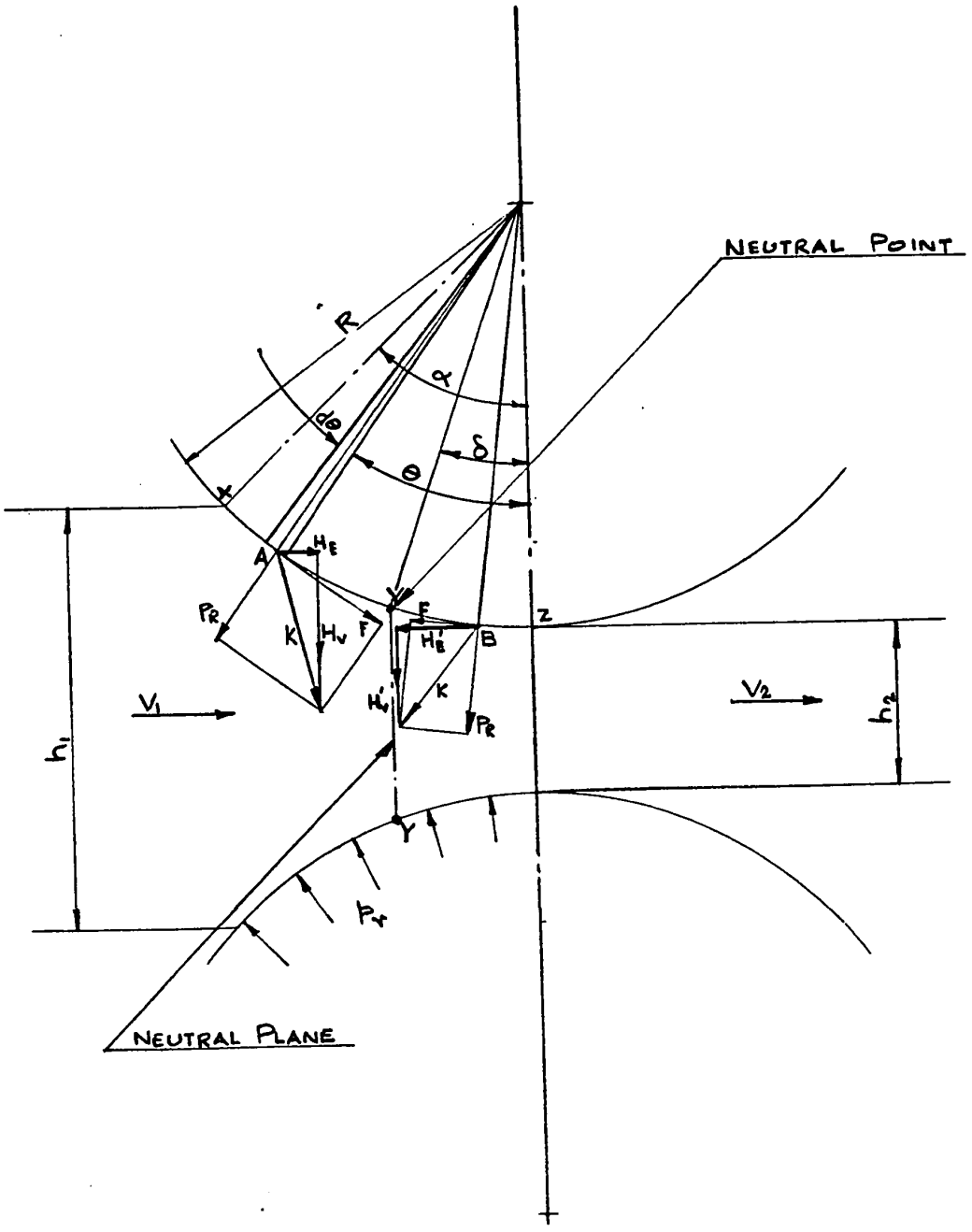

FIGURE 7 : Forces acting between rolls and material (3)

If ρ is the friction angle, i.e., $f = \tan\rho$ and θ is the angle between the radius to any point on the arc of contact and the line joining the roll centres, then we get from Figure 7,

$$\sum_{\delta}^{\alpha} K \cos(90^\circ - \rho + \theta) = \sum_{o}^{\delta} K \cos(90^\circ - \rho - \theta)$$

Since $K = \sqrt{P_R^2 + F^2}$, where $P_R = p_r \times R d\theta$ and

$F = f \cdot P_R$

We have $K = \sqrt{P_R^2 + F^2} \times \frac{p_r . R d\theta}{P_R} = P_R \cdot \sqrt{1 + f^2} \cdot p_r \cdot R d\theta$

then, $\int_{\delta}^{\alpha} \sin(\rho - \theta) d\theta = \int_{o}^{\delta} \sin(\rho + \theta)\, d\theta$, as f, p_r and R are assumed to be constant.

After integration, we get:

$$\sin\delta = \frac{\cos(\rho - \alpha) - \cos\rho}{2 \sin\rho} \qquad \text{.....2.3-8}$$

This may also be written as

$$\sin\delta = \frac{\sin\alpha}{2} - \frac{\sin^2 \alpha/2}{f}, \text{ or when } \alpha \text{ and } \delta \text{ are small and expressed in radians, } \delta = \frac{\alpha}{2} - \frac{1}{f}\left(\frac{\alpha}{2}\right)^2 \qquad \text{.....2.3-9}$$

We also know that $\sin\alpha = \frac{l_d}{R} = \sqrt{\frac{\Delta h}{R}}$

Thus we may obtain the following approximate form for the no-slip angle:

$$\delta = \sqrt{\frac{\Delta h}{2D}} - \frac{1}{f} \times \frac{\Delta h}{2D}, \text{ where} \qquad \text{.....2.3-10}$$

D is the roll diameter and δ is again in radians.

The formula shown on the previous page was derived by (4) Ekelund and, as mentioned earlier, is based on the assumptions that the radial roll pressure p_r is uniform along the arc of contact and the coefficient of external friction f is constant. It may be concluded that the formula is accurate only when the draught is small compared to the bar thickness.

The importance and role of "forward slip" is now introduced. As mentioned in the discussion on Neutral Angle, the material emerges from the roll gap at a velocity greater than the peripheral speed of the rolls. Forward slip is defined as equal to $\frac{V_2 - v}{v}$, where V_2 is the velocity of the material and v is the peripheral speed of the rolls. Forward slip is perhaps the most obvious and easily measured manifestation of external friction between rolls and stock, which, while being the most important phenomenon in the rolling process, is incapable of accurate determination. It is known that the manner in which the coefficient of friction changes from point to point along the arc of contact, has considerable effects on the magnitude and nature of pressure distribution between the roll and material, and hence on the power consumption of the mill. The direct measurement and evaluation of forward slip from rolling tests, offer a valuable tool in the verification of theories involving the behaviour of frictional forces and roll pressure distribution.

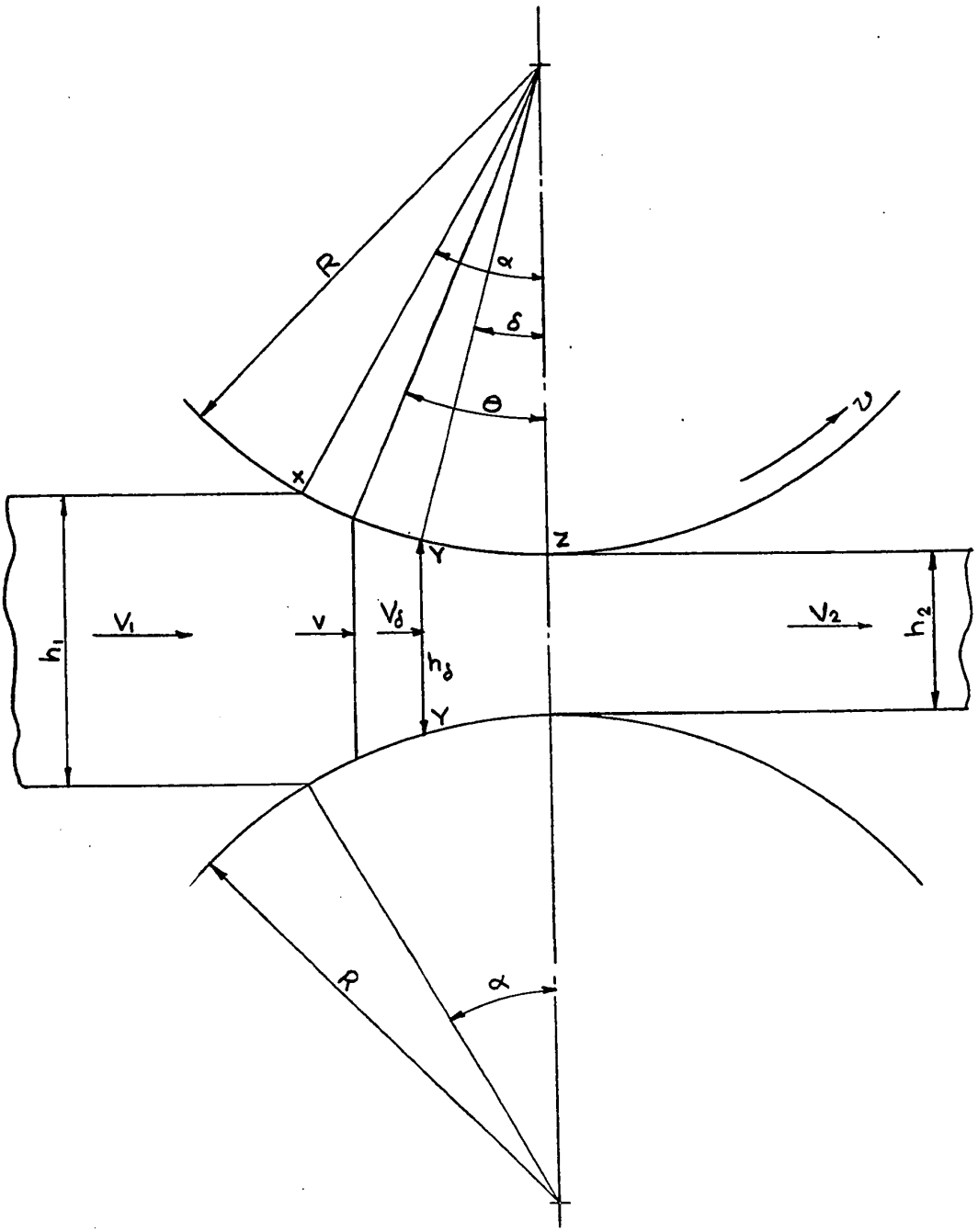

FIGURE 8 : Ekelund's derivation of forward slip (4)

Ekelund (4) deduced an expression for forward slip in terms of the no-slip angle based on the assumptions that initially plane vertical sections of the bar remain plane during rolling, that the density of the bar is constant, that lateral spread is negligible and that the rolls are rigid and no flattening takes place. Referring to Figure 8,

V_1 = Velocity of the bar entering the rolls

V_2 = Velocity of the bar leaving the rolls

V_δ = Horizontal velocity of the bar in the plane of the neutral point .

v = The peripheral velocity of the rolls

On the assumption of plane sections of the bar, the velocity V_1, V_2 and V_δ will be uniform throughout the thickness of the bar, at these planes.

Now, $V_\delta = v \cos \delta$ 2.3-11

and from the condition of constant density,

$$V_1 h_1 = V_2 h_2 = v h_\delta \cos \delta$$

From Figure 8, $h_\delta = h_2 + 2R(1-\cos \delta)$ 2.3-12

Thus, $V_2 = \frac{1}{h_2} \cdot v \cos\delta \; h_2 + D(1-\cos\delta)$

As earlier defined,

$$\text{Forward Slip} = \frac{V_2 - v}{v}$$

From the above, the following relation is obtained:

$$\text{Forward Slip} = (1 - \cos\delta) \cdot \left[\frac{D \cos\delta}{h_2} - 1\right] \quad ...2.3\text{-}13$$

When δ is expressed in radians, an approximate form of this expression may also be written as:

$$\text{Forward Slip} = \frac{1}{2}.\delta^2.\left[\frac{D}{h_2} - 1\right] \qquad \text{.....2.3-14}$$

Ekelund had conducted a series of rolling tests with rolls of various diameters and with bars having initial thickness ranging from 7.87" down to 0.47", width from 9" to 2" and at rolling temperatures of 1500°F to 2000°F, in order to examine the validity of the above formula on Forward Slip. The tests were carried out on a 2-HI slabbing mill and the exit velocity V_2 of the bar was found by noting the time taken by the bar to traverse a known distance marked out on the runout table, while the peripheral velocity of the rolls was determined by means of a revolution counter held against the roll surface. From these measurements the value of the Forward Slip could then be calculated by means of the defined relation of Forward Slip $= \frac{V_2 - v}{v}$. The tests were carried out at a low rolling speed. The theoretical values for Forward Slip were calculated in the following steps: (a) Coefficient of friction f was calculated from an empirical relation deduced by Ekelund, (b) The no-slip angle δ was determined, using this value of f, (c) The calculated value of δ was inserted into the expression for Forward Slip given earlier. The experimental and calculated data are as given in Table 1. Considering the nature of calculation and the doubt that is always associated with the correct value of f to be selected in any given case of rolling,

TABLE 1

Measured and Calculated Values of Forward Slip (Ekelund)

Roll diameter (D)	Height of bar		Width of bar (b)	Measured travel of bar (a)	Corresponding length of roll periphery (s).	Temperature of bar (t)	Calculated coefficient of friction	Calculated no-slip angle (δ)	Forward slip (per cent.)		Difference per cent.
	Initial (h_1)	Final (h_2)							forward slip measured	forward slip calculated	
in.	in.	in.	in.	in.	in.	^oF		(^{o})	in.	in.	
23.39	5.118	4.528	3.94	103.15	101.38	2012	0.5	5.0	1.75	1.57	+ 10.3
24.21	7.874	7.087	7.87	176.58	174.21	1832	0.55	5.7	1.35	1.21	+ 10.4
13.62	0.472	0.354	1.97	457.67	431.10	2012	0.5	3.3	6.17	6.07	- 1.6
28.27	1.969	1.476	8.86	234.25	224.41	1976	0.5	4.3	4.38	5.25	- 19.8
28.27	1.969	1.476	8.86	236.22	224.21	1652	0.6	4.5	5.38	5.67	- 5.4
28.27	1.000	0.630	9.06	236.22	212.01	1652	0.6	4.0	11.42	10.75	+ 5.9
28.27	0.630	0.433	9.06	236.22	216.14	1472	0.65	3.1	9.30	9.39	- 1.0

the agreement between experimental and calculated values is satisfactory. However, divergence appears to be noticed mostly in the results with thicker bars. This may be due to the fact that the assumption that plane sections remain plane during rolling is farther from the truth for thick than for thin bars.

For the case of rolling where lateral spread is not negligible, Ekelund's formula for Forward Slip takes for form:

$$\text{Forward Slip} = \frac{b}{b_2} \cdot \left(1 + \frac{D}{h_2}\right) \cos\delta - \frac{b}{b_2} \times \frac{D}{h_2} \cos^2\delta - 1$$

where b and b_2 are the widths of the bar at the neutral point and at exit respectively.

Several experiments were carried out by different researchers, to find the effect of various factors on Forward Slip. The effect of steel composition and rolling temperature were investigated by G. Weddige. He found that at a rolling (26) temperature of 685°C, the difference in Forward Slip exhibited by the various steels was very slight and that Forward Slip decreased as the temperature rose. At proper rolling temperatures, around 1200°C, non-scaling high alloy Ni-Cr steels exhibit very low Forward Slip (of the order of 1%), while the low carbon steels exhibit higher slip, of the order of 3%. This may be explained by the fact that carbon steels produce larger quantities of scale than alloy steels and thus we have more a case of friction between steel on

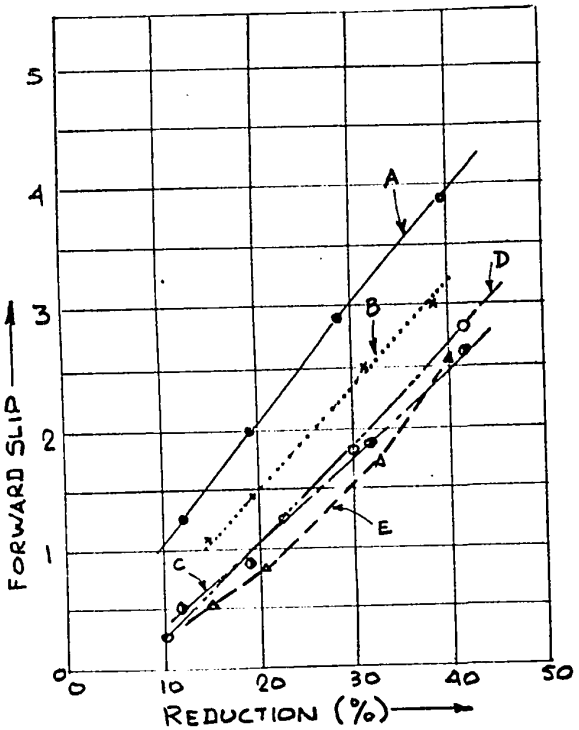

FIGURE 10 : Relation between forward slip and reduction (26)

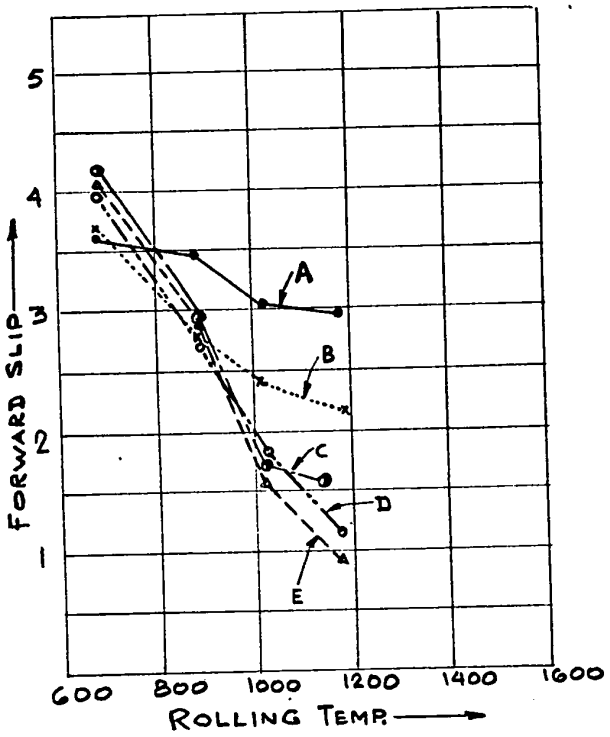

FIGURE 9 : Relation between forward slip and rolling temperature (26)

A - Low carbon steel
B - High carbon steel
C - Ferritic Si-Cr-Al steel
D - Non-corroding Austenitic Cr-Ni steel
E - Non-scaling Austenitic high Cr-Ni steel

Note: As is known (3) the neutral angle increases from zero (at $\alpha = 0$) to maximum (at $\alpha = \beta/4$) and drops to zero at ($\alpha = 2\beta$). This explains the decrease in the forward slip after reaching a maximum.

Note: The behaviour of the curve for 0.26 r.p.m. is probably due to non-uniform oil film at very low speeds, resulting in an increase of forward slip at higher reductions.

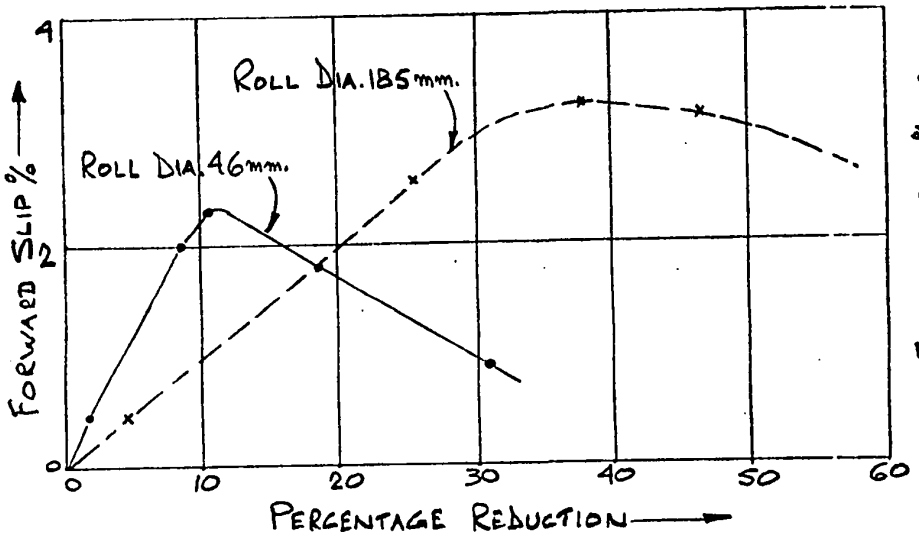

FIGURE 11 : Effect of roll diameter on relationship between forward slip and reduction (26)

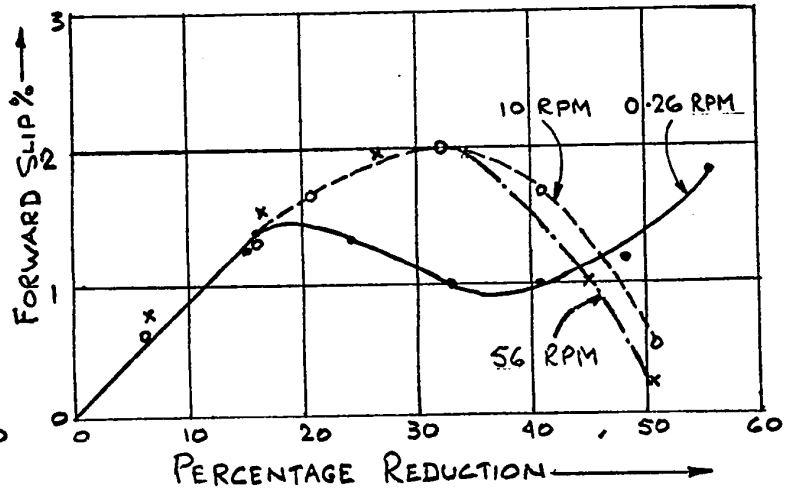

FIGURE 12 : Effect of rolling speed on the relationship between forward slip and reduction (26)

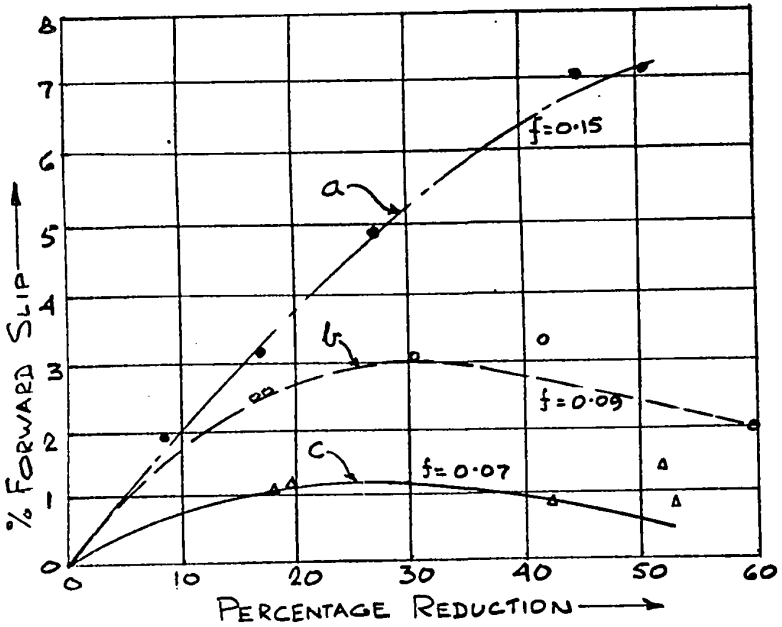

FIGURE 13 : Effect of external friction on the relationship between forward slip and reduction (26)

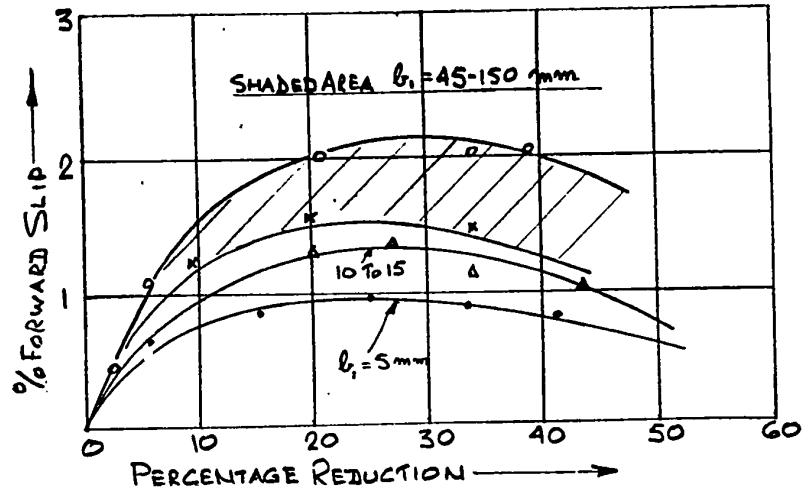

FIGURE 14 : Effect of strip width on the relationship between forward slip and reduction (26)

scale rather than steel on steel. Figure 9 shows the behaviour of Forward Slip as determined for different steels at various temperatures, under a constant reduction of 30%.

Weddige also carried out tests to determine the behaviour of Forward Slip in steels of different compositions with increasing percentage reduction, at a constant rolling temperature. As shown in Figure 10, it was found that the Forward Slip rises directly and proportionately with the reduction per pass; also, lower carbon steels have substantially higher forward slips than the high-alloy steels.

Other experimental findings regarding the influence on Forward Slip of factors such as roll diameter, width of stock, external friction and rolling speed are shown in Figures 11-14.

2.4 FLOW OF METAL IN ROLLING:

The first attempt to investigate the flow of metal during rolling was carried out in 1883 by A. Hollenberg, (29) using flat hot-rolled wrought-iron bars. A series of holes were drilled in the bar, perpendicular to the surfaces that would come in contact with the rolls. The holes were then filled with wrought-iron plugs. Subsequently, the bar was heated, fed into the rolls and the mill stopped after partial rolling had been done. After removal of the bar from the rolls, a longitudinal section was made, in the direction of rolling to examine the deformed shape of the plugs.

The test revealed that the plugs had curved in the direction opposite to that of the movement of the bar, indicating a flow of material in the inner portions of the bar relative to the surface in a backward direction.

Further tests were devised by subsequent researchers to prove the effect of elongation, spread and slip of the rolls with respect to the rolled stock. Ekelund carried out a series of tests on soft carbon steel rectangular bars which had been[4] covered by a grid of shallow V-shaped grooves, equally spaced longitudinally and transversely at a distance of 30 mm. The bars were rolled at temperatures of 1740°F and 2010°F between plain rolls of a 28-inch two-high reversing mill. Figure 15 a, b, c, d and e show the appearance and dimensions of the bars before and after rolling. It was observed that the vertical grooves on the sides of the bar in the region of contact show a backward bend with respect to the direction of rolling, this tendency originating at the beginning of the pressure zone, increasing up to a certain point, and then decreases as the bar is forced towards the plane of exit. Bending of the vertical lines was found to commence before the bar entered the rolls, reaches a maximum at the neutral point and decreases somewhat up to the exit plane. Regarding the behaviour of the horizontal surfaces, the tests indicated that the rectangular network of grooves before rolling remains rectangular after rolling, but the distance between the longitudinal lines increases during rolling, the increases in distance between the several lines being

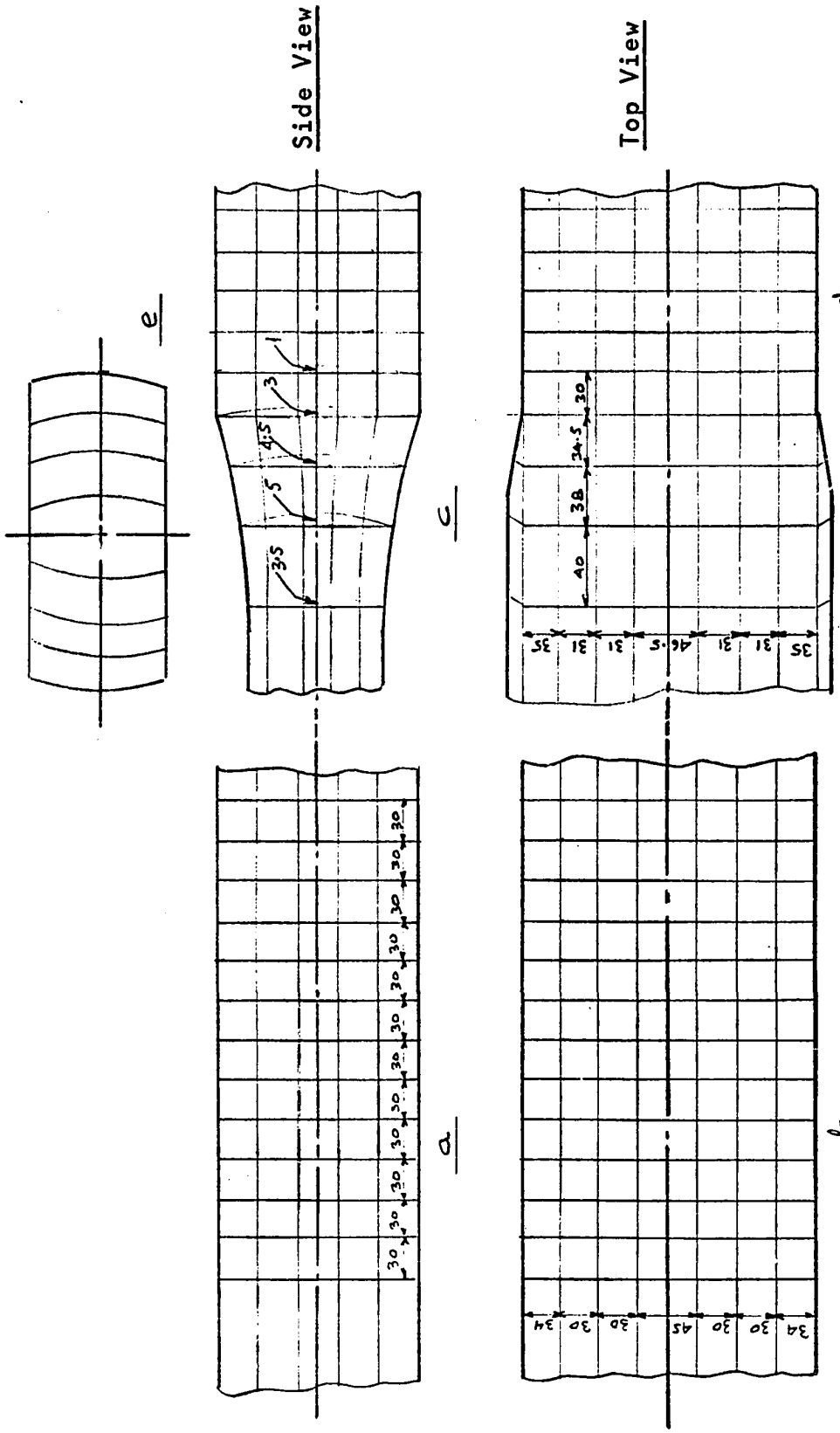

FIGURE 15 : Hot rolling tests on soft steel bars covered by network of grooves initially 30 mm apart (4)

approximately the same near the edge of the bar as near the centre. This distance between the longitudinal lines was found to increase with higher reductions, understandably, due to spread.

On the basis of Ekelund's tests and investigations by others, it is possible to make the following conclusions: In general, straight lines on the sides of the bar, perpendicular to the direction of rolling, do not remain straight during or after rolling, but become curved backward, as compared to the direction of rolling. This applies particularly to flat product. This, then, refutes the previous assumption of plane vertical sections remaining plane during rolling. Material within the bar tends to lag behind that on the rolled surfaces. Straight lines marked across the rolled surface, at right angles to the direction of rolling, remain approximately straight after rolling. This leads to the conclusion that material flows forward at en equal speed at all points from the edge to the centre of the bar. (3)

Refutation of the assumption, of plane vertical sections remaining plane during rolling, leads to the conclusion that internal slip occurs within the material at the same time that external slip occurs between the rolls and the bar. The existence of this internal slip shows that there is a definite possibility that the "neutral point", as described earlier, is really a neutral or no-slip "zone". Deformation of this nature is defined as "inhomogeneous". Orowan (10) conducted a classical experiment of rolling specially prepared

laminated plasticine bars through wooden rolls. The coefficient of friction between the wooden rolls and the plasticine bars being of the order of 1, a value much higher than in any case of practical rolling, one would expect to see a much exaggerated departure, in the behaviour of the stock, from the hypothetical assumption of homogeneous compression as discussed earlier. The shape of the laminated plastic bars, as shown in Figure 16, clearly bear this out, as the initially plane vertical sections become markedly curved in a direction opposed to that of rolling. It can also be observed that the extension of the surface of the bar takes place mainly near the plane of entry, while for a large part of the remainder of the arc of contact, the distances between the ends of the laminae remain approximately the same, indicating that little or no slip takes place here. It may also be observed that, at the plane of entry, the deformation is localised near the surface of the bar, with no deformation at the centre; while as the material passes between the rolls, the deformation penetrates deeper into the bar. This may be interpreted as proof of the existence of a non-plastic region in the plane of entry. Figure 17 indicates the non-plastic region at entry, as readily deducible from the deformation pattern of the laminated plasticine bar shown in Figure 16. As discussed later, there are also two wedge-shaped regions of non-plasticity near the middle of the arc of contact similar in character to slip-cones noted in parallel-plate compression of cylinders, etc. Another region of non-plasticity, though not proven by tests, is deduced to exist

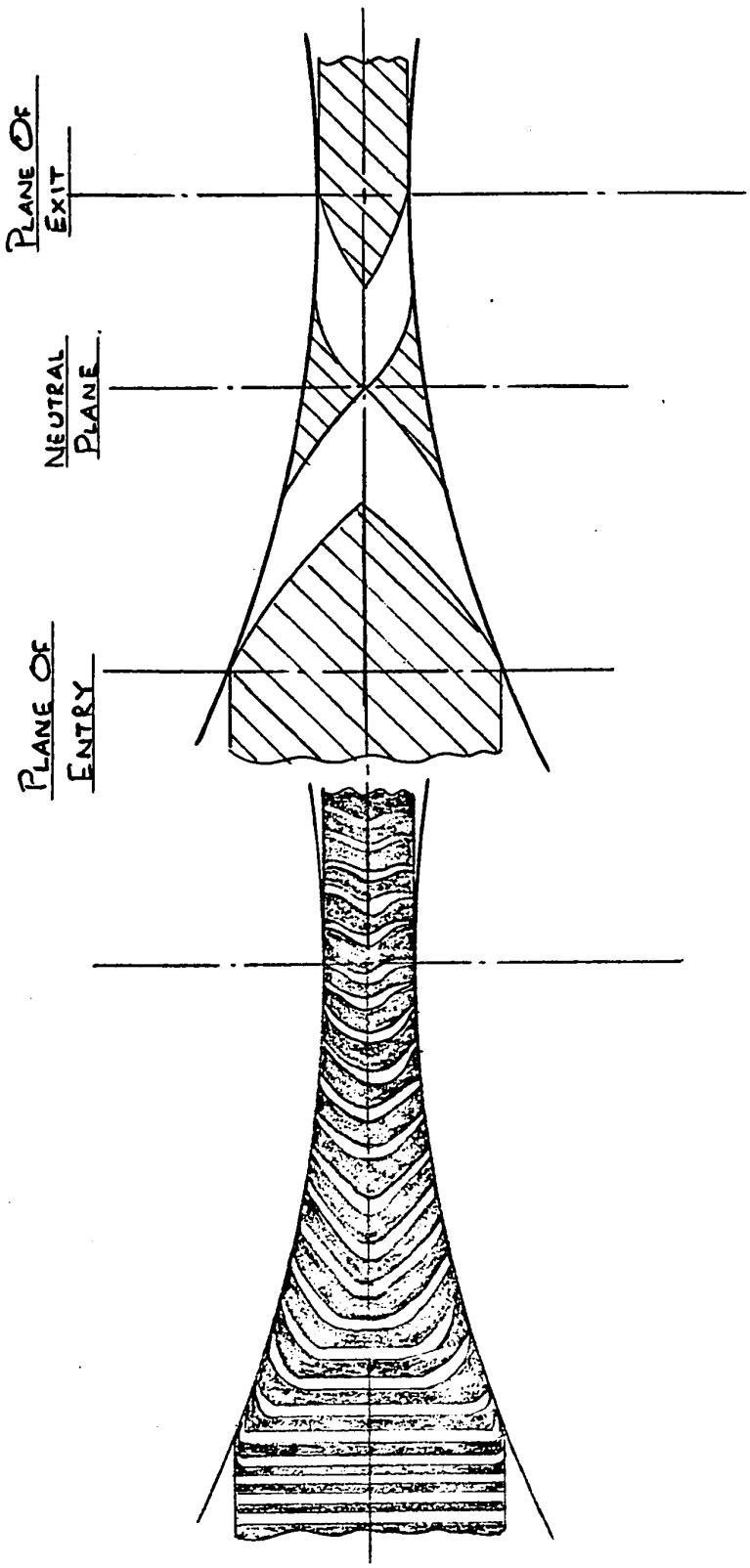

FIGURE 16 : Flow of material in a composite plasticine bar rolled between wooden rolls (10)

FIGURE 17 : Inhomogeneous deformation of material between rolls. Shaded areas are non-plastic regions (10)

at the plane of exit. As shown in Figure 17, the unshaded portion of the diagram represents the zones of plastic deformation, while the shaded portion represents the non-plastic areas. The boundary between the plastic and non-plastic regions runs along the slip-lines which, in the ideal case where the material has a sharp yield point and suffers no work-hardening, are approximately cycloid at the plane of entry.

2.5 PLASTIC DEFORMATION IN ROLLING FACTORS AFFECTING YIELD STRESS

2.5.1 CRITERIA FOR PLASTIC YIELDING

Rolling is a process of plastic deformation and achieves its object by subjecting the material to forces of such magnitude that the resulting stresses produce permanent change of shape. A typical stress-strain curve for, say, mild steel at room temperature, would show that the strain or extension of unit length of the specimen under test is extremely small until a stress of the order of 62000 p.s.i. is reached, after which a further increase of stress produces a proportionately much greater strain. This point which is the yield point is sharply defined for steel, and does not necessarily exist for several other ductile materials such as copper alloy in the fully annealed condition.

The forces which act between the rolls and the material are complex. Reduced to their simplest form and with the assumptions of homogeneous compression and neglecting the

effect of shearing forces on the yield of the material, these forces may be represented by vertical pressures, horizontal pressures which act with and against the direction of rolling and are induced by friction, and lateral pressures which restrict flow in the direction of the roll axes. With these simplifications, any element of the material between the rolls may be considered as being acted upon by three mutually perpendicular stresses, all compressive.

To determine the conditions under which a body will yield under the action of external forces, i.e., to determine the "Criteria for Yielding", various theories have been offered. One of these theories states that yielding occurs when the "maximum principal stress" S_1 reaches a certain value. Another theory states that yielding occurs when the "maximum principal strain" reaches a certain value, while a third theory states that the governing factor is the energy of deformation. However, these theories all fail when applied to material subjected fo hydrostatic pressure as, according to them, the material should yield under this condition, whereas experiment has shown the contrary. The "Maximum Shear Stress Theory", which does not have the above flaw, states that the intermediate principal stress S_2 has no influence whatsoever on yielding and that the material yields plastically when the maximum shear stress in the material reaches the yield stress in shear. Under these conditions, we get the criteria for yielding according to the theory, as

$$\tau_{max} = \frac{S_1 - S_3}{2} = \text{Constant} = \text{Yield stress in shear}$$

It follows from this theory that permanent deformation should take place in the planes of maximum shear, which are at 45^{o} to the maximum and minimum principal stresses S_1 and S_3.

This theory gives a better approximation to the yielding of metal in plastic deformation than the previous two theories. However, it has been proved experimentally that the intermediate principal stress S_2 does have an influence on the yield strength of the material, and cannot be neglected. Most theories of rolling are based on the theory of Maximum Strain Energy which offers one of the most recent explanations of plastic deformation.

The Von Mises-Hencky Theory (32) of "Maximum Shear Strain Energy" gives an expression for the condition of plasticity in which the intermediate principal stress S_2 has a definite effect on yielding and this has been proved by experiment. The criterion of yielding, as defined by his theory, can be deduced as follows:

> If we consider a point P in a body, having principal stresses S_1, S_2 and S_3 and if P is visually represented by rectangular co-ordinates S_1, S_2 and S_3, then the totality of the points P, representing different states of stress in the body and at the point of yielding, would, according to Nadai, form a surface which is referred to as the (18) "limiting surface of yielding". Nadai further showed

that this surface, as would be derived by the Maximum Shear Stress Theory of Yielding", is a regular hexagonal prism whose axis makes equal angles with the three co-ordinate axes. Thus the limiting surface of yield, by the Maximum Shear Stress Theory, consists of six different planes in the stress space. The discontinuities revealed by this theory were eliminated by Von Mises who assumed an expression for a continuous surface: (33)

$$(S_1 - S_2)^2 + (S_2 - S_3)^2 + (S_3 - S_1)^2 = 8k^2 = \text{a constant},$$

which represents a circular cylinder circumscribed about the regular hexagonal prism of the maximum shear stress theory.

Now, the elastic strain energy per unit volume of a material subjected to the action of the principal stresses S_1, S_2 and S_3 is:

$$u = \frac{1}{2}\left[\frac{1}{9K_B}(S_1 + S_2 + S_3)^2 + \frac{1}{6C_R}\left\{(S_1 - S_2)^2 + (S_2 - S_3)^2 + (S_3 - S_1)^2\right\}\right] \qquad \text{.....2.5.1-1}$$

where K_B = Bulk modulus = $\dfrac{E}{3(1 - 2\gamma)}$

C_R = Modulus of Rigidity = $\dfrac{E}{2(1 + \gamma)}$

E = Young's Modulus

and γ = Poisson's ratio for the material.

If K_B is assumed infinite, then :

$$u = \frac{1}{12C_R}\left[(S_1 - S_2)^2 + (S_2 - S_3)^2 + (S_3 - S_1)^2\right] \quad \text{.....2.5.1-2}$$

Thus $(S_1 - S_2)^2 + (S_2 - S_3)^2 + (S_3 - S_1)^2 =$

$u \times 12C_R = 8k^2 = \text{Constant}$

by the Von Mises-Hencky criterion for plastic yielding.

To find the Constant, we consider the case of pure tension for which $S_2 = S_3 = 0$

Then $u \times 12 C_R = 2 S_1^2$

If S_o is the yield stress in tension, than at the time of yielding, $S_1 = S_o$ and $u \times 12C_R = 2 S_o^2$

Thus the Von Mises-Hencky criterion for plastic yielding is

$$(S_1 - S_2)^2 + (S_2 - S_3)^2 + (S_3 - S_1)^2 = 2 S_o^2, \quad \text{.....2.5.1-3}$$

assuming $S_1 \geqslant S_2 \geqslant S_3$.

Now, if we are to assume a plane state of strain, i.e., for rolling conditions without spread, the lateral strain ϵ_2 is zero, and, we obtain the magnitude of the average stress for the plastic range of the material:

$$\epsilon_2 = \frac{1}{E} \cdot \left[S_2 - \frac{S_3 + S_1}{2}\right] = 0$$

Hence $$S_2 = \frac{S_1 + S_3}{2}$$

By substituting this in the Von Mises-Hencky equation, the first boundary condition is obtained:

$$S_1 - S_3 = \frac{2}{\sqrt{3}} S_o$$

or $$S_1 - S_3 = 1.155\, S_o = S \quad .....2.5.1\text{-}4$$

The Constant S is termed by Nadai as the "Constrained Yield Strength" for tension since it is the tensile stress in a bar which is allowed to contract freely in one of the lateral directions, while it is constrained against deformation in the other lateral direction.

The factors which affect yield stress vary with cold or hot rolling. In cold rolling, the chief factors which influence the yield stress are the nature of the material, the amount of cold reduction, or the deformation work which has been applied to the material before it is rolled in the pass considered, i.e. the amount of work-hardening the material has undergone before the pass, the extra amount of work-hardening that occurs during the pass and the nature of the deformation, either homogeneous or inhomogeneous. In cold rolling, the strain rate, or the rate at which the deformation takes place is a minor factor, usually of little importance. In hot rolling, the chief factors influencing the yield stress are the nature of the material, the temperature at which the material is rolled and the strain rate, i.e.

the rate of deformation. When the working temperature is only slightly higher than the temperature of recrystallisation, the speed of recrystallisation and grain growth in the hot metal is usually so slow that the deformed structure is maintained to the next pass. This results in partial strain-hardening of metal, similar to that occurring in cold working.

2.5.2 YIELD STRESS IN HOT ROLLING

The accurate determination of yield stress in hot rolling is a difficult proposition, as it depends on material composition, temperature of rolling and strain rate. The last two criteria pose the biggest problems for any accurate and meaningful calculations to be made and most researchers have been forced to make different degrees of approximation in the prediction of temperature and true strain rate in the rolling operation. Several methods of testing have been evolved, in an effort to determine the yield stress under laboratory conditions approximating the actual working process during hot rolling: (7)

a) Tension testing which is more conveniently carried out at or below room temperatures, but fails to be suitable for testing hot material. The reasons for these are that 1) necking and fracture do not allow sufficiently large strain rates, approximating the rolling process, to be applied, and 2) the tensile tester is incapable of applying a high enough strain rate. The normal tester has a maximum strain rate

of about 10^{-1} sec^{-1}, i.e., about 10% per second, while strain rates during rolling operations can go as high as 10^{3} sec^{-1}.

b) Compression testing of hot specimens is more suitable, since the stress system is closer to those found in deformation processes and basic instabilities of tension testing, such as necking do not occur. It is possible to determine the complete true stress-true-strain curve, however, the friction between the specimen and the anvils can lead to erroneous results, caused by barreling of the cylindrical test specimen at the mid-section.

To obtain plane strain deformation, a narrow band across a wide strip is compressed by means of (Fig.18) platens, which are wider than the strip specimen. Fairly high strains, up to 2.3, have been attained by this method. The constraints of the undeformed shoulders on both sides of this platen prevent extension parallel to the long dimensions of the platens. The result is a groove and extension normal to the long dimension of the platen, approximating the conditions in flat rolling, which is also a form of plane strain compression. In this test also, if lubrication between platen surface is insufficient, a dead zone will form in the specimen next to the face of each platen, and the

effect of friction will increase with increasing reduction.

c) The Cam Plastometer: For strain rates between (43) 1 sec^{-1} to 10^3 sec^{-1}, applicable to rolling conditions, the Cam Plastometer is eminently suited for compression testing. The equipment, originally developed by the British Iron and Steel Research Association (B.I.S.R.A.), consists of platens which are driven together by a cam whose radius increases with the angle of rotation, so that a constant strain rate can be maintained through the deformation period. With the specimen inserted between the anvils, the test is carried out by inserting a block, called the cam follower, between the movable anvil and the rotating cam at the instant the minimum radius of the cam is opposite the anvil. After compression is done, the cam follower is withdrawn with equal rapidity, both these actions being performed by fast-acting pneumatic cylinders. The cam driveshaft is driven by an oversized motor and flywheel, to maintain constant angular speed during compression. Different strain rates can be obtained by changing the speed of the drive motor. The cam plastometer produces the deformation defined by the cam in a single operation. The strain rate profile of a

particular process can be reproduced with the proper cam contour. The stress can be measured by a load cell on the fixed anvil. The strain is defined by the cam, with allowance for elastic distortion. The strain, strain rate and uniformity of strain are observed for room temperature experiments by the high-speed photography of specimens marked with a gridwork. The cam plastometer was extensively used by Cook & McCrum in the B.I.S.R.A. experiments to determine specific rolling properties of different grades of steel under varying conditions of rolling. Their results were widely utilised through the B.I.S.R.A. publication, "The Calculation of Loads & Torques in Hot Flat Rolling". (15)

d) The Hot Torsion Test: This test, which consists of twisting a specimen with a heated gauge section, is capable of producing strains of the order of 20. The shear stresses and strains as measured, are converted to equivalent tensile stresses and strains by the Von Mises criterion. The torsion flow curves are found to be almost identical to tension or compression flow curves for the same strain rate and temperature. The difficulties with the hot torsion test arise from the variation in the axis to the surface strain and strain rate, and the influence on the ductility of a shear-to-

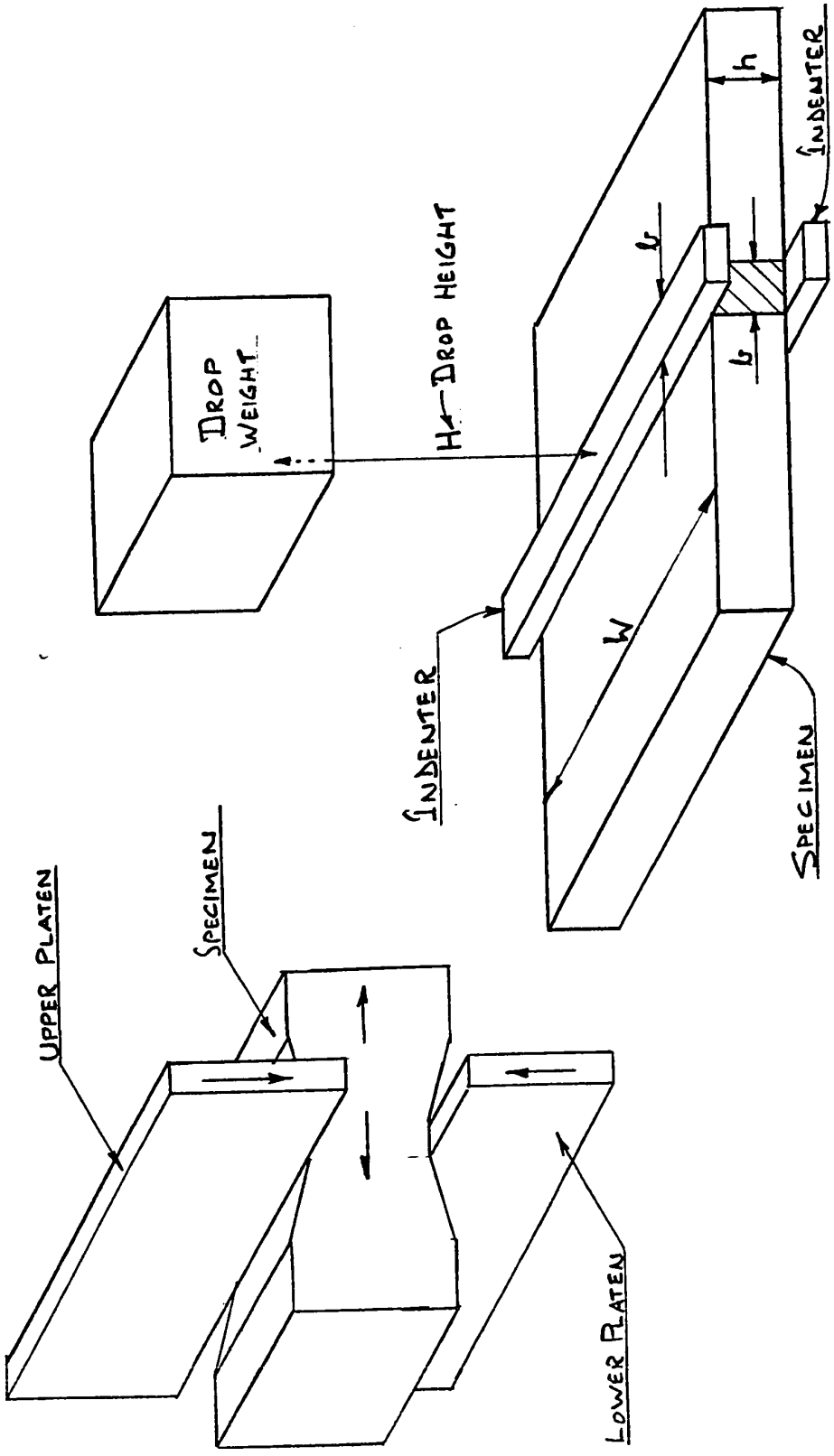

FIGURE 18 : Plane-strain compression test (7)

FIGURE 19 : Plane-strain drop test (9)

normal stress ratio of unity, which is much higher than that commonly found in forming operations. When a solid cylinder is twisted, the strain and stress rate vary from zero at the axis to a maximum at the surface. This variation gives rise to problems of interpretation because the surface work-hardens more than the core and the mechanism of deformation may also be different from that in rolling operations. However, correction factors can be introduced into calculations with hot tension test data, to arrive at more meaningful figures. In torsion testing, the strain rate is altered by changing the rate of rotation. It is possible to achieve strain rates from 10^{-5} to 10^{3} sec^{-1} by this test.

e) The Plane-Strain Drop Test: This test was developed by A.S. Weinstein and A. Matsufuji as part of an (8) A.I.S.E. (Association of Iron and Steel Engineers) research program. The plane-strain drop test appears to be the most promising among all the hot-testing methods, for the prediction of resistance to deformation of metal, mill loads and torques.

Since its issue in 1958, the B.I.S.R.A. publication of Cook and McCrum's "The Calculation of Loads and Torques in Hot Flat Rolling", has been most widely used for calculation to predict mill forces and torques.

After the publication of the B.I.S.R.A. results using the Cam Plastometer, and their wide usage, it became apparent that reliable prediction of rolling torques was not always possible, particularly for rolling conditions of high average strain rate and large reductions. This deficiency was shown very clearly by Dahl who compared resistance to deformation figures, calculated from actual (45) rolling mill tests, with the B.I.S.R.A. figures, and found large variations. Generally, he found that the B.I.S.R.A. data underestimated the deformation resistance at higher values of mean strain rate and reduction. Weinstein and Matsufuji argued that this divergence could be explained by the fact that in addition to the approximations inherent in basic theory, there were two additional assumptions which had to be made in order to use the deformation resistance obtained from uniaxial compression tests at constant strain rate, in the theory of hot flat rolling: (a) the deformation process occurring in flat rolling is very nearly one of plane strain and not uniaxial compression. Thus it was necessary to assume that the theory, relating the deformation resistance in uniaxial compression to that in plane-strain compression, was valid. This has been demonstrated for cold deformation of steel at low strain rates, however,

it has not been verified for hot deformation at high strain rates. (b) Furthermore, the B.I.S.R.A. data were obtained by compressing cylindrical specimens at constant strain rate. As is well known, the strain rate, within the contact arc during rolling, varies significantly. Typically, the maximum strain rate occurs near the entry of the contact arc and is of the order of twice the mean value for the process, while decreasing to zero at the exit plane. Thus, to use the constant strain rate data in the rolling model, it was also necessary to assume that the characteristic behaviour of the deformation resistance during rolling varied with overall changes in reduction and mean strain rate in the same way as that observed from the constant strain rate tests on the cam plastometer. It was tentatively concluded that the most likely cause of the disagreement between hot rolling theory and experiment was due primarily to the use of constant strain rate, uniaxial compression test data to simulate the plain strain, variable strain rate behaviour of metal occurring in the actual hot rolling process.

Weinstein and Mastufuji devised and built a drop hammer (Fig.19) to carry out the plane-strain drop test. By adjusting the amount of weight and the distance through which it was dropped, they obtained varying reductions and mean strain rates

on $\frac{1}{4}$" and $\frac{1}{2}$" thick samples of hot steel, through indenters of $\frac{1}{2}$" and 1" width, by 6" inch length. The test pieces $\frac{1}{2}$" x 4" x 4" and $\frac{1}{4}$" x 4" x 4". Figure 20 shows one of the many curves that were drawn by Weinstein and Matsufuji in their comparison of variable and constant strain rate deformations. The first observation to be made is the distinctly different local behaviour of the plane-strain stress curves compared to that of uniaxial compression. The stress level in plane-strain compression reaches a peak value very soon after the beginning of deformation and then continually decreases to the end of the process. The second point to be noted is the contrast in the behaviour of the mean stress levels, in relation to different amounts of reductions.

There was a considerable amount of work done by these two researchers, in trying to explain the differences between the B.I.S.R.A. data and values deduced from actual rolling experiments. Although their drop test results showed better qualitative agreement with the rolling tests, there were discrepancies in the magnitude of the deformation resistance. The drop test also showed that the stress-strain curve for steel at high temperatures has a different character for different reductions, even though the mean strain rate is kept constant. This effect is not revealed by the uniaxial constant strain-rate tests. Furthermore, it was found that the mean stress, as determined from a drop-test, is more sensitive to differences in mean strain rate but is less

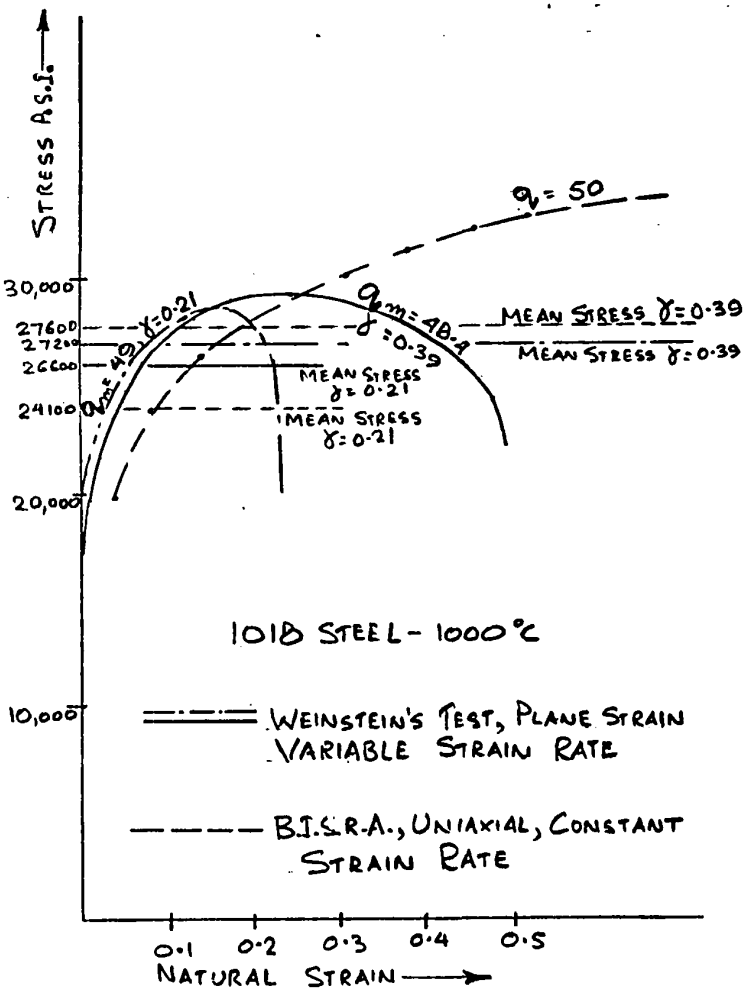

FIGURE 20 : Comparative stress-strain curves for different reductions: drop test and plastometer (7)

FIGURE 21: Variation of resistance to deformation with temperature for 0.22% C Steel (3)

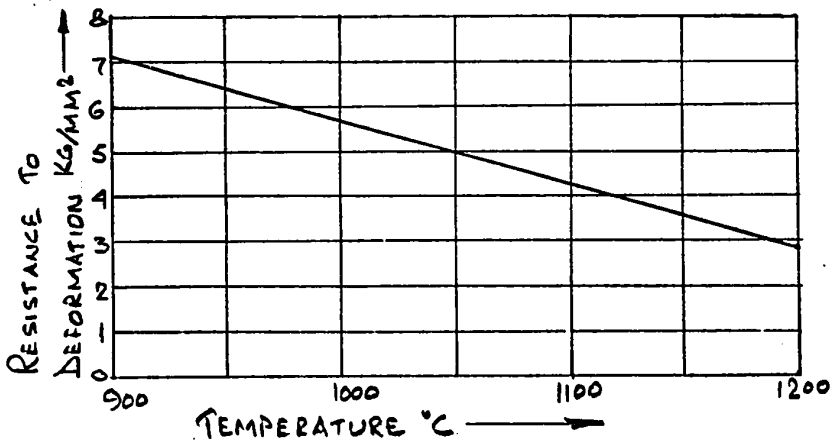

sensitive to differences in reduction than given by the uxiaxial constant strain-rate tests.

Weinstein and Matsufuji, in spite of their pioneering work in the evaluation of deformation resistance, could not explain the discrepancy between their results and those of Dahl's rolling tests, whereby values were calculated from actual observed values of load and torques in a rolling operation.

2.5.3 MEAN STRAIN RATE IN ROLLING

In the determination of yield stress and deformation resistance, it is thus evident that, in the usage of the various available curves and monograms put out by B.I.S.R.A. and other researchers, one of the first steps is to determine the mean strain rate that applies to the rolling process being considered. There is quite a diversity of formulae put out by various workers.

Very basically, the mean strain rate undergone by a material during any deformation process is defined as:

$$q_m = \frac{\epsilon}{t_o} \qquad \text{.....2.5.3-1}$$

where

q_m = the mean strain rate ($^1/_{sec.}$)

ϵ = the logarithmic strain of the material ($^{in}/_{in.}$)

t_o = the total time taken to achieve the strain (sec.)

To relate this expression to the rolling process, the time that an element of the material is in the roll gap, must be calculated. By assuming the rolls to be rigid and that the material assumes the tangential velocity of the roll at only one point in the contact arc, the neutral point, the mean strain rate can be shown to be

$$q_m = \frac{2\pi N}{60}\left(\frac{3h_\delta}{h_1 + 2h_2}\right)\frac{1}{\sqrt{r}} \times \sqrt{\frac{R}{h_1}} \times \ln\left(\frac{r}{1-r}\right) \quad \text{.....2.5.3-2}$$

where N = the roll speed (r.p.m.)

h_δ = the strip thickness at the neutral point (in.)

h_1, h_2 = entry and exit strip thicknesses, respectively (in.)

r = reduction = $\frac{h_1 - h_2}{h_1}$

R = the roll radius (in.)

Except for the strip thickness at the neutral point, all parameters in the above equation are known or can be calculated. To obviate the problem of determining the thickness h_δ, several different assumptions have been made by various investigators. Among these are that the material has the same tangential velocity as the roll throughout the contact arc, or that the neutral point thickness is the average thickness of the strip during reduction. Depending upon the assumptions, there results a different expression for the mean strain rate. For example, Sims' assumption of the (11)

correspondance of material and roll velocities at every point in the contact arc, i.e., an assumption of "sticking", results in:

$$q_m = \frac{2\pi N}{60} \times \frac{1}{\sqrt{r}} \times \sqrt{\frac{R}{h_1}} \times \ln\left(\frac{1}{1-r}\right) \quad \text{.....2.5.3-3}$$

Wusatowski's formula for mean strain rate in the case of "sticking" is: (50)

$$q_m = \frac{2\pi N}{60} \times \sqrt{\frac{R}{h_1}} \times \sqrt{r} \quad \text{.....2.5.3-4}$$

Still another formula, by Ford and Alexander, gives the form:

$$q_m = \frac{2\pi N}{60} \times \frac{1}{\sqrt{Rh_1}} \times \left(1+\frac{r}{4}\right) \quad \text{.....2.5.3-5}$$

2.5.4. EFFECT OF TEMPERATURE ON YIELD STRESS

As is to be expected, there is a marked reduction of resistance to deformation with increase of temperature, for the same rate of deformation. The yield stress for carbon steels under hot working conditions can be calculated, without taking into account the rate of deformation, i.e., under assumption of nearby static conditions of deformation, by using the formula given by S. Ekelund:

$$S = (14 - 0.01\ t)\ (1{\cdot}4 + C + Mn + 0.3\ Cr)\ Kg/mm^2, \quad \text{.....2.5.4-1}$$

FIGURE 22 : Variation of yield stress with temperature and strain-rate (2)

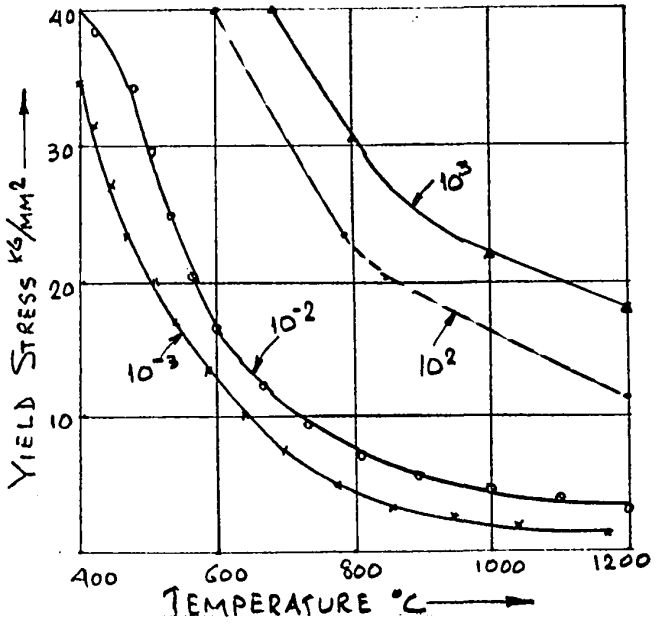

FIGURE 23 : Tensile true stress-strain curves for various metals (3)

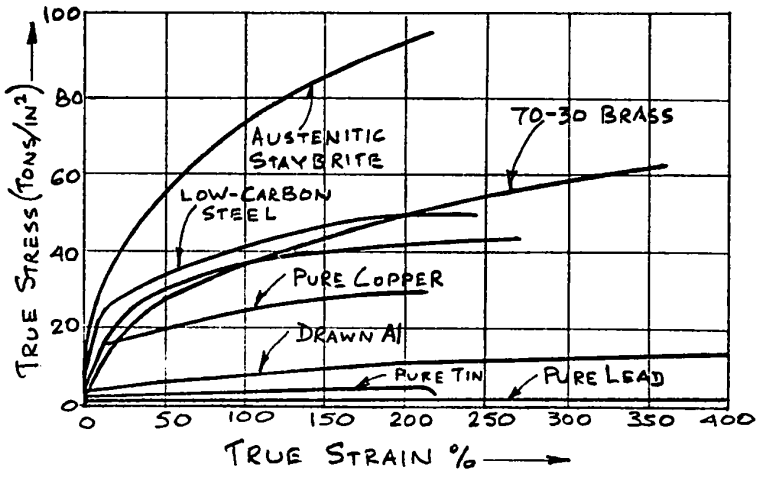

where t = temperature of steel in C

C = carbon content of steel, %

Mn = Manganese content of steel, % (max. 1%)

Cr = Chromium content of steel, %

This formula is applicable only for values of t above 700°C.

Certain steels show a "hump" in the resistance to deformation/ temperature curve near the temperature at which the steel changes from α- structure to γ- structure. This (3) phenomenon was noticed by Houdremont and Kallen. Figure 21 shows the change in deformation resistance with temperature, as deduced with the Ekelund formula, for 0.22% C steel.

Geleji (51) considers the values obtained from the Ekelund formula to be too high and has arrived at the following formula for steels with C 0.6%, Si 0.5% and Mn 0.8%:

$$= 0.015 \ (1400 - t) \ \text{Kg/mm}^2 \qquad .....2.5.4\text{-}2$$

The variation of yield stress at different temperatures and strain-rates is shown in Figure 22.

2.5.5. YIELD STRESS IN COLD ROLLING

It has been stated before that the yield stress in cold working depends on the kind of metal, amount of cold work or initial strain-hardening, strain-hardening during the rolling pass being considered and, to a very small degree,

the strain-rate of deformation. The yield-stress-percentage reduction curve naturally depends on the material concerned. In commercial testing practice, such diagrams are plotted by calculating the stress at any elongation, or compression, from the measured load and the original cross-sectional area of the test specimen. For purposes of studying the relationship between stress and strain under plastic conditions, it is better to consider the actual reduced area in case of tension or the actual enlarged area in the case of compression. The stresses are termed "true stresses". Figure 23 shows some true stress-strain curves obtained by tension tests for some common metals. From this, it may be noted that not only does the initial stress, at which plastic flow commences, vary widely for the different metals, but also that the variation of resistance to deformation with increasing strain is markedly different between the various metals.

Regarding the effect of strain-rate on the yield stress in cold rolling, it has been found by accurate tests that, at very low strain rates, there is an increase in the yield stress of the material. Figure 24 shows the results of tension tests on mild steel at strain rates varying from .00003 sec^{-1} to .074 sec^{-1}. It will be observed that as the strain rate increases, the initial yield point also increases appreciably, but that after an extension of about 8%, the effect of strain-rate on yield stress is very much reduced. In cold rolling, compression rates or strain rates

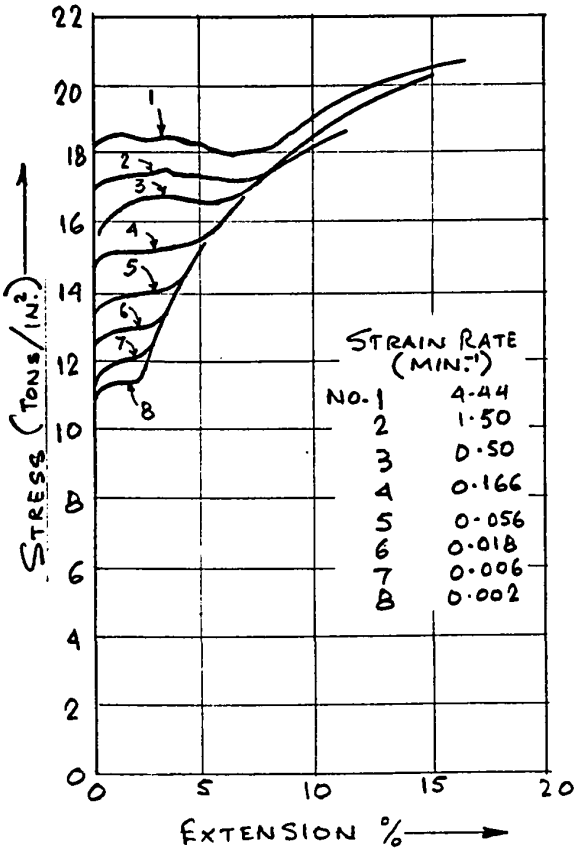

FIGURE 24 : Effect of strain-rate on yield stress in mild steel (35)

rarely fall below 15 sec^{-1} and maybe up to 3,000 sec^{-1}, in modern continuous strip mills. It may thus be inferred, and this fact has been borne out by actual rolling tests, that at the rates of strain prevalent in cold rolling, the effect of strain-rate variation is almost negligible.

There is, however, a major influence on yield stress in cold rolling, brought about by work-hardening or strain-hardening. It is a common property of most metals that cold plastic deformation results in an increased yield strength. As is seen from Figure 23, the true-stress increases with strain, for most metals, with the exception of tin and lead which exhibit almost no strain hardening. The British Iron and Steel Research Association (B.I.S.R.A.) developed an indentation test and published yield stress curves for different metals, corresponding to measuring amounts of reductions from the annealed condition of the metals. Figure 25 shows typical curves for carbon steels. For rolling calculations, it is necessary to evaluate a mean value of the yield stress during the pass. It has been experimentally determined that the yield stress at a total reduction r_m corresponding to 60% of the reduction in the pass, can be taken as this mean. This may be expressed as: (25)

$$r_m = r_1 + \frac{60}{100} \cdot (r_2 - r_1) = 0.4\ r_1 + 0.6\ r_2$$

where r_1 = Initial reduction of strip from annealed

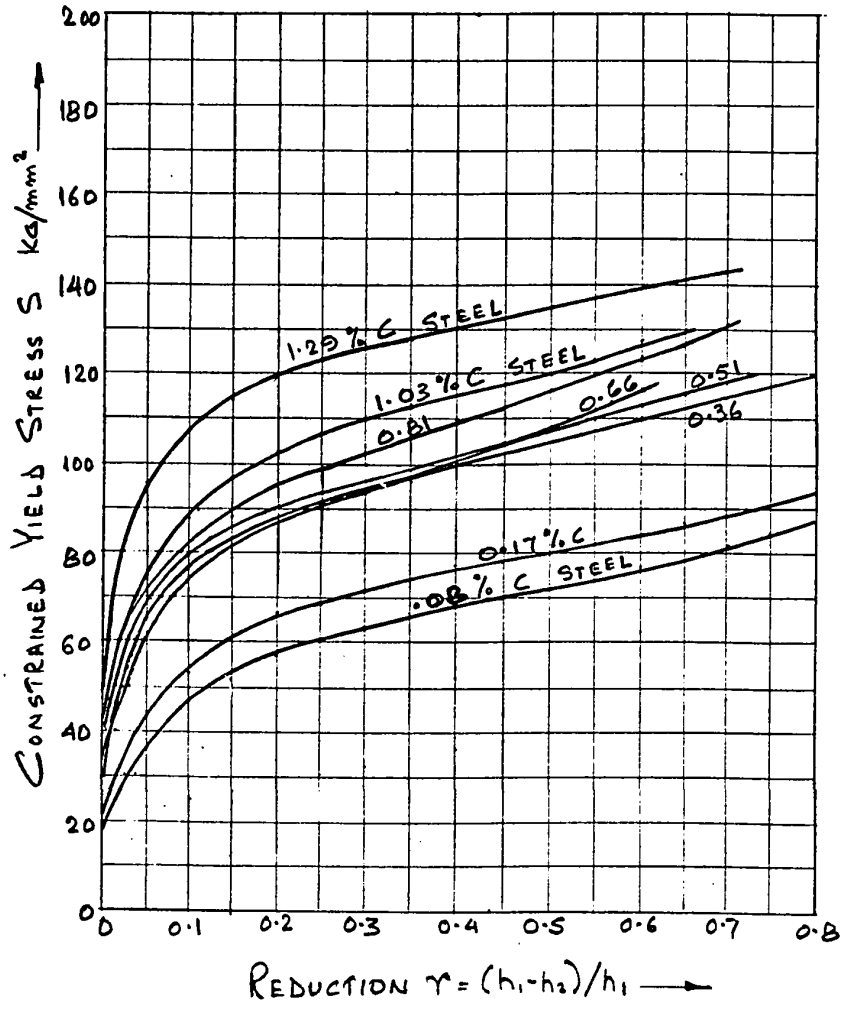

FIGURE 25 : Variation of yield stress with reduction for various steels (25)

condition, prior to pass being considered $= \frac{h_o - h_1}{h_o}$

r_2 = Reduction of strip from annealed condition, after pass being considered $= \frac{h_o - h_2}{h_o}$

The initial and final yield stresses are read off the curves in Figure 25, for values of r_1 and r_2, and the mean yield stress is computed thereafter.

2.6 SPECIFIC ROLL PRESSURE, ROLLING LOAD AND TORQUE

One of the first quantities that has to be determined in any systematic procedure for mill design, is the specific roll pressure and, from it, the rolling load, corresponding to the assumed data of material specifications, rolling temperature, rolling speed, reduction in the pass, etc. This, naturally, has been the prime objective of various rolling mill researchers and experimentalists, leading to several qualitatively-approximate theories and also empirical formulae which are evolved and modified from actual rolling mill tests.

The "rolling load" (P) is defined as the vertical force with which the rolls press on the stock, thus causing it to reduce in height and cross-sectional area. It is also referred to as the "separating force" in the mill. The "mean specific roll pressure" (p_r) by definition, is the rolling load divided by the horizontally projected contact

area between the rolls and the material being rolled. This applies particularly in the case of hot rolling, where elastic deformation or "flattening" of the roll surface is usually negligible. As given earlier, the horizontal projection of the arc contact, from which the area of contact is usually contacted, is given by:

$$l_d = \sqrt{R(h_1 - h_2) - \frac{(h_1 - h_2)^2}{4}} \qquad \ldots\ 2{\cdot}5 - 1.$$

Hence mean specific roll pressure can be expressed as:

$$p_r = \frac{P}{b_m \times l_d}$$

where b_m = mean width of the material between the rolls.

The various theories of rolling, however, attempt at first to establish an expression for the mean specific roll pressure. It is known that the specific roll pressure varies along the arc of contact, between the rolls and the material, rising sharply from zero at the plane of entry, reaching a maximum value somewhere along the arc of contact and falling sharply to zero at the plane of exit. Friction is one of the factors causing non-uniform pressure distribution during rolling. The frictional forces arising in the roll gap act in two directions opposite to each other. The zone in which the slipping forces disappear and static friction arises is, as mentioned earlier, called the neutral zone. Other factors

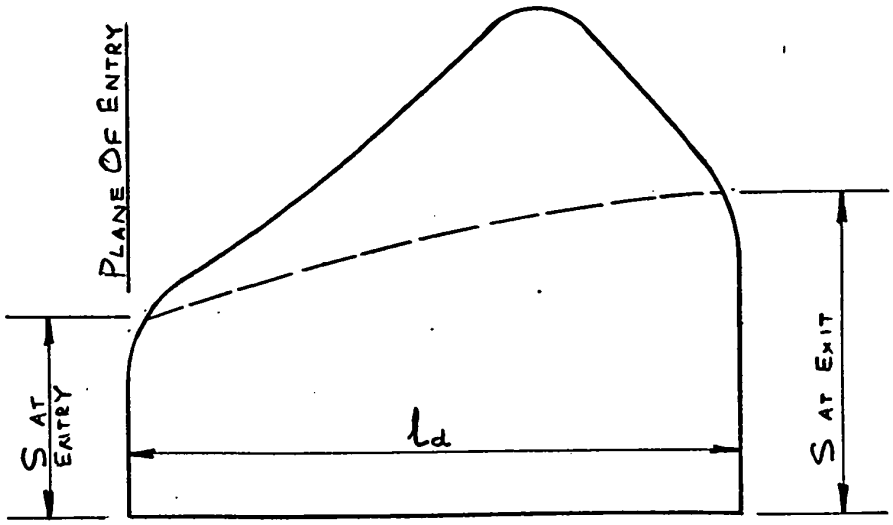

FIGURE 26 : Influence of strain hardening on roll pressure distribution (2)

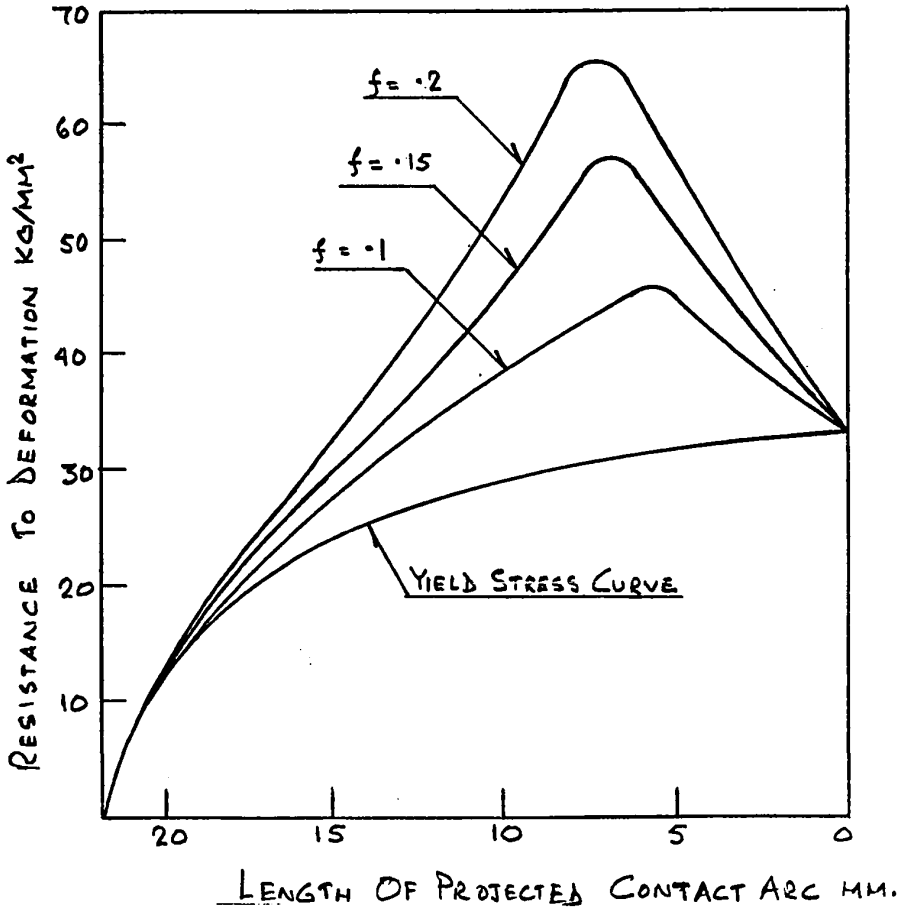

FIGURE 27 : Influence of coefficient of friction on resistance to deformation (13)

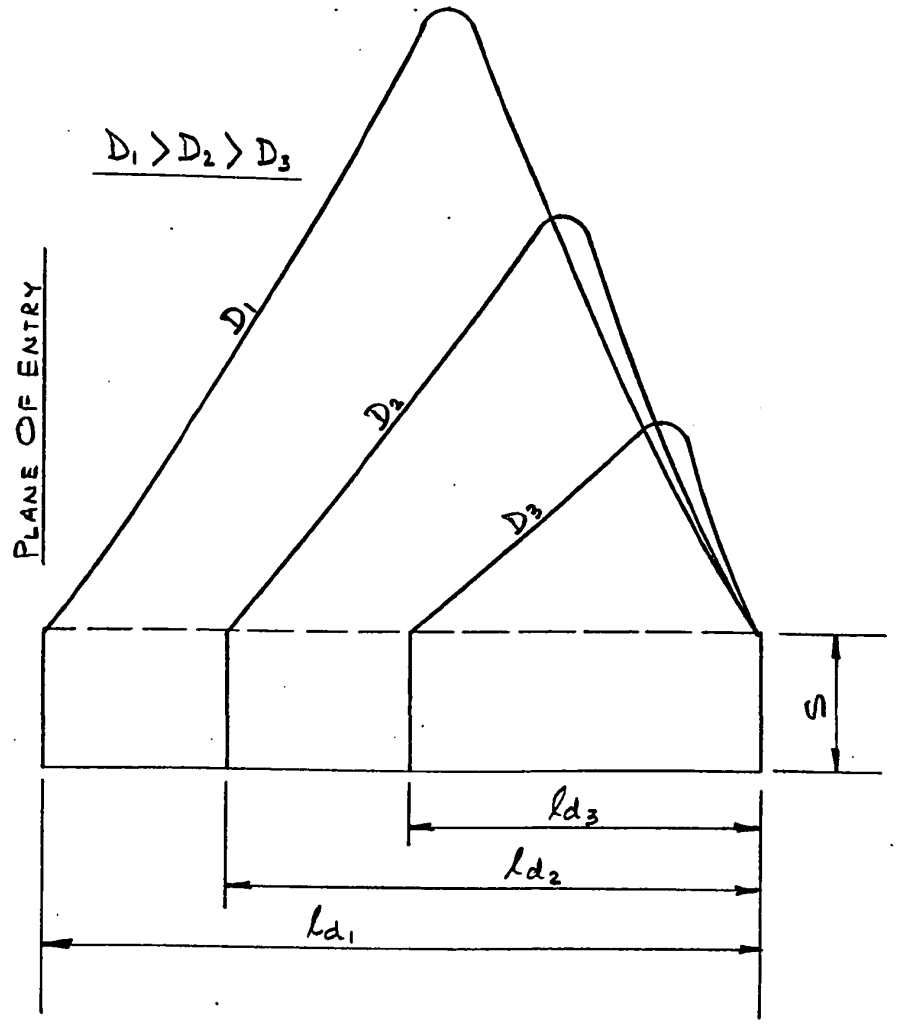

FIGURE 28 : Influence of roll diameter on resistance to deformation (2)

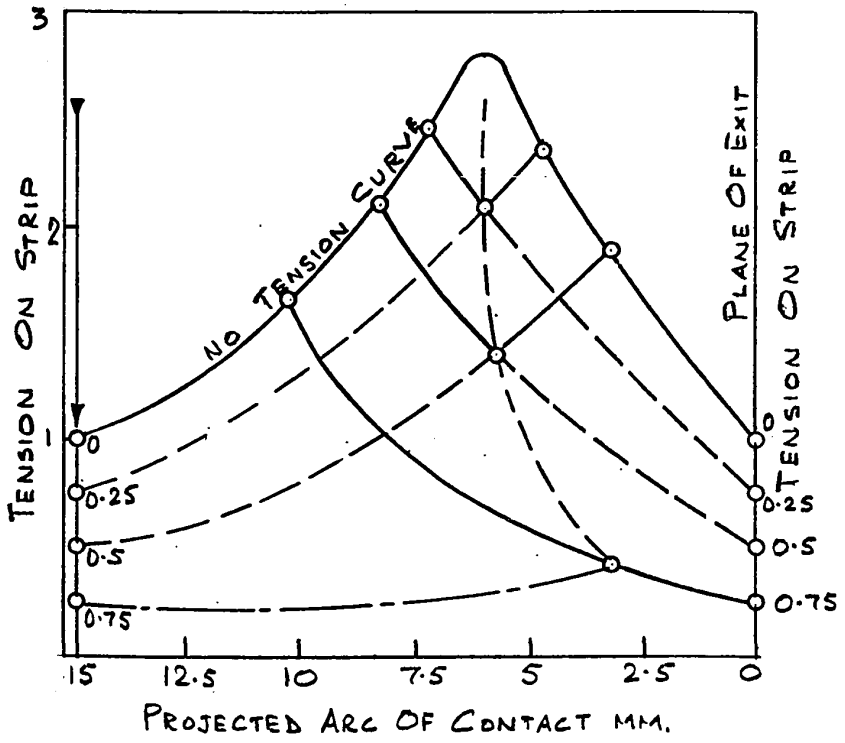

FIGURE 29 : Effect of front and back tension on roll pressure distribution (2)

which affect the distribution of specific pressure along the contact arc are: 1) the roll diameters, 2) the speed of rolling which influences the variation of strain rate which, in turn, affects the constrained yield stress of the material, 3) the amount of reduction which, in cold rolling, affects the strain-hardening and thus the constrained yield stress and 4) in general, all the factors discussed earlier which affect the constrained yield stress of the material during rolling. Figures 26, 27, 28 and 29 show the influence of some parameters on the specific pressure distribution.

It is important to determine the true nature of this pressure distribution as this will decide the position of the resultant vertical force acting on the rolls, and its distance from the roll centers, in order to be able to determine the torque required to be applied on the roll, for a given reduction.

Siebel and Lueg (19) were one of the earliest researchers to carry out experiments, with a specially-constructed scaled-down mill, in order to actually measure the pressure distribution along the contact arc, for several metals under mostly cold and some hot rolling conditions. Using a pressure sensing device mounted in the surface of the roll, pre-calibrated and wired to amplifying and recording instruments, they obtained detailed readings for pressure distribution. Figures 30 and 31 show some typical curves

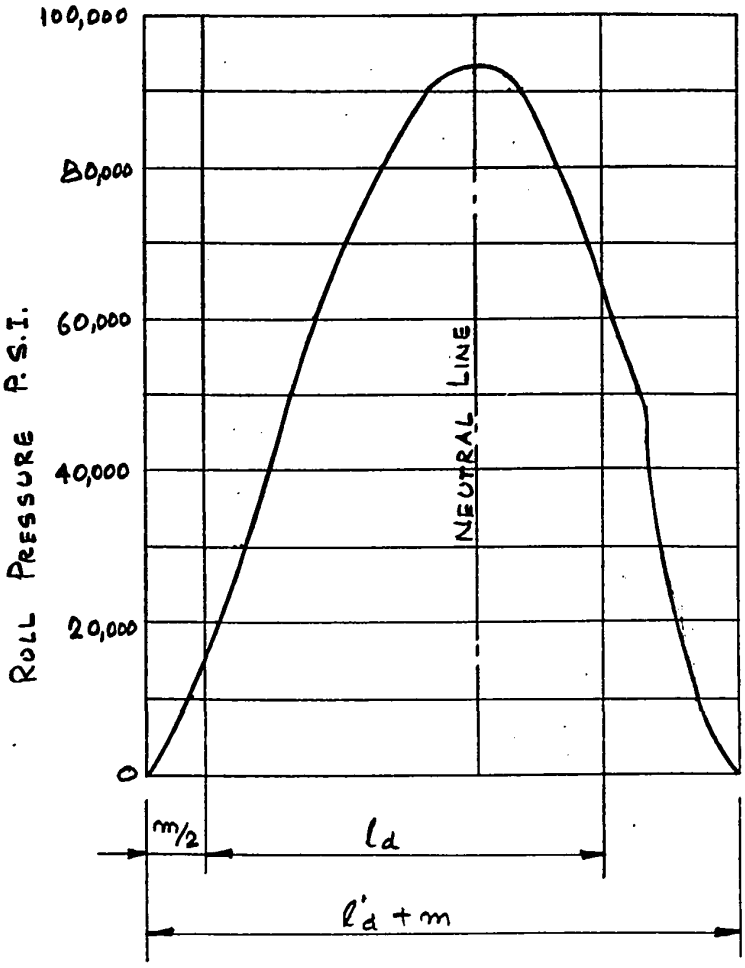

FIGURE 30 : Pressure distribution along contact arc for cold rolling of copper strip without tension (19)

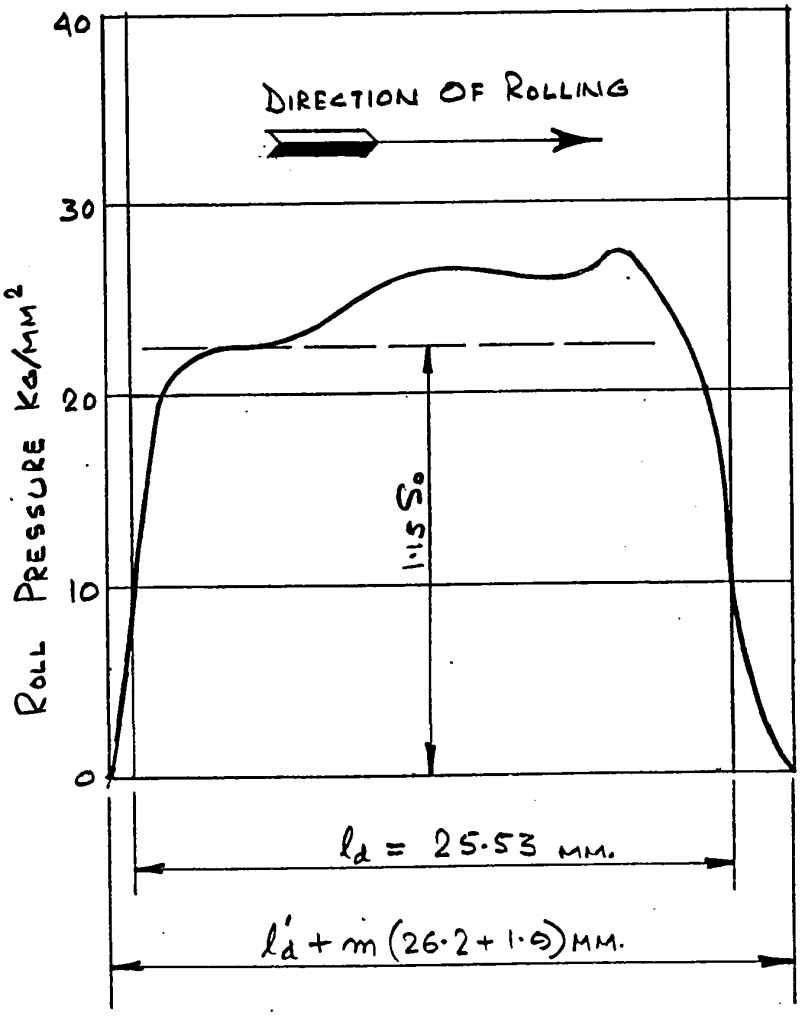

FIGURE 31 : Pressure distribution along contact arc for hot rolling mild steel flat bar (19)

obtained by them. Figure 31 which shows the pressure distribution during a hot rolling operation, seems to suggest that in hot rolling of a thick bar, the radial pressure distribution is approximately uniform. This is in sharp contrast to Figure 30, which shows a distinct rise of pressure to a peak and a decrease to zero thereafter. Further experiments by Smith, Scott and Sylwestrowicz (37) and Korolev (36) have also corroborated the findings of Siebel and Lueg.

2.6.1 CALCULATION OF ROLLING LOAD

The rolling load may be obtained by integrating the vertical component of the specific roll pressure over the length of the contact arc and multiplying by the mean width of the material in the pass.

$$\text{Thus, } P = A_h \int_{\theta=0}^{\theta=\alpha} p.d = A_h . K_{wm} \qquad \ldots\ldots 2.5\text{-}2$$

where P = the Rolling Load

α = Contact angle

A_h = Projected horizontal area of contact

$= l_d \times b_m$

K_{wm} = Mean resistance to deformation.

l_d = Length of contact arc $= \sqrt{R(h_1 - h_2) - \frac{(h_1-h_2)^2}{4}}$

p = Specific vertical rolling pressure, which

for small angles of contact may be, without much error, assumed to be = p_r, the specific radial roll pressure.

$$b_m = \frac{b_1 + b_2}{2} \quad \text{or} \quad = \frac{b_1 + 2b_2}{3}$$

It is in the treatment of Kwm, i.e., the integral in equation 2.5-2 that much of the divergence of the theories of rolling and their proposed calculation methods and formulae, is present.

2.6.2 CALCULATION OF TORQUE

Figure 32 shows the case of stock being rolled between rolls of equal diameter and equal circumferential speeds and the resultant rolling load is shown passing through the center of gravity of the roll pressure distribution diagram, at a horizontal distance a_1 from the line of the roll centers. This distance a_1 is referred to as the "lever arm" and from this the torque acting upon the roll can be calculated. The lever arm a_1 is normally expressed in terms of the horizontal projection l_d of the contact arc:

$$a_1 = c_1 \cdot l_d \qquad \ldots\ldots\ldots\ldots \text{2.5-3}$$

The value of c_1 has again been a matter of extensive research and experimentation and various formulae have been published by several researchers for different rolling conditions. Underwood (3) published values of c_1 varying from 0.39 to 0.5, depending on the type of operation.

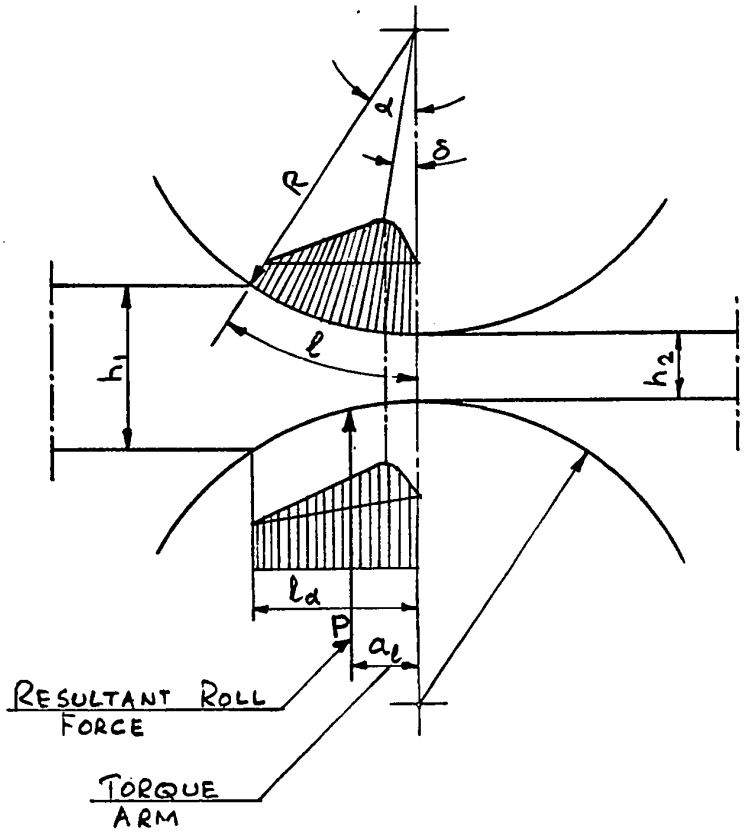

FIGURE 32 : Resultant roll force and torque arm relative to projected arc of contact (2)

Thus, the general expression for rolling torque may be written as:

$$M_w = A_h \cdot a_1 \cdot \int_{\theta=0}^{\theta=\alpha} p \cdot d\theta \qquad \ldots 2.5\text{-}4$$

CHAPTER 3

THEORIES OF STRIP ROLLING

The theories of strip rolling aim at providing means and methods of calculating roll force and torque in terms of certain measurable quantities. These are the ingoing and outgoing thickness of the strip and the roll radius, all of which are easily measured; the yield stress of the strip which is measured, not on the strip itself in the roll gap, but on a sample taken from it or on the basis of experimentally determined curves and empirical average values; and the coefficient of the friction, a factor assumed to be constant in the roll gap and measurable only by rolling experiments carried out for condition similar to those for which a calculation is being made.

Much of the classical work in the theory of rolling was done by Siebel, Von Karman, Tselikov and Nadai. All of these theories had similar assumptions, many of which have later been proven to be erroneous. They all have as their starting point, a differential equation which represents the condition of equilibrium of an elementary vertical plane section of the strip between the rolls. The theories differ in the further development of this differential equation.

3.1 THE BASIC DIFFERENTIAL EQUATION FOR PRESSURE DISTRIBUTION IN THE ROLL GAP

The following assumptions are made in the derivation of the basic differential equation:

1. The material does not spread laterally, i.e., a condition of plane strain exists. This condition is approximately satisfied if the thickness of stock is small compared to the width.
2. The coefficient of external friction between the stock and the rolls is constant at all points in the arc of contact.
3. Plane vertical sections before rolling remain plane after rolling.
4. There is no elastic deformation of the rolls.
5. Elastic deformations in the arc of contact are negligible in comparison to plastic deformations.
6. The metal being deformed is a continuous isotropic medium.
7. The Hencky-Von Mises criterion for plastic yielding, i.e., $S_1 - S_3 = 1.15\ S_o = S$, holds for the material and the rolling conditions.
8. The yield stress of the material, S, remains constant throughout the contact length, i.e., there is no work-hardening of the material or variation of yield stress due to the variable strain-rate conditions in the roll gap.

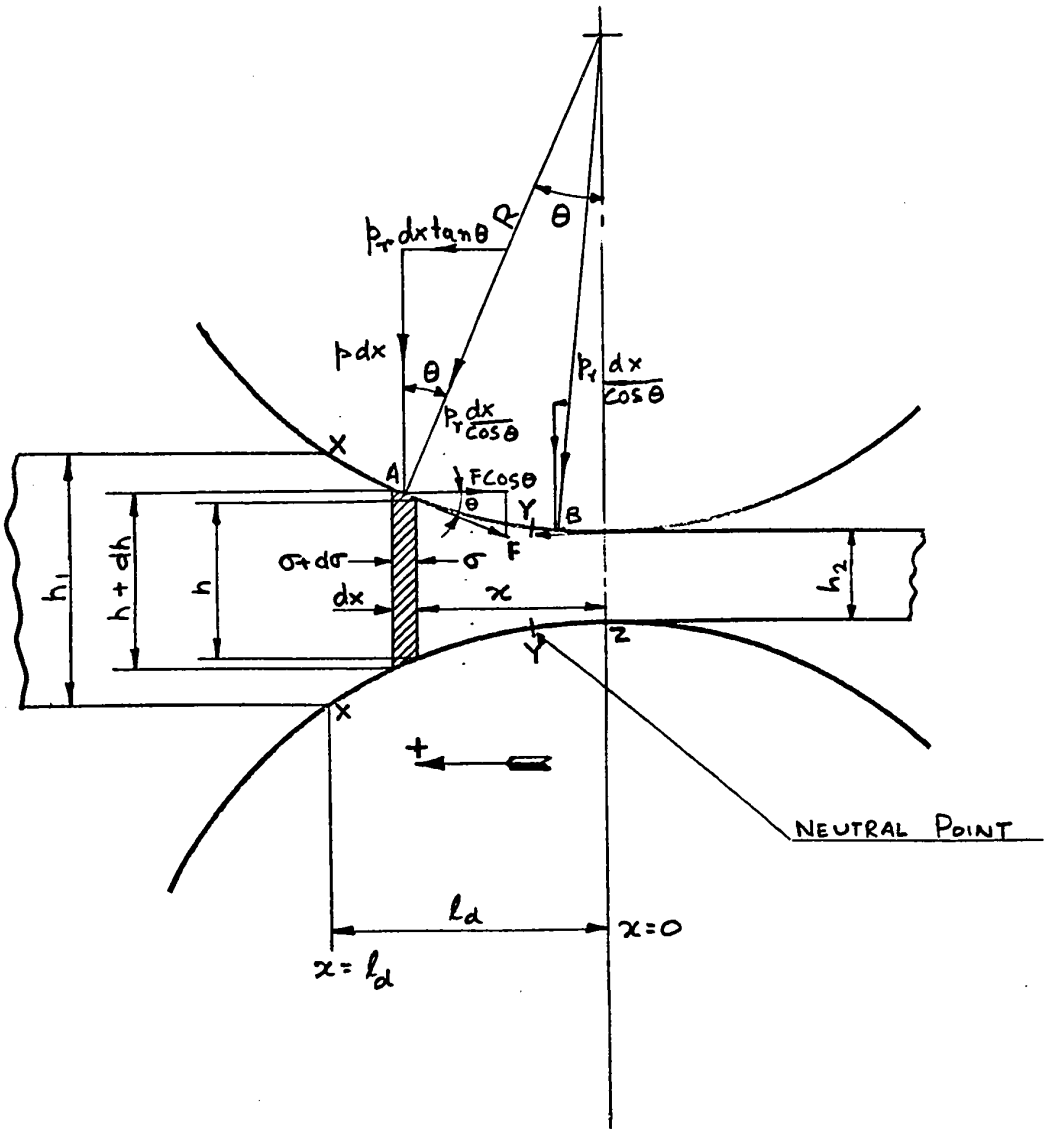

FIGURE 33 : Forces and stresses acting upon an elemental vertical section of the sheet between the rolls (3)

9. The peripheral velocity of the rolls is uniform, i.e., that the rolls are neither accelerating nor decelerating.

10. Slipping takes place along the arc of contact at all points except the neutral point.

11. The contact angle is small.

Figure 33 shows the reduction of a sheet, of initial thickness h_1, between plain cylindrical rolls, down to a final thickness h_2. The equilibrium conditions are considered, for a vertical elemental plane section of height h and width dx. With reference to Figure 33, the following may be stated:

Normal force on elemental section $= p_r \times \frac{dx}{\cos\theta}$

Horizontal component of normal force, tending to oppose entry $= p_r \cdot \frac{dx}{\cos\theta} \times \sin\theta$

$= p_r \tan\theta \, dx.$

Tangential frictional force $= F = f.p_r \frac{dx}{\cos\theta}$

Horizontal component of tangential force tending to draw the bar between the rolls $= f.p_r \cdot \frac{dx}{\cos\theta} \cdot \cos\theta$

$= f.p_r dx$

Hence, for equilibrium of the section under the influence of the horizontal forces, we have

$$2p_r \tan\theta dx - 2f\, p_r dx = (h + dh)(\sigma + d\sigma) - h\sigma = d(h\sigma) \quad \ldots\ldots\ldots\ldots\ldots\ldots 3\cdot1\text{-}1$$

From Figure 33, we also get:

$p.dx$ = Vertical component of the normal force $p_r \cdot \frac{dx}{\text{Cos}}$.

$$= p_r \frac{dx}{\text{Cos}\theta} \times \text{Cos}\theta$$

$$= p_r\, dx$$

$$\therefore \quad p = p_r.$$

Substituting this and writing $f = \tan\rho$, where ρ is the friction angle, we get:

$$p\,(\tan\theta - \tan\rho)dx = d\left(\frac{h\sigma}{2}\right) \quad \ldots\ldots 3\cdot1\text{-}2$$

As is seen from the figure, the elemental section was considered between the plane of entry and the neutral plane. If a similar elemental section is considered between the neutral plane and the plane of exit, with the direction of frictional forces reversed, we would get

$$p\,(\tan\theta + \tan\rho)\,dx = d\,(\frac{h\sigma}{2}) \quad \ldots 3.1\text{-}3$$

Combining these equations and substituting $\tan\theta = \frac{1}{2}\,\frac{dh}{dx}$,

we get $\frac{1}{2} p . \frac{dh}{dx} \mp p \tan\rho = \frac{d\left(\frac{h\sigma}{2}\right)}{dx}$ .....3·1-4

In order to express σ in terms of p, the criterion for plastic yielding, $S_1 - S_3 = S$ is applied along with the assumption of the mean vertical pressure and mean horizontal stress acting on the section dx, as principal stresses, in this case both compressive.

Now, total vertical force on element = $pdx + F \sin\theta$

$= pdx + fp \tan\theta\, dx$

$= p(1 + f \tan\theta)dx.$

Assuming $S_1 = p(1 + f \tan\theta)$

and $S_3 = \sigma$

we get, from $S_1 - S_3 = S$

$p(1 + f \tan\theta) - \sigma = S$

When a further assumption is made, of small angles of contact, it is possible to conclude that $f \tan\theta \doteq 0$.

This then gives $p - \sigma = S$.

Substituting this in the differential equation, we get:

$$\frac{1}{2} p . \frac{dh}{dx} \mp p \tan\rho = \frac{d\left\{\frac{h}{2}(p - S)\right\}}{dx} \quad \ldots 3.1\text{-}5$$

or $$\frac{d\left\{\frac{h}{2}(p - S)\right\}}{dx} - \frac{p}{2} \cdot \frac{dh}{dx} \pm p \tan\rho = 0$$

which expressed thus or in other alternative forms, is the starting point of the work of the classical theories of rolling.

3.2 VON KARMAN'S THEORY (17)

In the formulation of his theory (in 1925), Von Karman considered the forces acting on an elemental vertical section of the material between the rolls and made further approximations whereby he assumed that:

Radial pressure p_r is replaced by a vertical pressure p and x is small compared to R.

This gave the relation $\frac{d\left(\frac{\sigma h}{2}\right)}{dx} = p(\sin\theta \mp f \cos\theta)$ which is also given as $\frac{d\left(\frac{\sigma h}{2}\right)}{dx} = p \cos\theta (\tan\theta \mp \tan\rho)$

He next assumed that for small angles of contact $\cos\theta \doteq 1$, thus obtaining $d\left(\frac{\sigma h}{2}\right) = p(\tan\theta \mp \tan\rho)\, dx$ ..... 3·2-1

or: $$d\left\{\frac{h}{2} \cdot (p - S)\right\} = p(\tan\theta \mp \tan\rho)\, dx$$ 3.2-2

The solution was of the form:

$$p = e^{\mp \int \tan \rho / h \, dx} \left[C + \frac{K}{h} e^{\pm \int \tan \rho / h \cdot dx} \cdot dh \right] \quad \ldots 3.2\text{-}3$$

T.L. Smith of the Carnegie Institute of Technology, (3) attempted a simplification of the Von Karman equations on the following basis: In equations 3.1-4 and 3.1-5, $\frac{1}{2}\frac{dh}{dx}$ represents the slope of the arc of contact at any point distant x from the roll centre line. Smith's approach was to try and replace the circular arc of contact by a curve of another form which very nearly coincides with the circular arc, so that $\frac{dh}{dx}$ is a simple function of x, thus greatly simplifying equations 3.1-4 and 3.1-5. He assumed a parabolic arc of contact whose equations, referred to the rolling direction and the vertical roll centres, can be expressed as:

$$\frac{1}{2} \cdot h = \frac{1}{2}\left[h_2 + \Delta h \left(\frac{x}{l_d}\right)^2 \right] \text{ as in Figure 34,}$$

where $\Delta h = h_1 - h_2$, The draught

and l_d = The projected contact length.

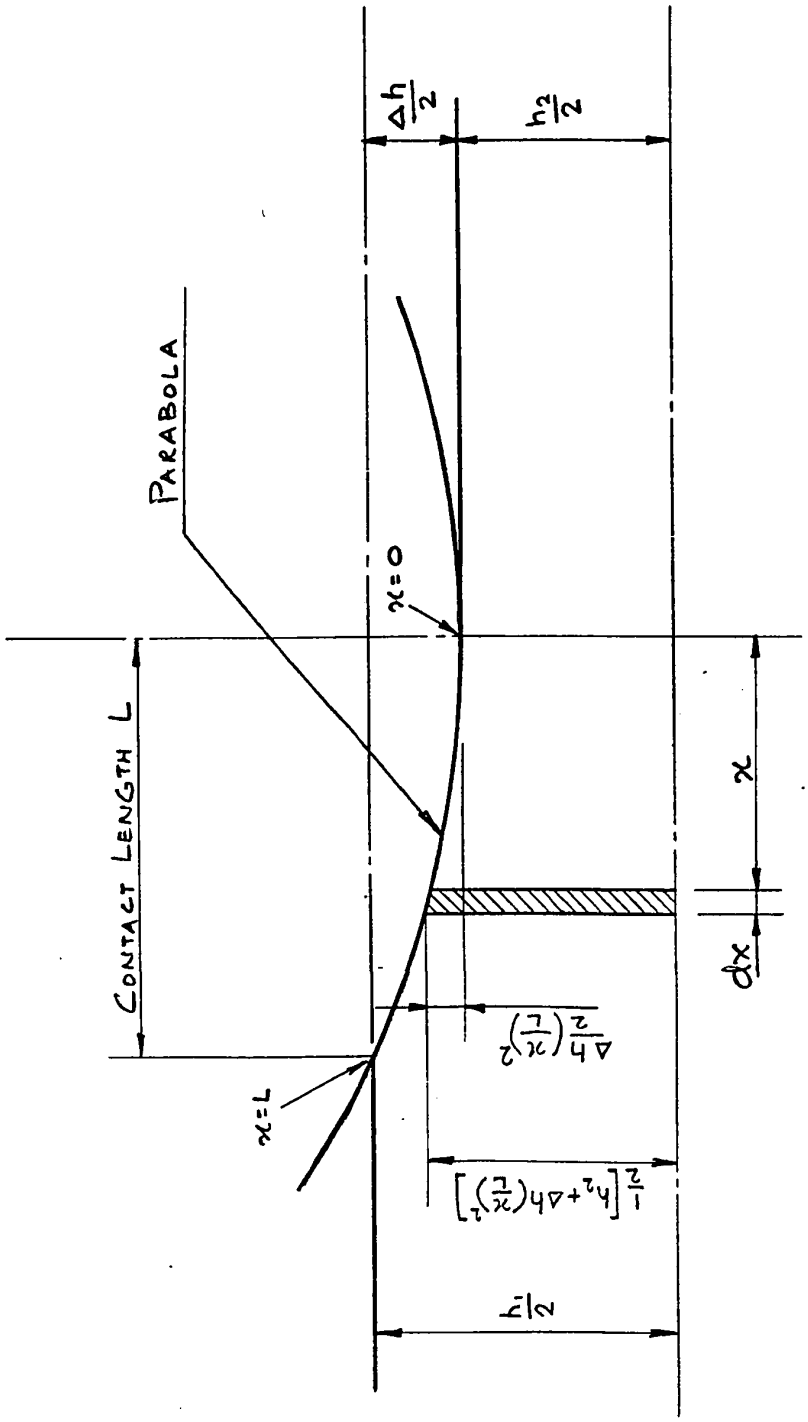

FIGURE 34 : Parabolic arc of contact between material and roll (3)

Differentiating, we get $\frac{1}{2} \cdot \frac{dh}{dx} = \Delta h \cdot \frac{x}{l_d^2}$

Substituting this expression in Equation 3·1-4,

$$\frac{d\left(\frac{h\sigma}{2}\right)}{dx} = \frac{\Delta h}{l_d^2} px \mp p \tan\rho = p\left[\frac{\Delta hx}{l_d^2} \mp \tan\rho\right]$$

Substituting $\sigma = P - S$ and $h = h_2 + \Delta h\left(\frac{x}{l_d}\right)^2$,

$$\frac{d}{dx}\left[(P - S)\left\{\frac{1}{2} h_2 + \frac{1}{2} \cdot \Delta h \left(\frac{x}{l_d}\right)^2\right\}\right] = p\left[\frac{\Delta hx}{l_d^2} \mp \tan\rho\right]$$

$$\text{or} \quad \left(\frac{h_2}{2} + \frac{\Delta hx^2}{2l_d^2}\right) \cdot \frac{dp}{dx} + \frac{\Delta hx}{l_d^2}(p - S) = p\left(\frac{\Delta hx}{l_d^2} \mp \tan\rho\right)$$

$$\text{or} \quad \frac{d\left(\frac{p}{S}\right)}{d\left(\frac{x}{l_d}\right)} = \frac{\frac{2\Delta h}{h_2}\left(\frac{x}{l_d} \mp \frac{p}{S} \times \frac{l_d}{\Delta h} \times \tan\rho\right)}{1 + \frac{\Delta hx^2}{h_2 l_d^2}} \quad \text{.....3·2-4}$$

Equation 3·2-4 cannot be directly integrated and thus the pressure curves represented by it can only be traced by a point to point summation method or by computer. The application of this equation to a specific rolling operation is thus a complex proposition. However, using this equation, Trinks had worked out several thousand point by point (41) integration calculations and published a family of curves as shown in Figure 35.

3.3 NADAI'S THEORY (20)

Nadai, in solving basic differential equation for

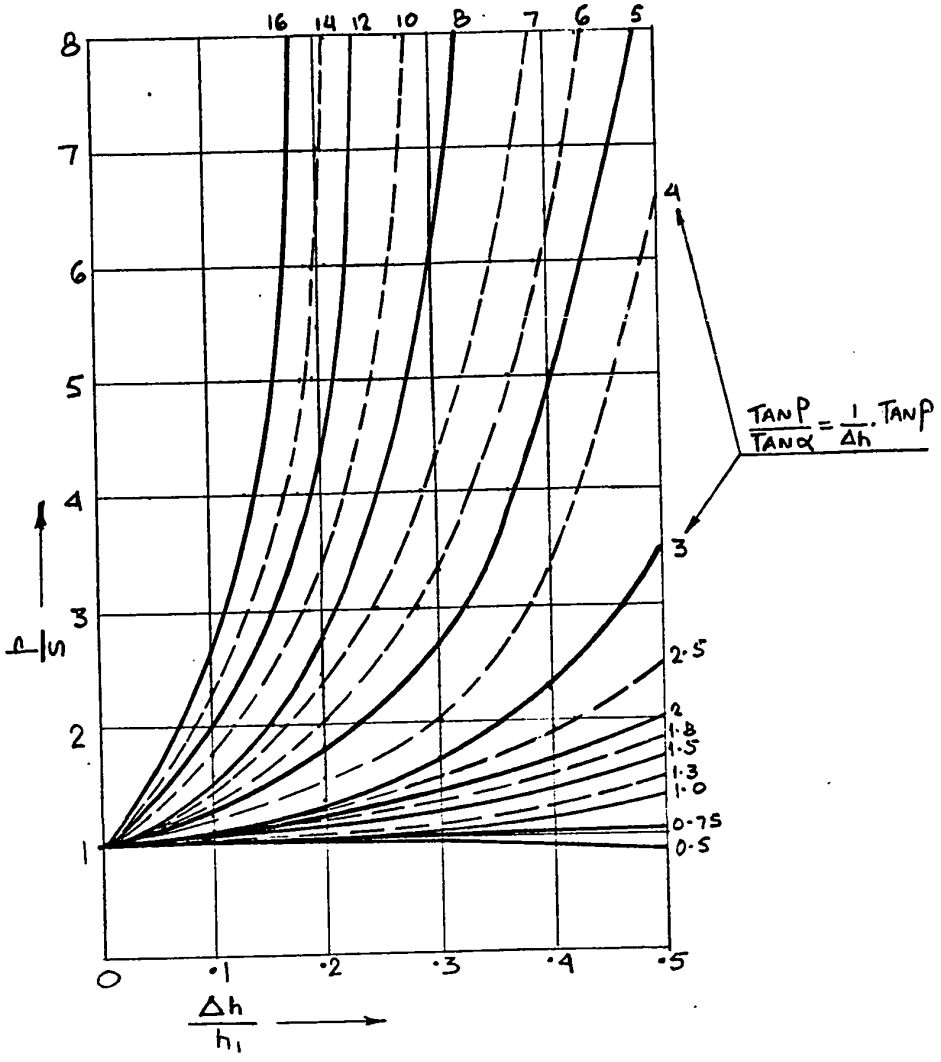

FIGURE 35 : Trinks' graphical solution of Von Karman's equation (41)

specific pressures, introduced the additional factor of external tension on strip, applicable to cold strip rolling. He gave the following form to the Von Karman equation:

$$\frac{d(h\sigma)}{dx} \pm 2fp_r + 2p_r \frac{x}{R} = 0 \quad \ldots\ldots\ldots\ldots\ldots 3.3\text{-}1$$

The assumption of small angle is made, i.e., $\tan\theta = \theta = \frac{x}{R}$.

Nadai also uses the following terms in developing the equation:

$$y = \frac{p_r}{S} \quad , \quad \gamma_1^2 = \frac{h_2}{R} \quad , \quad Z = \frac{x}{\gamma_1 R} \quad ,$$

and $\tau = \pm fp_r$ = tangential shear stress.

Also, with respect to Figure 33, $h = h_2 + 2R(1 - \cos\theta)$ which, with the assumption of small angles of contact, gives the approximation $h = h_2 + R\theta^2$

$$= h_2 + \frac{x^2}{R} = h_2(1 + Z^2)$$

Now, the condition for plastic flow, when considered with strip tension, becomes

$$p_r - (-\sigma) = S$$

Combining all the above conditions and substitutions, Nadai converted Equation 3·3-1 to this form:

$$(1 + Z^2)\frac{dy}{dZ} - \left(\frac{2}{\gamma_1 S}\right)\tau = 2Z \quad \ldots\ldots\ldots\ldots 3\cdot3\text{-}2.$$

He arrived at this form of Von Karman's equation, in order to evaluate the influence, on specific roll pressure, of different assumptions regarding the frictional force, viz., a) the assumption that $\tau = f p_r$, b) τ = a constant and c) frictional resistance proportional to the relative velocity of slip between the strip and the roll.

a) Here, $\tau = f p_r$ for forward slip and $\tau = - f p_r$ for backward slip.

Also, since $y = \frac{p_r}{S}$, $\tau = fSy$ for forward slip,

and $\tau = -fSy$ for backward slip.

Now: $\frac{2\tau}{\gamma_1 S} = \frac{2.fSy}{\gamma_1 S} = K_f.y$, since f and γ_1 are constant.

Where $K_f = \frac{2f}{\gamma_1}$

Then equation 3·3-2 becomes

$$(1 + Z^2)\frac{dy}{dZ} - K_f y = 2Z \quad \text{.....3·3-3}$$

Substituting $Z = \tan v_1$ where v_1 is another variable, we get $dv_1 = \frac{dZ}{1 + Z^2}$

or $\frac{dy}{dv_1} - K_f y = 2 \tan v_1$

The solution of this differential equation is:

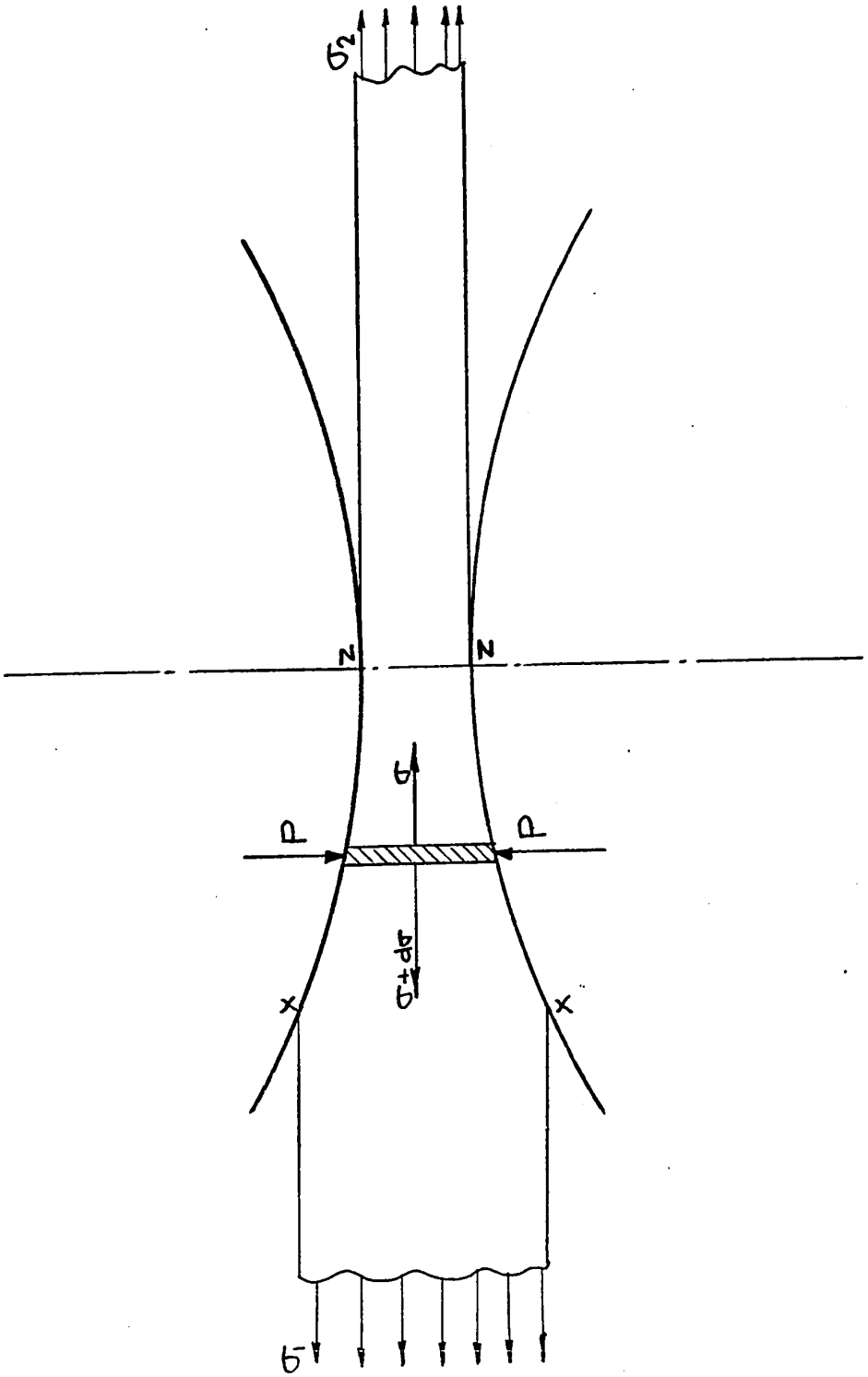

FIGURE 36 : Effect of front and back tension (3)

$$y = \frac{p_r}{S} = e^{K_f v_1} \left(C + 2\int e^{-K_f v_1} \tan v_1 \, dv_1\right) \quad \ldots.3.3\text{-}4$$

The integral can be computed by replacing tan v_1 by a series in v_1 and integrating. Thus, for the region of forward slip, we obtain

$$y = \frac{p_r}{S} = C_2 e^{K_f v_1} - 2\,(1 + K_f v_1) \Big/ K_f^2$$

and for backward slip,

$$y = \frac{p_r}{S} = C_2 e^{-K_f v_1} - 2\,(1 - K_f v_1) \Big/ K_f^2$$

The constants C_1 and C_2 are determined from the boundary constants at the end of the contact zones, where front tension σ_2 and back tension σ_1 are applied, as shown in Figure 36.

After finding C_1 and C_2, the roll pressure corresponding to any point in the arc of contact distant x from the line of roll centres is given by the following two equations:

1. In the area of backward slip, i.e., the entry side of the mill,

$$p_r = S \left[\left\{Y_1 + \frac{2\,(1 - K_f v_2)}{K_f^2}\right\} e^{K_f (v_2 - v_1)} - \frac{2\,(1 - K_f v_1)}{K_f^2}\right] \quad \ldots.3.3\text{-}5$$

2. On the exit side,

$$p_r = S \left[Y_2 + \frac{2}{K_f^2} e^{K_f v_1} - \frac{2\,(1 + K_f v_1)}{K_f^2}\right] \quad \ldots.3.3\text{-}6$$

where $\tan v_1 = \dfrac{x}{\delta R}$

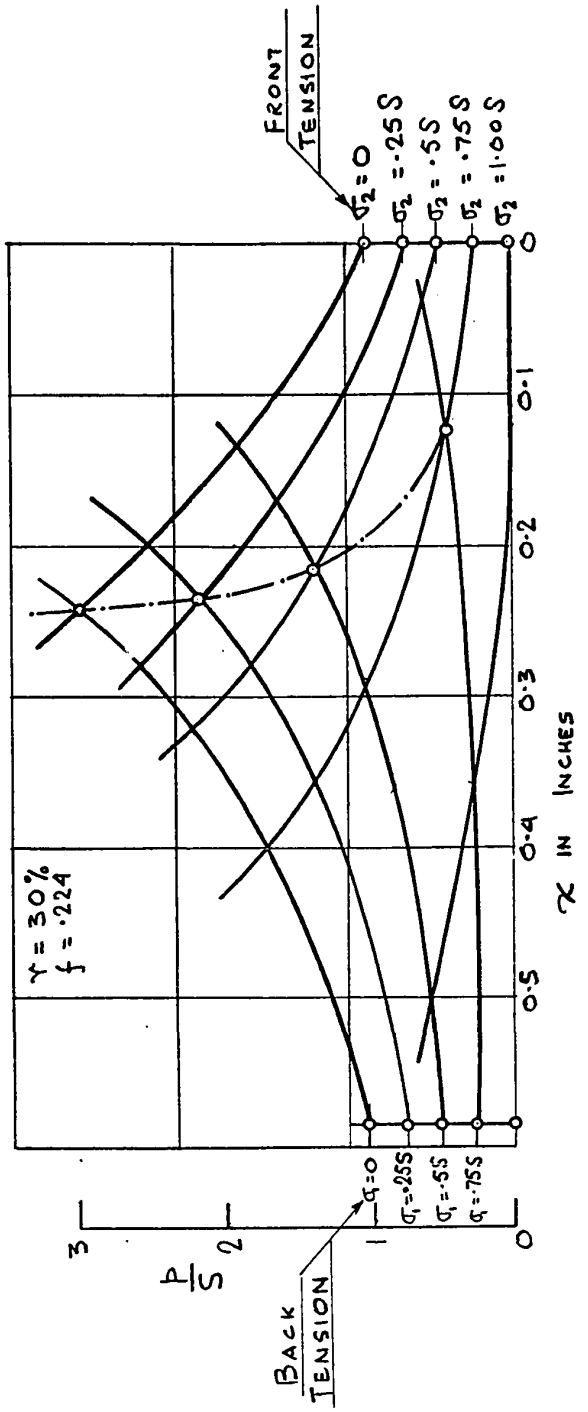

FIGURE 37a : Pressure distribution with and without strip tension using Nadai's equations (20)

$$\tan v_2 = \frac{r}{1 - r}$$ where r is the reduction

$$Y_1 = \frac{S - \sigma_1}{S}$$

$$Y_2 = \frac{S - \sigma_2}{S}$$, where σ_1 and σ_2 are the back and front tensions respectively.

On the basis of equations 3·3-5 and 3·3-6, Nadai has calculated pressure curves for a number of rolling conditions. Figure 37a shows some typical curves for a particular set of rolling conditions. The top pressure curve refers to the case in which front and back tensions are zero, while the other curves indicate conditions with progressively increasing tensions. These curves clearly lead to the conclusions that the application of front or back tension or a combination of both, leads to a reduction in roll pressure and also shifts the position of the neutral point or plane.

2. The magnitude of the surface friction force is assumed to be constant, i.e., $\pm \tau$ = constant.

   Then, with the substitution $\frac{2\tau}{\gamma S} = K_g$, equation 3·3-2 becomes:

$$\frac{dy}{dZ} = \pm \frac{K_g}{1 + Z^2} + \frac{2Z}{1 + Z^2}$$

After integration, this equation gives:

$$y = \frac{p_r}{S} = \pm K_g \tan^{-1} Z + \log_e (1 + Z^2) + C \quad .. \; 3·3-7$$

Here, the plus sign in front of $\pm \tan^{-1} Z$ applies in the region of forward slip between the neutral and exit planes while the minus sign applies in the region of backward slip. Applying boundary conditions at the entry and exit planes and assuming no front or back tension, we get,

$$C_1 = 1 \quad \text{and} \quad C_2 = K_g \tan^{-1} Z_1 - \log_e (1 + Z_1^2)$$

Figure 37b shows a typical pressure curve based on the above equations.

3. The surface friction is assumed to be proportional to the relative velocity of slip between the rolls and the material being rolled. This was the first attempt by any researcher, to consider the variable nature of surface friction within the arc of contact. The case considered was one of cold strip rolling with oil where, according to Nadai, the frictional force is a function of the dynamic viscosity of the lubricating oil, the oil film thickness and the relative speed between rolls and strip.

   Thus, $\tau = \frac{\eta}{\delta_t} (V - v)$,where

   v = the peripheral velocity of roll

   V = the variable horizontal velocity of strip, corresponding to any angle .

   η = mean value of dynamic viscosity of the rolling oil

δ_t = the mean thickness of the oil layer.

Nadai postulated the frictional law :

$$\tau = \frac{\eta}{\delta_t}(V - v) = \frac{\eta V_2}{\delta_t}\left(\frac{1}{1 + Z^2} - \frac{1}{1 + Z_o^2}\right) \quad ..3.3\text{-}8$$

where Z_o = the value of Z corresponding to the neutral point.

V_2 = velocity of strip at plane of exit.

Now, the variable strip velocity, V at any strip height h, can be said to be:

$$V = \frac{V_2 h_2}{h} = \frac{V_2}{1 + Z^2}$$

Also, at the neutral point $V_\delta = v = \frac{V_2}{1 + Z_o^2}$

Hence, we get $\tau = \frac{\eta}{\delta_t}(V - v) = \frac{\eta}{\delta_t} \cdot V_2\left(\frac{1}{1 + Z^2} - \frac{1}{1 + Z_o^2}\right)$

Substituting $\tau_o = \frac{\eta}{\delta_t} \cdot V_2$, equation 3·3-8 assumes the form:

$$\tau = \tau_o\left(\frac{1}{1 + Z^2} - \frac{1}{1 + Z_o^2}\right)$$

Substituting this in equation 3·3-2, we get

$$(1 + Z^2)\frac{dy}{dZ} - \frac{2\tau_o}{\gamma_1 S}\left(\frac{1}{1 + Z^2} - \frac{1}{1 + Z_o^2}\right) = 2Z$$

Putting $K_h = \frac{2\tau_o}{\gamma_1 S}$, we get

$$(1 + Z^2)\frac{dy}{dZ} = K_h\left(\frac{1}{1 + Z^2} - \frac{1}{1 + Z_o^2}\right) + 2Z \quad ...3\cdot3\text{-}9$$

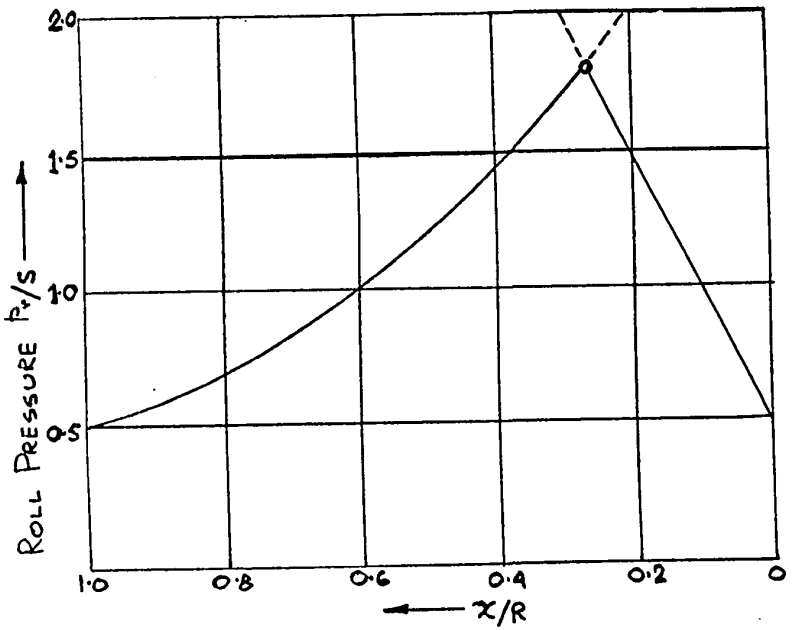

FIGURE 37b : Pressure distribution assuming constant frictional force (20)

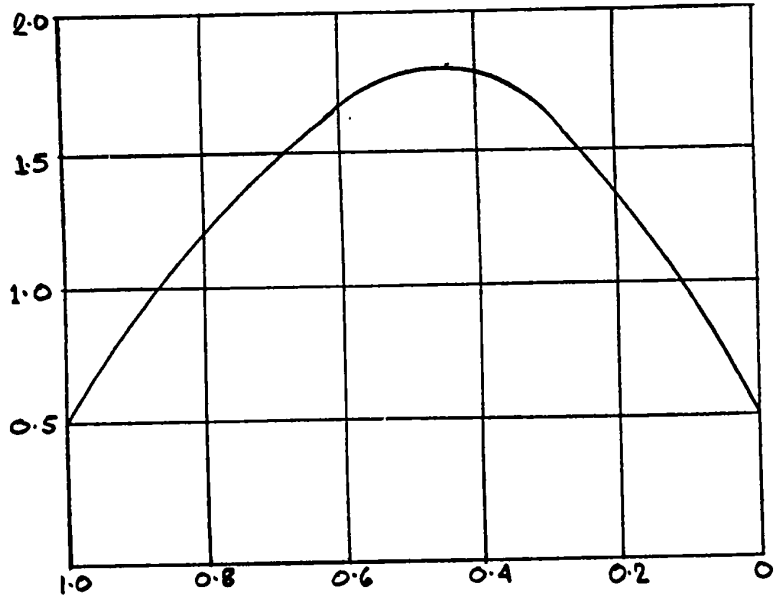

FIGURE 37c : Pressure distribution with friction proportional to relative velocity of slip (20)

The solution of this was found to be:

$$y = \frac{p_r}{S} = 1 + \log_e (1 + Z^2) + \frac{K_h}{2} \left[\frac{Z}{1 + Z^2} - \frac{1 - Z_o^2}{1 + Z_o^2} \cdot \tan^{-1} Z \right] \quad \ldots\ldots 3.3\text{-}10$$

Figure 37c shows the pressure distribution for rolling without tension, as given by equation 3.3-10. It may be observed that there is no break point or discontinuity in this curve, as in the other pressure distribution curves so far shown. Furthermore, the neutral plane is not coincident with the plane of maximum pressure. This can be explained in the following way:

In the neutral plane, $v = V$, hence $\tau = 0$.

From this, we obtain $Z = Z_o$, and substituting this in equation 3.3-9,

$$\left(1 + Z_o^2\right) \frac{dy}{dZ} = 2Z_o$$

or

$$\frac{dy}{dZ} = \frac{2Z_o}{1 + Z_o^2}$$

Since $\frac{dy}{dZ}$ is not equal to zero at the neutral plane, it follows that the roll pressure p_r $(= y \times S)$ is not a maximum at this plane.

Siebel and Lueg's experimental pressure curve shown in Figure 30, also exhibits a rounded profile at the peak. In the light of Nadai's theory, this may have been caused by

variations of the friction coefficient.

3.4 TSELIKOV'S THEORY (39)

Tselikov, in addition to making the assumption stated for the basic differential equation of roll pressure as deduced by Von Karman, made some additional assumptions by which he reduced the Von Karman equation to a form which could be integrated. Tselikov re-wrote equation 3·1-2 in the form:

$$2p\,(\tan\theta - \tan\rho)\,dx = h.d\sigma + \sigma.dh \quad \ldots\ldots \quad 3\cdot4\text{-}1$$

He also deduced $p(1 + f\tan\theta) - \sigma = S$

or $$\sigma = p\,(1 + f\tan\theta) - S \quad \ldots\ldots \quad 3\cdot4\text{-}2$$

Differentiating this equation,

$$d\sigma = (1 + f\tan\theta)\,dp$$

Substituting the values of σ and $d\sigma$ in 3.4-1, putting $\frac{dh}{2\tan\theta} = dx$ and dividing through by $(1 + f\tan\theta)$, we get:

$$\left[1 + \left\{\frac{\tan(\rho - \theta)}{\tan\theta}\right\} p - \frac{S}{1 + f\tan\theta}\right] dh + h.dp = 0 \quad \ldots.3\cdot4\text{-}3$$

At this point, Tselikov made the additional assumption that for small contact angles, θ may be assumed to be nearly constant and equal to half the contact angle. This would be true for a typical section near the neutral plane. Additional substitutions are made:

$$\frac{\tan(\rho - \theta)}{\tan \theta} = \varsigma = \text{constant}$$

and:
$$\frac{S}{1 + f \tan\theta} = S_1 = \text{constant since } \theta \text{ is constant.}$$

Then, 3.4-3 is written as

$$\frac{dp}{(1 + \varsigma)\, p - S_1} = - \frac{dh}{h}$$

This equation may be integrated and results in

$$\frac{1}{1 + \varsigma} \log_e \left\{ (1 + \varsigma)\, p - S_1 \right\} = \log_e \frac{1}{h} + C_o \quad \ldots\ldots\ldots 3.4\text{-}4$$

The constant C_o can be found by applying the boundary condition at the point of entry where $h = h_1$, and $p = p_1$, say. Thus equation 3.4-4, after solving for p, gives:

$$p = \frac{S_1}{1 + \varsigma} \left[\left\{ \frac{p_1}{S_1} (1 + \varsigma) - 1 \right\} \left(\frac{h_1}{h}\right)^{1+\varsigma} + 1 \right] \ldots\ldots\ldots 3.4\text{-}5$$

This is the general expression for Tselikov's formula for specific roll pressure. When tensions are not applied to the strip, we have $\sigma = 0$, and from equation 3.4-2,

$$p_1 = \frac{S}{1 + f \tan\theta} = S_1$$

Thus the expression for roll force, when applied to a point between the entry plane and the neutral plane, becomes:

$$p = \frac{S}{(1 + f \tan\theta)\, \varsigma_1} \left[\varsigma_1 \left(\frac{h_1}{h}\right)^{\varsigma_1 + 1} + 1 \right] \ldots\ldots\ldots 3.4\text{-}6$$

where $\varsigma_1 = \dfrac{\tan(\rho - \theta)}{\tan \theta}$, and the roll force, considering a point between the neutral point and the exit plane,

$$p = \frac{S}{(1 - f\tan\theta)\varsigma_2} \left[\varsigma_2 \left(\frac{h}{h_2}\right)^{\varsigma_2 - 1} - 1 \right] \ldots\ldots 3.4\text{-}7$$

where $\varsigma_2 = \dfrac{\tan(\rho + \theta)}{\tan \theta}$

Tselikov deduced a series of curves, showing the effect of varying coefficient of friction, varying reductions and varying roll diameters, on the specific roll pressure, over the length of the contact arc, as shown in Figure 38.

Tselikov went further, to determine a "mean" specific roll pressure for the case of rolling without tensions, which he expressed as $p_s = \dfrac{\text{Total Rolling Load } P}{\text{Contact Area}}$. He deduced this by integrating the expression for vertical force on the elemental section in Figure 33, over the length of the contact arc.

Thus $P = b\int_{x=0}^{x=l_d} p(1 \mp f \tan\theta)\, dx$ 3.4-8

where b = mean width of material. For rolling without tensions, the expression for p_s, was deduced from equations 3.4-7 and 3.4-8, after assuming $\varsigma_1 - 1 \doteq \varsigma_2 - 1 = f/\tan\frac{\alpha}{2}$ and $f \tan \alpha/2 \doteq 0$.

$$p_s = \frac{2h_\delta \cdot S_1}{(h_1 - h_2)(\phi - 1)} \left(\frac{h_\delta}{h_2}\right)^{\phi - 1} \qquad \text{..... 3.4-9}$$

where $\phi = \dfrac{f}{\tan \alpha/2}$

α = total contact angle

δ = neutral angle

h_δ = height of bar at neutral plane, determined by

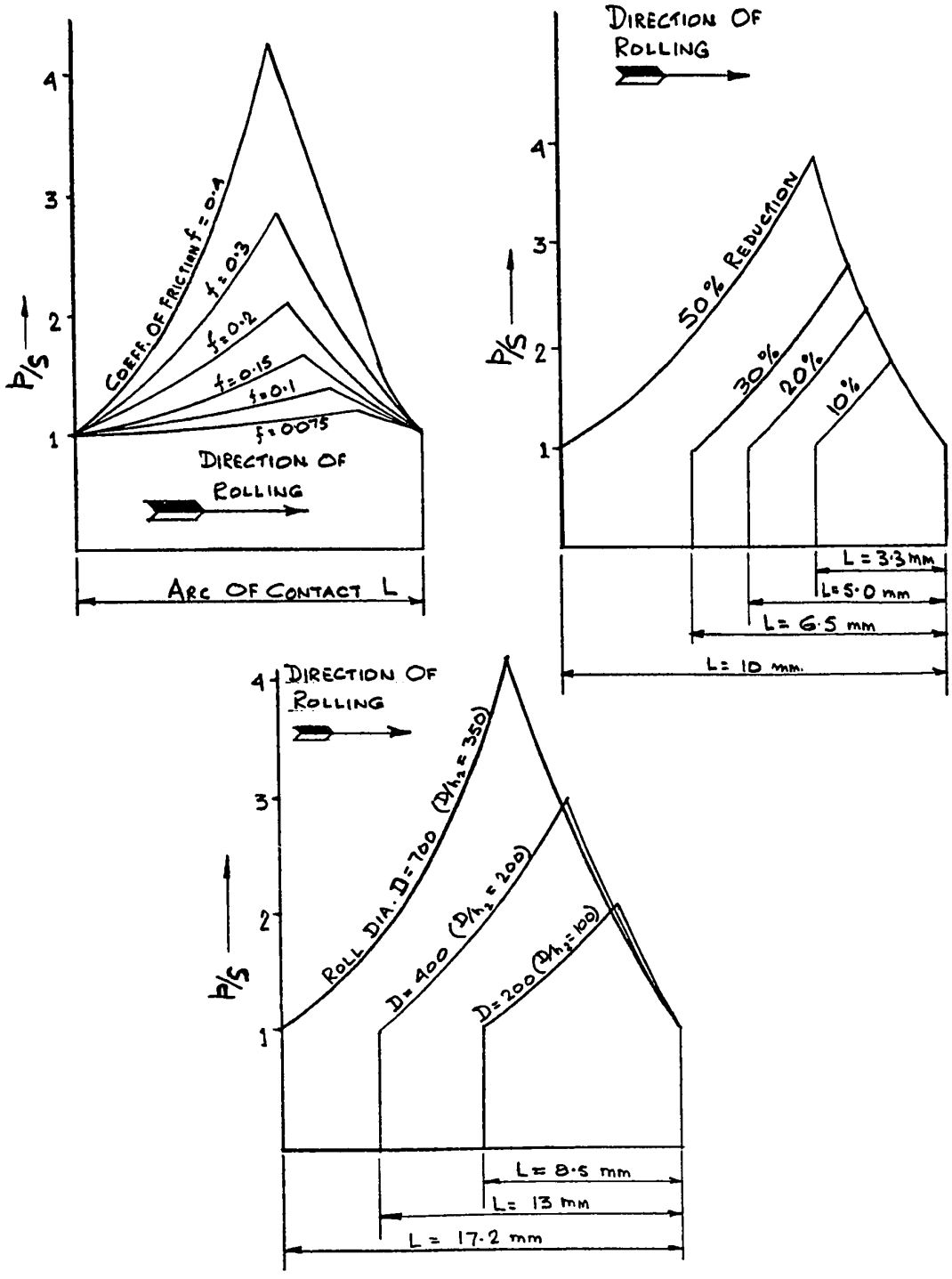

FIGURE 38 : Variation of pressure distribution by Tselikov's equations (39)

calculating the value of h at the point of intersection of the forward and backward slip pressure curves. It was shown that

$$\frac{h_\delta}{h_2} = \left[\frac{1 + \sqrt{1 + (\phi^2 - 1)(h_1/h_2)^\phi}}{\phi + 1}\right]^{1/\phi} \qquad \ldots\ldots\ldots 3.4\text{-}10$$

To facilitate computation of mean specific roll pressure using these formulae, Tselikov prepared a series of curves for $\frac{h_\delta}{h_2}$ against ϕ for different values of reduction.

3.5 DISCUSSION ON THE THEORIES OF VON KARMAN, NADAI AND TSELIKOV

The chief drawbacks of the preceding theories, complex as they are, lies in the initial assumptions made in the development of Von Karman's equation and then further assumptions and simplifications made by Nadai and Tselikov in order to transform Karman's equation to a more manageable form. It has been proven that plane vertical sections before rolling do not remain plane after rolling, that during cold-rolling, the material undergoes strain-hardening in the roll-gap, that in hot rolling, there is a variation of yield stress in the roll-gap due to the variable strain-rate, and also that the coefficient of friction f is not necessarily constant. The assumption of small angles of contact may be valid for rolling of thin strip in fairly large conventional 4-HI or 2-HI mills, however, they do not apply in the case

of cold rolling in cluster mills with small-diameter work rolls, in which case the angles of contact are much higher than 4^{o}-5^{o} as assumed in these theories. The same comments would apply when one considers slabbing of ingots with heavy draught.

3.6 OROWAN'S THEORY (10)

The theory proposed by Orowan, in 1943, enables the pressure distribution between the rolls and the material to be obtained by a graphical method of integration of the roll-pressure/arc-length curve for the case of variable coefficient of friction and variable constrained yield stress. This theory avoids most of the mathematical approximations and assumptions used in the classical theories, and can be used for both cold and hot rolling, provided that aside from geometry, the basic physical properties of yield stress and coefficient of friction and their variations within the contact arc can be known. The usual assumption is not made here, of homogeneous compression of the material. Instead, the non-homogeneity of stress distribution and hence deformation is approximated by using the results derived by Prandtl and Nadai, from the Hencky treatment of two- (18)(42) dimensional plastic deformation. The assumption, of the rolls slipping on the material at all points along the arc of contact except at the neutral point, is not made. Instead, Orowan provides criteria for determining the areas of the contact arc that are subject to slipping and sticking. The

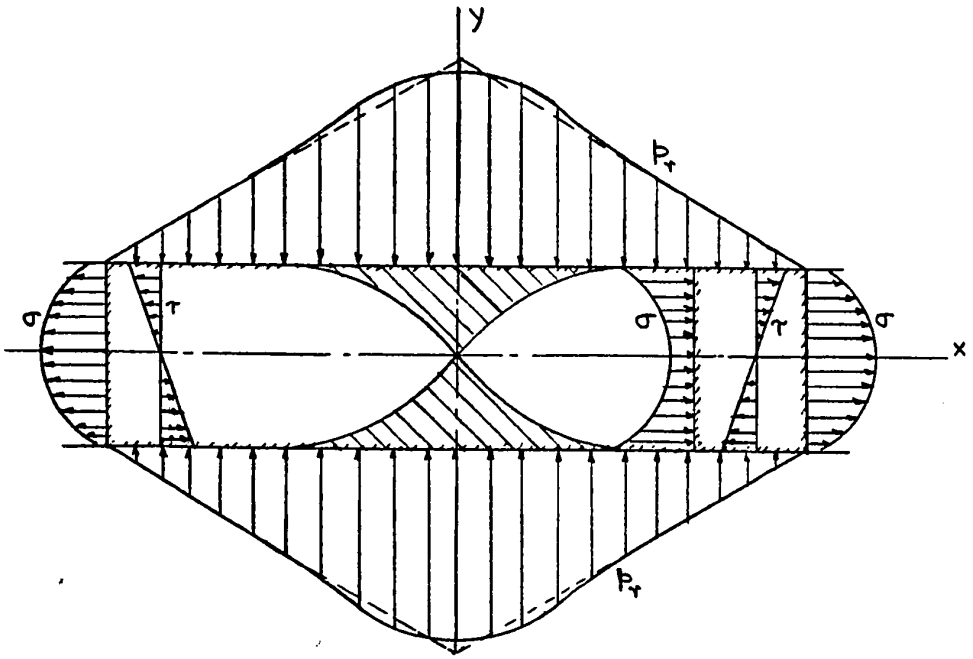

FIGURE 39 : Pressures in compressed plastic strip (10)

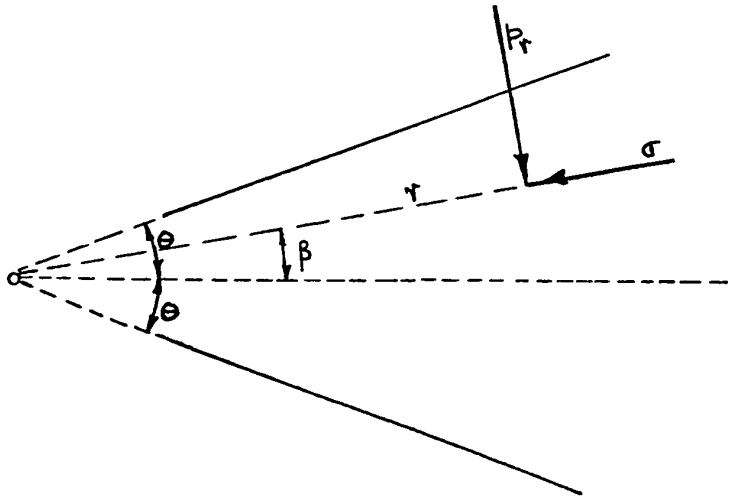

FIGURE 40 : Stresses between non-parallel plates (10)

Figure 39 shows the corresponding stress distribution.

This analogy is difficult to apply to the rolling case. However, Orowan considered an extension of the above, by Nadai, in which the mass is compressed between plane rough plates inclined at a small angle 2θ, as shown in Figure 40. For flow of material toward the apex of the angle, Nadai obtained the following relations:

$$\sigma = p_r - S\sqrt{1 - \frac{\beta^2}{\theta^2}} \qquad \ldots\ldots 3{\cdot}6\text{-}3$$

$$\tau = \frac{S}{2\theta} \cdot \beta \qquad \ldots\ldots 3{\cdot}6\text{-}4$$

These relations for parallel and inclined plates all apply to a case of "sticking" between the material and the compression plates. To consider the case of slipping, Orowan assumed a condition that the stress distribution given by the equations applies if a new value of the thickness h is so chosen, that the shear stress at the surface equals fp_r instead of $S/2$ as with sticking. For parallel plates, this is expressed by:

$$h^* = \frac{S}{2\,fp_r} \cdot h$$

For inclined plates, the same considerations applied between a wedge-shaped mass and the inclined plates, give:

$$\theta^* = \frac{S}{2\,fp_r} \cdot \theta$$

and from this, $\tau = - \frac{fp_r}{\theta} \cdot \beta$

and $$\sigma = p_r - S\sqrt{1 - \left(\frac{2fp_r}{S}\right)^2 \cdot \left(\frac{\beta}{\theta}\right)^2} \qquad \ldots\ 3\cdot6\text{-}5$$

Thus, we obtain the equations for slipping which would revert to the equations for sticking if $fp_r = \frac{S}{2}$. These relationships were next applied by Orowan to the generalized equation for the equilibrium of a segment of the rolled material.

In Figure 41, consider a thin vertical section of arbitrary shape bounded by surfaces A and A' . The following relations are obtained:

$F(\theta)$ = resultant horizontal force per unit width on surface A.

$F(\theta) - \frac{dF}{d\theta}.d\theta$ = horizontal force across surface A' per unit width

p_r = normal pressure acting on ends of the segment.

$2p_r \sin\theta \cdot Rd\theta$ = horizontal component of normal pressure p_r

τ = frictional drag (without assuming sticking or slipping).

$\pm 2\tau \cos\theta . Rd\theta$ = horizontal component of frictional drag τ.

For horizontal equilibrium:

$$\frac{dF}{d\theta} = \left(p_r \sin\theta \pm \tau\cos\theta\right)D \qquad \ldots\ 3\cdot6\text{-}6$$

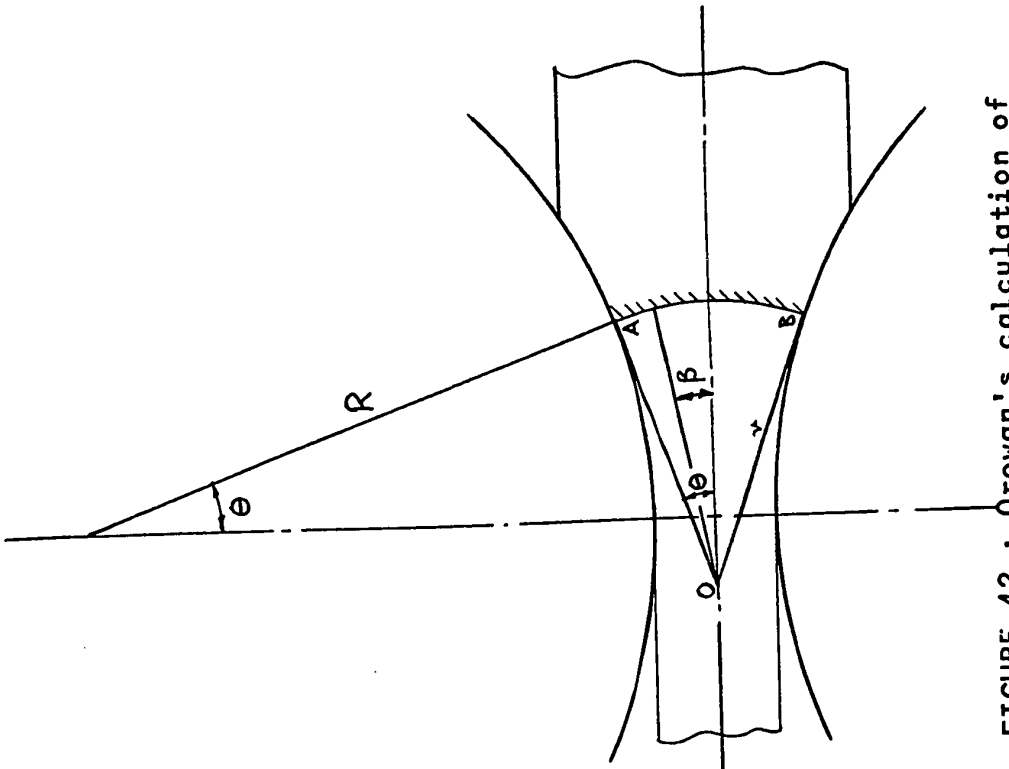

FIGURE 42 : Orowan's calculation of horizontal force in the sheet between rolls (10)

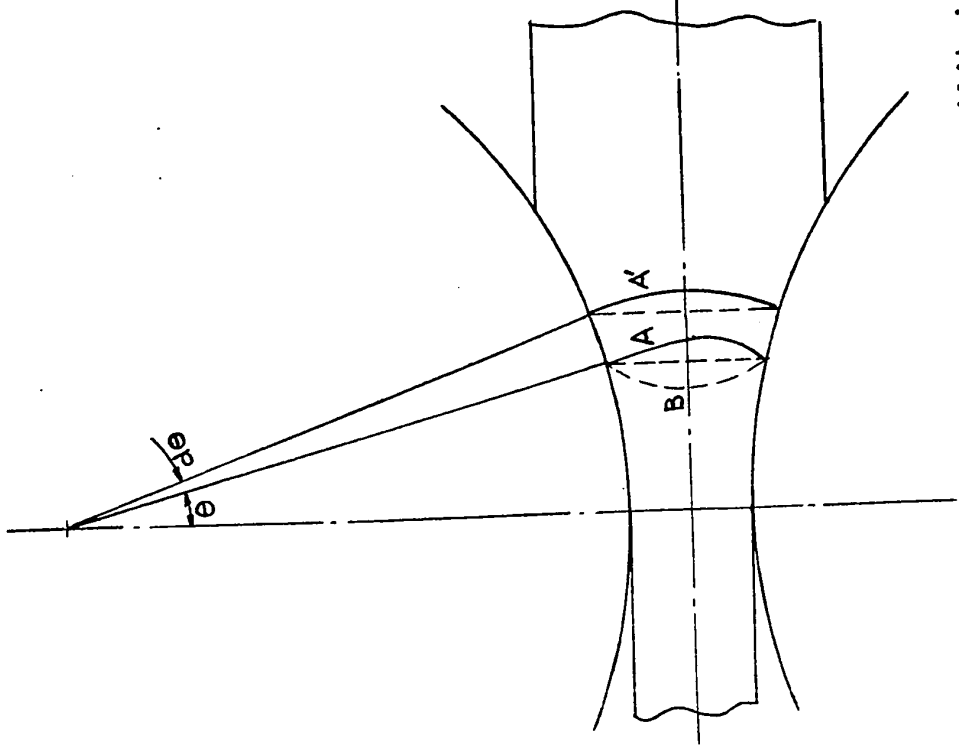

FIGURE 41 : Orowan's treatment of equilibrium of thin segment of rolled stock (10)

Differential Equation for slipping:

As is shown in Figure 42, the surface of the elemental section is represented by a cylindrical surface AB, with an included angle of 2θ, at O. Other geometrical data are as shown in the figure. It is then assumed that the stresses acting across AB will be distributed in similar manner to those acting on a plastic wedge-shaped body contained by the tangents at A and B, and the previously derived equations are applied.

On the surface AB, we now consider an element which subtends an angle $d\beta$ at O and which has unit width in a plane perpendicular to the paper.

The area of this element $dA = r.d\beta = \dfrac{h}{2 \sin \theta} \cdot d\beta$ ... 3.6-7

Now the horizontal force $F(\theta)$, acting across AB, may be assumed to have an element dF of F acting across the area dA, and would be consisting of:

1) The contribution of the radial pressure σ is

$$\sigma \operatorname{Cos} \beta \, dA = \sigma \operatorname{Cos} \beta \, \frac{h}{2 \sin \theta} \cdot d\beta \quad \ldots 3.6\text{-}8$$

Substituting σ from 3·6-5, and integrating from $\beta = -\theta$ to $\beta = +\theta$, we obtain the contribution of σ to (θ) as

$$F_{\sigma}(\theta) = hp_r - \frac{hS}{\operatorname{Sin}\theta} \cdot \int_0^{\theta} \left[\sqrt{1 - \left(\frac{2 f p_r}{S} \right)^2 \left(\frac{\beta}{\theta} \right)^2} \right] \cdot \operatorname{Cos}\beta \, d\beta \ldots 3.6\text{-}9$$

Put $a = \dfrac{2 f p_r}{S}$

and $w(\theta, a) = \dfrac{1}{\sin\theta} \int_0^{\theta} \left[\sqrt{1 - a^2 . \frac{\beta^2}{2}}\right] \cos\beta \, . \, d\beta$

As mentioned earlier, slipping occurs when $a < 1$

and sticking occurs when $a \gg 1$

Orowan plotted a curve of w against "a" and found that for values of $\theta = 0^\circ - 30^\circ$, which covers the most common range of rolling, w is not affected by θ. Thus, we may write 3·6-9 as:

$F_\sigma(\theta) = h \, . \, p_r - h \, . \, S \, . \, w$, where θ as an independent variable of w is omitted in view of its negligible influence on w.

2) The contribution of the shear stress τ, is expressed by $\tau \sin\beta . dA = \dfrac{f . p_r}{\theta} \, . \, \beta \, . \sin\beta . \dfrac{h}{2 \sin\theta} \, . \, d\beta$, with

a positive sign being applicable when considering on the entry side and a negative sign on the exit side. Integrating again between the limits of $\beta = -\theta$ to $+\theta$, we get:

$$F_\tau(\theta) = \pm \, h f p_r \left(\frac{1}{\theta} - \frac{1}{\tan\theta}\right) \quad \ldots\ldots\ldots\ldots 3\cdot6\text{-}10$$

Hence the total horizontal force on the section AB is:

$$F(\theta) = F_{\sigma}(\theta) + F_{\tau}(\theta) = h\left[p_r\left\{1 \pm f\left(\frac{1}{\theta} - \frac{1}{\tan\theta}\right)\right\} - Sw\right] \quad 3.6\text{-}11$$

For most cases of slipping, particularly in cold rolling where $f < 0.2$ to 0.25, θ is less than 10^{o}-12^{o}, the term $hp_r f\left(\frac{1}{\theta} - \frac{1}{\tan\theta}\right)$ is very small compared to hp_r.

For cold rolling, $F(\theta) = h\,(p_r - Sw)$

$$\text{or} \quad p_r = \frac{F}{h} + Sw \quad \ldots\ldots\ldots\ldots\ldots 3.6\text{-}12$$

Making substitution of $\tau = fp_r$ and the expression for p_r, we obtain the following from equation 3.6-6 :

$$\frac{dF}{d\theta} = F \cdot \frac{D}{h}\,(\mathrm{Sin}\theta \pm f\,\mathrm{Cos}\theta) + DSw(\mathrm{Sin}\theta \pm f\,\mathrm{Cos}\theta) \quad 3.6\text{-}13$$

which gives the differential equation for slipping.

<u>Differential Equation for Sticking</u> : For sticking, fp_r is replaced by $\frac{S}{2}$, so we get $a = \frac{2\,fp_r}{S} = 1$.

For sticking, equation 3.6-11 takes the form:

$$F(\theta) = h\left[p_r - S\left\{w \mp \frac{1}{2}\left(\frac{1}{\theta} - \frac{1}{\tan\theta}\right)\right\}\right] \quad \ldots\ldots\ldots 3.6\text{-}14$$

$$\text{and} \quad p_r = \frac{E}{h} + S\left[w \mp \frac{1}{2}\left(\frac{1}{\theta} \quad \frac{1}{\tan\theta}\right)\right] \quad \ldots\ldots\ldots 3.6\text{-}15$$

and the differential equation for sticking is:

$$\frac{dF}{d\theta} = F.\frac{D}{h}.\,\mathrm{Sin}\theta + DS\left[\left\{w \mp \frac{1}{2}\left(\frac{1}{\theta} - \frac{1}{\tan\theta}\right)\mathrm{Sin}\theta\right\} \pm \frac{1}{2}\,\mathrm{Cos}\theta\right] \quad 3.6\text{-}16$$

Substituting $m^{+}(\theta) = \left[w(\theta, 1) - \frac{1}{2}\left(\frac{1}{\theta} - \frac{1}{\tan\theta}\right)\mathrm{Sin}\theta \pm \frac{1}{2}\,\mathrm{Cos}\theta\right]$

and $m^{-}(\theta) = \left[w(\theta,1) + \frac{1}{2}\left(\frac{1}{\theta} - \frac{1}{\tan\theta}\right)\mathrm{Sin}\theta - \frac{1}{2}\,\mathrm{Cos}\theta\right]$

Equation 3·6-16 is written as:

$$\frac{dF}{d\theta} = F.\frac{D}{h}.\,\mathrm{Sin}\theta + D.S.m \quad \ldots\ldots\ldots\ldots\ldots\ldots \quad 3\cdot6\text{-}17$$

where m has values of $m^{+}(\theta)$ or $m^{-}(\theta)$ on the exit side or entry side respectively. This gives the differential equation for sticking and may be expressed as:

$$\frac{dF}{d\theta} + A(\theta)\,F(\theta) + B(\theta) = 0 \quad \ldots\ldots\ldots\ldots\ldots\ldots \quad 3\cdot6\text{-}18$$

whose solution is $F(\theta) = Z(\theta)\left[\int_{\theta_x}^{\theta} \frac{B(\theta)}{Z(\theta)}\,d\theta + F_o\right]$ 3.6-19

where F_o is strip tension

and $Z(\theta) = \exp\left[\int_{\theta_x}^{\theta} A(\theta)\,d\theta\right]$

$A(\theta) = \frac{D}{h}.\,\mathrm{Sin}\theta$

$B(\theta) = D.S.m$ (m^{+} on exit side and m^{-} on entry side).

If h_2 is the material thickness leaving the rolls, D is the roll diameter and γ_2 is the thickness ratio h_2/D, we get

$$\log_e Z(\theta) = \int_{\theta_x}^{\theta} A(\theta)\, d\theta = \int_{\theta_x}^{\theta} \frac{\mathrm{Sin}\theta}{\gamma_2 + 1 - \mathrm{Cos}\theta} \cdot d\theta,$$

from which we get $Z(\theta) = \dfrac{\gamma_2 + 1 - \mathrm{Cos}\theta}{\gamma_2 + 1 - \mathrm{Cos}\theta_1} = \dfrac{h(\theta)}{h(\theta_x)}$ ...3.6-20

On the exit side, we have to put $\theta_x = \theta_2 = 0$ and so

$$Z^{+}(\theta) = \frac{h}{h_2}$$

On the entry side, $\theta_x = \theta_1$ and so

$$Z^{-}(\theta) = \frac{h}{h_1}$$

Orowan carried out the computation of $F(\theta)$, by graphical integration of equation 3·6-19. He prepared two sets of calculations in order to compare his method with measured data by Siebel and Lueg. The curves are as shown in Figure 43. The normal roll pressure is found for each point in the contact arc, by $p_r = \frac{F}{h} + \frac{\pi}{4} \cdot S$.
This permits the solution of the differential equation, in the case of sticking between material and rolls.

When "slipping" occurs, as mentioned in equation 3·6-13 , the solution is arrived at as follows:

We have, from equation 3·6-13,
by similar substitutions as in equation 3·6-17, and since w is considered to be independent of θ , we may write :

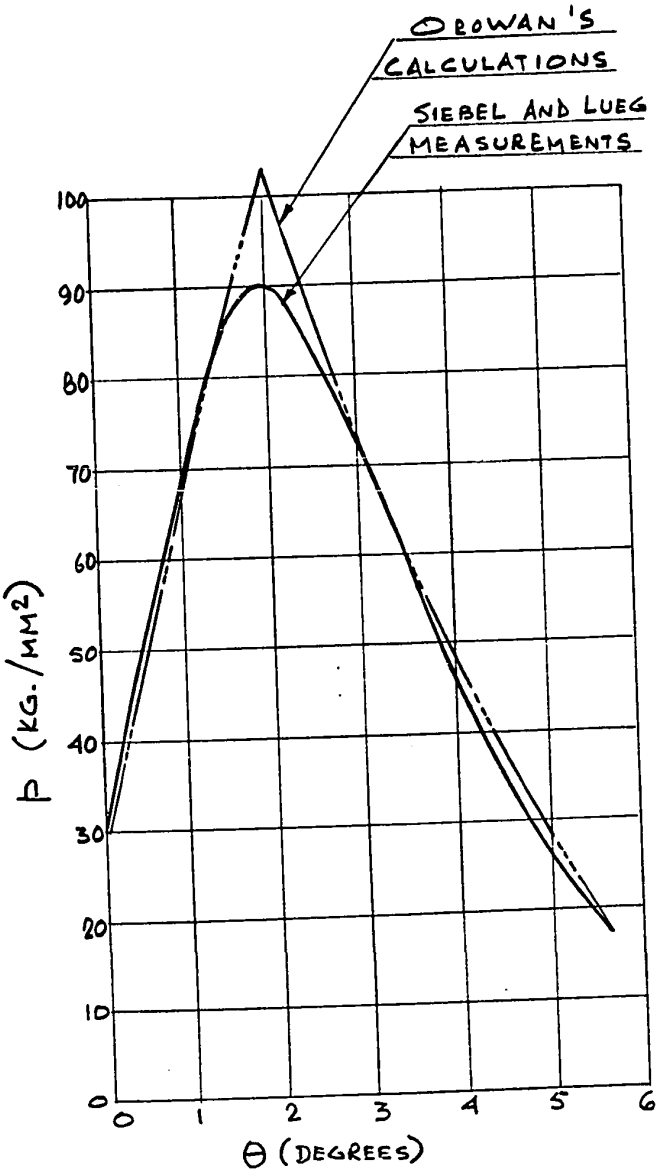

FIGURE 43 : Roll pressure distribution curves calculated by Orowan, for comparison with Siebel and Lueg's experimental curves (10)

$$\frac{dF}{d\theta} + A(\theta)\, F(\theta) + B(\theta) = 0$$

where $A(\theta) = \frac{D}{h} (\mathrm{Sin}\theta \pm f\, \mathrm{Cos}\theta)$

and $B(\theta) = D\, Sw\, (\mathrm{Sin}\theta \pm f\, \mathrm{Cos}\theta)$

Here again, the solution is of the form

$$F(\theta) = Z(\theta)\left[\int_{\theta_x}^{\theta} \frac{B(\theta)}{Z(\theta)} \cdot d\theta + F_o\right] ,$$

where $Z(\theta) = \exp\left[\int_{\theta_x}^{\theta} \frac{D}{h} \cdot \mathrm{Sin}\theta\, d\theta \pm \int_{\theta_x}^{\theta} \frac{fD}{h} \cdot \mathrm{Cos}\theta\, d\theta\right]$

The first integral is solved as in equation 3·6-20. For the second integral, since $h = h_2 + D(1 - \mathrm{Cos}\theta)$ and $\gamma_2 = \frac{h_2}{D}$,

$$f\int_{\theta_x}^{\theta} \frac{\mathrm{Cos}\theta}{\gamma_2 + 1 - \mathrm{Cos}\theta} \cdot d\theta = f\,(H - H_2) \qquad \ldots\ 3\cdot6\text{-}21$$

Orowan plotted the function H against γ_2, for values of θ varying from $\frac{1}{2}^{\circ}$ to 30°, as shown in Figure 44. For the function $Z(\theta)$, he obtains:

For exit side, $\log_e Z^{+}(\theta) = \log_e \frac{\gamma_2 + 1 - \mathrm{Cos}\theta}{\gamma_2} + fH$

For entry side, $\log_e Z^{-}(\theta) = \log_e \frac{\gamma_2 + 1 - \mathrm{Cos}\theta}{\gamma_2 + 1 - \mathrm{Cos}\alpha} + f(H_1 - H)$

where α is angle of contact and H_1 is the function H at entry.

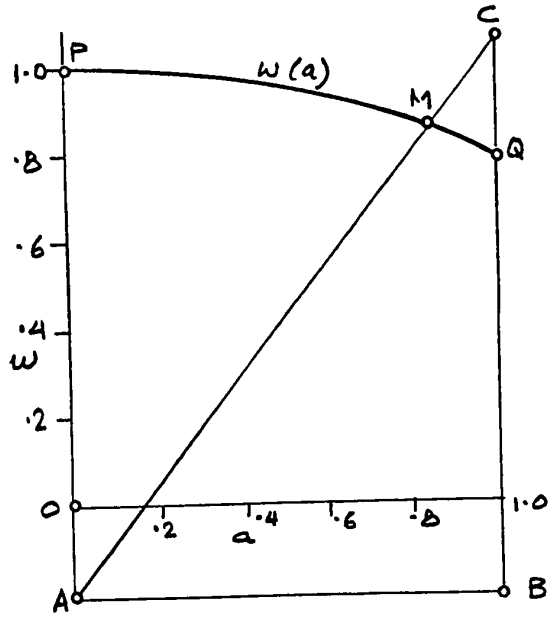

FIGURE 45

Orowan's criteria for calculating whether material sticks or slips (10)

FIGURE 44 : Variation of Orowan's function H against γ_2(10)

From this, he obtains:

$$Z^{+} = \frac{h}{h_2} \cdot e^{fH} \quad \ldots\ldots\ldots\ldots\ldots\ldots \quad 3{\cdot}6\text{-}23$$

$$Z^{-} = \frac{h}{h_1} \cdot e^{f(H_1 - H)} \quad \ldots\ldots\ldots\ldots\ldots \quad 3{\cdot}6\text{-}24$$

Here again, the function $F(\theta)$ is calculated by the graphical integration method, progressing from the ends of the arc of contact, inwards. At each point, one has to apply Orowan's criterion for deciding whether material sticks or slips, as shown in Figure 45. If the point M in this figure slips off the curve PQ, the end of the region of slipping has been reached and the computation must be carried on by means of the differential equation for sticking.

The normal roll pressure is then found for each point in the contact arc from the relation

$$p_r = \frac{F}{h} + wS \quad \ldots\ldots\ldots\ldots\ldots\ldots 3{\cdot}6\text{-}25$$

Here, also in the case of sticking, the value of the constrained yield stress S at every point of the arc, is variable and must be computed separately from strain-rate or strain-hardening curves. Orowan further states that since the compression between the material and the rolls is not homogeneous, the amount of work imparted to it for a given reduction is greater than for homogeneous compression.

To obtain the yield stress in inhomogeneous compression, Orowan states that the only practical method for doing this would be to experimentally determine the correction factor that must be applied to the yield stress calculated for homogeneous compression. Interrupted rolling tests are suggested with subsequent ball indentations made on the deformed part of the material that was in the contact arc. However, as ball indentation tests cannot be done for hot rolling, Orowan suggests that the simplest way is to determine these correction factors by actual rolling tests and comparing the experimental yield stress to the yield stress calculated as a function of strain rate in homogeneous compression.

3.7 DISCUSSION OF OROWAN'S THEORY

Orowan's theory provides the means for calculating roll pressures, loads, torques, power requirements and rolling efficiency, without most of the limitations inherent in the other theories of rolling discussed before. The theory visualises rolling conditions ranging from complete slipping to complete sticking. He also introduces corrections in his general differential equation, to allow for flattening of rolls. However, to return to the basis of Orowan's theory, i.e., that of compression of a wedge-shaped plastic mass between two inclined plates, it may be said that, although this is a closer approximation to the pressure distribution in the arc of contact, it is still not fully

representative of the conditions existing in the roll gap. Although regarded as a yardstick against which other theories of rolling are often compared, his equations of the roll pressure have not been generally applied to mill design and operation because of the time needed to complete the laborious numerical calculations required for a set of passes. Orowan himself made only two sets of calculations to compare with the experimental results of Siebel and Lueg. Should there be further development of his mathematical models and efforts made by iterative computer solution to prove the correctness of his theory, he may well have propounded the most basic and accurate of the general theories of rolling.

3.8 SIMS' THEORY (11)

Sims' analysis, while partially based on Orowan's theory, makes certain assumptions and deviations in order to reduce the computation time, without much loss in accuracy, of results. Sims' theory also serves as the basis for the Cook and McCrum data published by the B.I.S.R.A. which, to this day, serve as the most widely used basis for basic flat rolling mill calculations of load and torque.

One of the additional assumptions made by Sims, as compared to Orowan, is the one of small angles of contact, for which $\sin\theta = \tan\theta = \theta$. Sims starts with the Von Karman equation, assumes complete sticking friction, applies Orowan's condition for deformation between rough inclined plates, makes a further assumption of constant mean yield stress in the roll gap

and comes up with expressions for normal roll pressure on the entry side and exit side, as follows:

$$\frac{p^+}{S} = \frac{\pi}{4} \log_e \left(\frac{h}{h_2}\right) + \frac{\pi}{4} + \sqrt{\frac{R^1}{h_2}} \cdot \tan^{-1} \sqrt{\frac{R^1}{h_2}} \cdot \theta \quad \ldots\ldots 3\cdot8\text{-}1$$

and

$$\frac{p^-}{S} = \frac{\pi}{4} \log_e \left(\frac{h}{h_2}\right) + \frac{\pi}{4} + \sqrt{\frac{R^1}{h_2}} \tan^{-1} \sqrt{\frac{R^1}{h_2}} \cdot \alpha - \sqrt{\frac{R^1}{h_2}} \tan^{-1} \sqrt{\frac{R^1}{h}} \theta \ldots 3\cdot8\text{-}2$$

where p = Normal roll pressure

S = Constrained yield stress

h = Thickness of material at any point in contact arc

h_2 = exit thickness

h_1 = entry thickness

R^1 = Radius of curvative of elastically deformed roll

θ = Angular co-ordinate at material thickness h_1

α = Total angle of contact.

Sims stated that when the angular co-ordinate θ is small, the differences between the normal roll pressure and the vertical pressure are negligible, and with plane deformation, the specific roll load may be written as:

$$P = R^1 \int_0^{\alpha} p \cdot d\theta \quad \ldots\ldots\ldots\ldots \qquad 3\cdot8\text{-}3$$

Substituting from 3·8-1 and 3·8-2 into 3·8-3, we get

$$P = R^1 . S\left[\int_{\delta}^{\alpha}\left\{\frac{\pi}{4}\log_e\frac{h}{h_1} + M(\alpha) - M(\theta) + \frac{\pi}{4}\right\}.d\theta + \int_{o}^{\delta}\left\{\frac{\pi}{4}\log_e\frac{h}{h_1} + M(\theta) + \frac{\pi}{4}\right\}.d\theta\right]$$

where $M(\theta) = \sqrt{\frac{R^1}{h_2}} . \tan^{-1}\sqrt{\frac{R^1}{h_2}} . \theta$.

and δ = neutral angle.

After integration and simplification, Sims obtained the equation for specific roll force as:

$$P = R^1 S\left[\frac{\pi}{2}\sqrt{\frac{h}{R^1}}\tan^{-1}\sqrt{\frac{r}{1-r}} - \frac{\pi\alpha}{4} - \log_e\frac{h_\delta}{h_2} + \frac{1}{2}\log_e\frac{h_1}{h_2}\right]$$

where r = Reduction in pass = $\frac{h_1-h_2}{h_1}$

h_δ = Thickness at neutral plane

P can be expressed in the form

$$P = S\sqrt{R^1\Delta h} . Q_p\left(\frac{R^1}{h_2}, r\right) \qquad .....3·8\text{-}4$$

where Δh = Draught = $h_1 - h_2$

and $$Q_p\left(\frac{R^1}{h_2}, r\right) = \frac{\pi}{2}\sqrt{\frac{1-r}{r}}\tan^{-1}\sqrt{\frac{r}{1-r}} - \frac{\pi}{4} - \sqrt{\frac{1-r}{r}}\sqrt{\frac{R^1}{h_2}}\log_e\frac{h_\delta}{h_2} + \frac{1}{2}\sqrt{\frac{1-r}{r}}\sqrt{\frac{R^1}{h_2}}\log_e\frac{1}{1-r}$$

Figure 46 shows variation of Q_p with r. Sims argues that in equation 3·8-4, the term $S\sqrt{R^1 \Delta h}$ provides the component of the specific roll force due to plane homogeneous deformation. The function Q_p provides the contribution due to the friction and the inhomogeneity of deformation.

Specific Roll Torque: The specific torque in rolling is defined as the torque, per inch width of the strip, required to deform the material. Sims' equation for the specific roll torque was

$$Mw = 2\ R.R^1 \int_0^{\alpha} p\ \theta .\ d\theta$$ which, after substitution

from equations 3·8-1 and 3·8-2, and integration, becomes:

$$Mw = 2R\ .\ R^1\ S\ \left(\frac{\alpha}{2} - \delta\right) \quad \ldots\ldots\ldots\ldots\ldots\ldots\ 3.8\text{-}5$$

which Sims represents as

$$Mw = 2R\ .\ R^1\ S\ .\ Q_G\ \left(\frac{R^1}{h_2},\ r\right) \quad \ldots\ldots\ldots\ldots\ldots\ 3.8\text{-}6$$

where $$Q_G\ \left(\frac{R^1}{h_2},\ r\right) = \frac{\alpha}{2} - \delta$$

Figure 47 shows variation of Q_G with r.

For elastic deformation of rolls, particularly in cold rolling, Sims used Hitchcock's formula, which replaces the actual pressure distribution over the whole surface with an elliptical distribution giving the same total load. The roll, in its arc of contact with the material, is then of constant radius

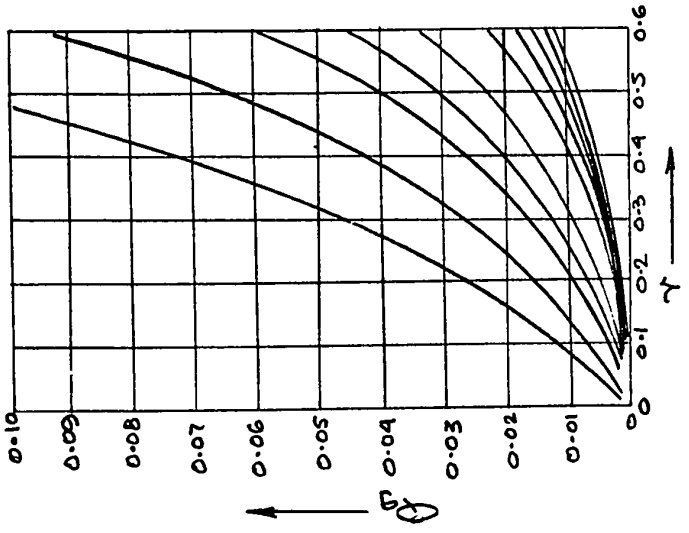

FIGURE 47 : Variation of Sims' function Q_G with r (11)

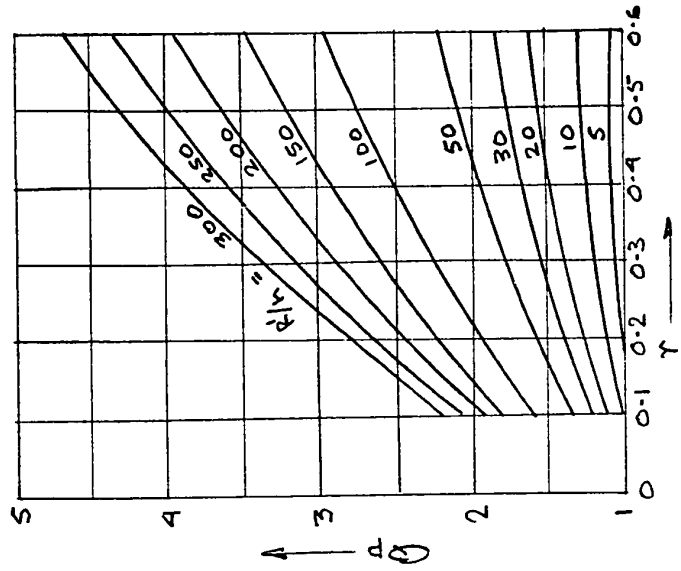

FIGURE 46 : Variation of Sims' function Q_P with r (11)

of curvature, which may be calculated from the equation:

$$R^1 = R \left(1 + \frac{CP}{\Delta h}\right), \quad \text{where C is a constant and}$$

equal to 3.45×10^{-4} for steel rolls.

Mean yield strength: Sims makes the allowance, in cold rolling, for the effect of strain-hardening, by assuming the mean yield stress given by:

$$K_p = \frac{1}{\alpha} \int_o^{\alpha} S \, d\theta, \quad \text{and in the calculation}$$

of roll torque, the material is assumed to have a constant yield strength given by

$$K_g = \frac{1}{r} \int_o^{r} S \, d\epsilon, \text{ where } \epsilon = \frac{h_1 - h}{h_1}$$

Bland and Ford[52] have experimentally proven the accuracy of these formulae to within 2% and Sims also conducted a large number of experiments to prove the validity of these formulae.

In the case of hot rolling, it is known that yield stress depends on the material, temperature and strain rate q_m, which is defined by $q = \frac{1}{h} \cdot \frac{dh}{dt}$. The form of the relation between the yield strength and the variable is quite complex

and for steel, the relation is expressed as:

$$S = f(r) + B(r) \log_e q$$

The values of K_p and K_g are calculated for the various strains and the mean between the two is taken to be the yield strength in hot rolling.

3.9 COOK AND McCRUM'S DEVELOPMENT OF SIMS' THEORY (15)

Cook and McCrum based their work on the Sims theory and carried out extensive tests on the Cam Plastometer to establish data for curves that would permit a graphical method of calculation of roll force and torque.

They deduced the following formulae for their calculations:

$$\text{Specific Roll force } P^1 = R^1 \cdot Cp \cdot Ip \quad \ldots\ldots 3\cdot9\text{-}1$$

$$\text{Specific Roll Torque } M_w = 2R \cdot R^1 \cdot Cg \cdot Ig \quad \ldots\ldots 3\cdot9\text{-}2$$

where:

$$C_p = Q_p \sqrt{\frac{h_2}{R} \cdot \frac{r}{1+r}} \quad \ldots\ldots 3\cdot9\text{-}3$$

$$C_g = Q_g \sqrt{\frac{1-r}{1+r}} \quad \ldots\ldots 3.9\text{-}4$$

Q_p and Q_g are as defined in Sims' theory.

$$I_p = K_p \sqrt{\frac{1+r}{1-r}} \quad \ldots\ldots\ldots\ldots 3\cdot9\text{-}5$$

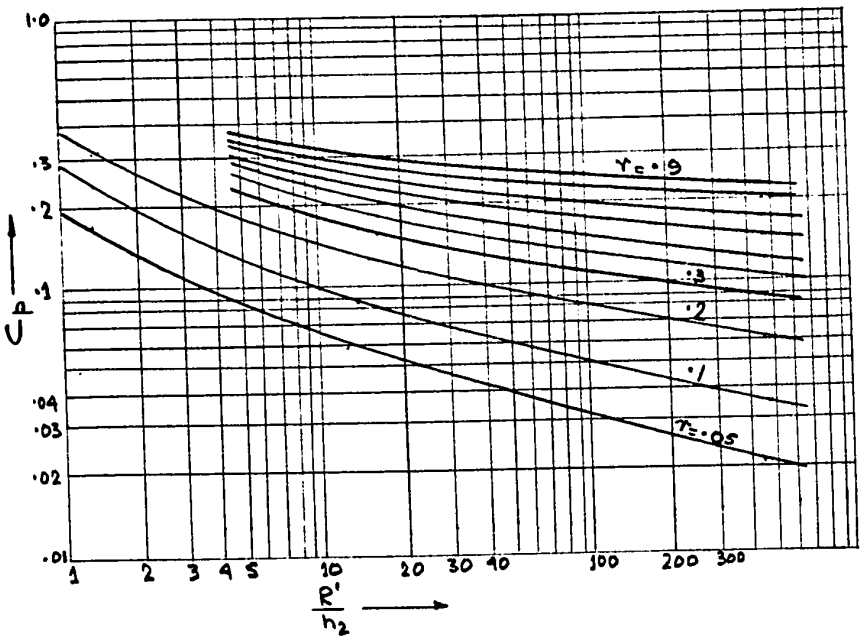

FIGURE 48 : C_p functions from Cook and McCrum (15)

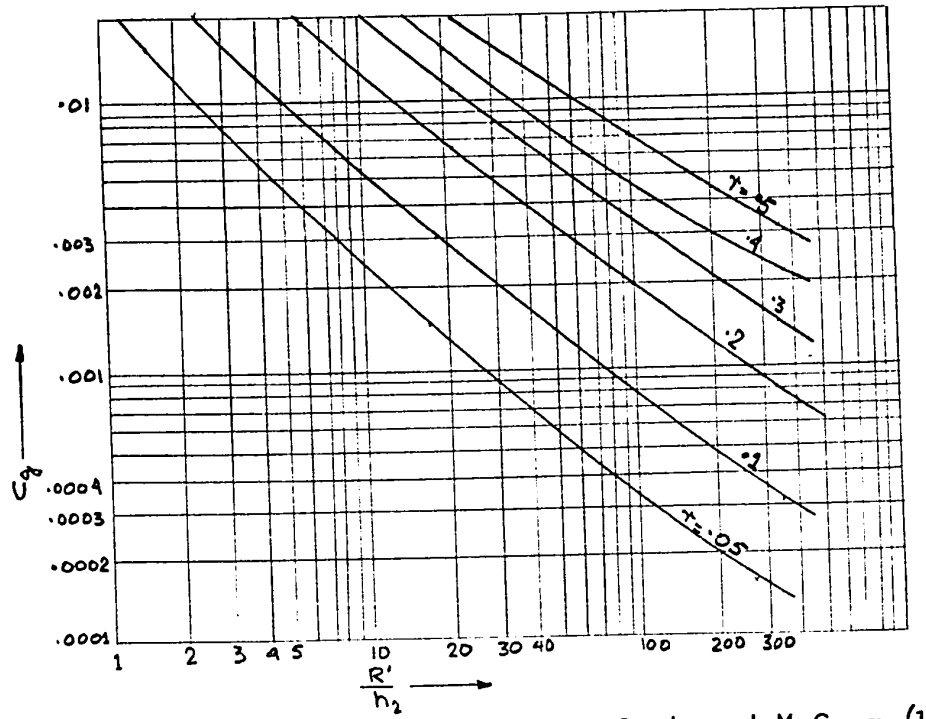

FIGURE 49 : C_q functions from Cook and McCrum (15)

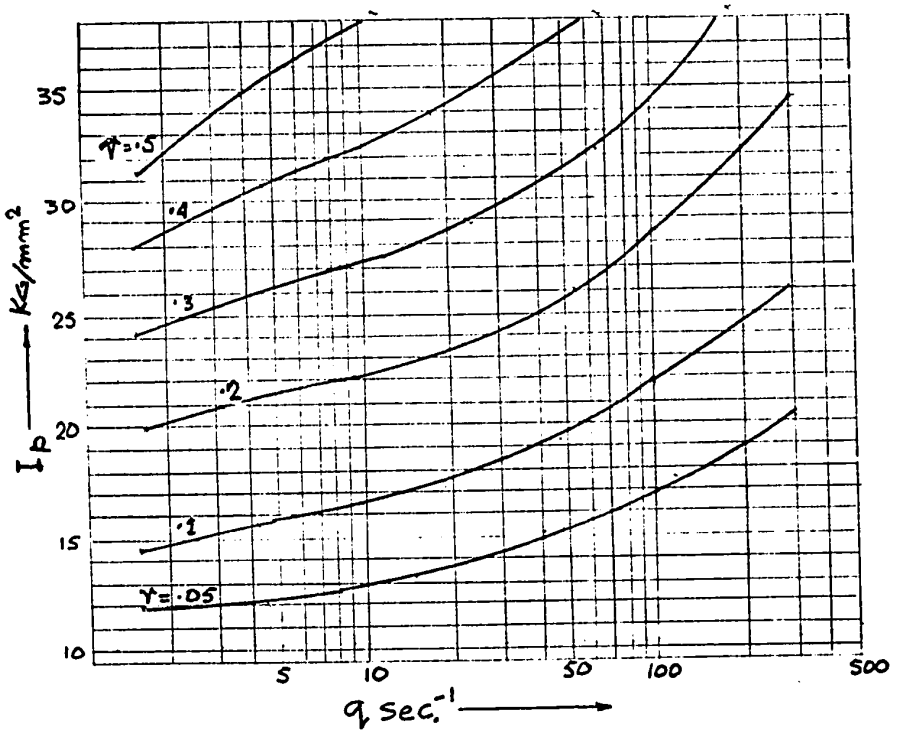

FIGURE 50 : I_p functions from Cook and McCrum for low carbon steel at 1000°C (15)

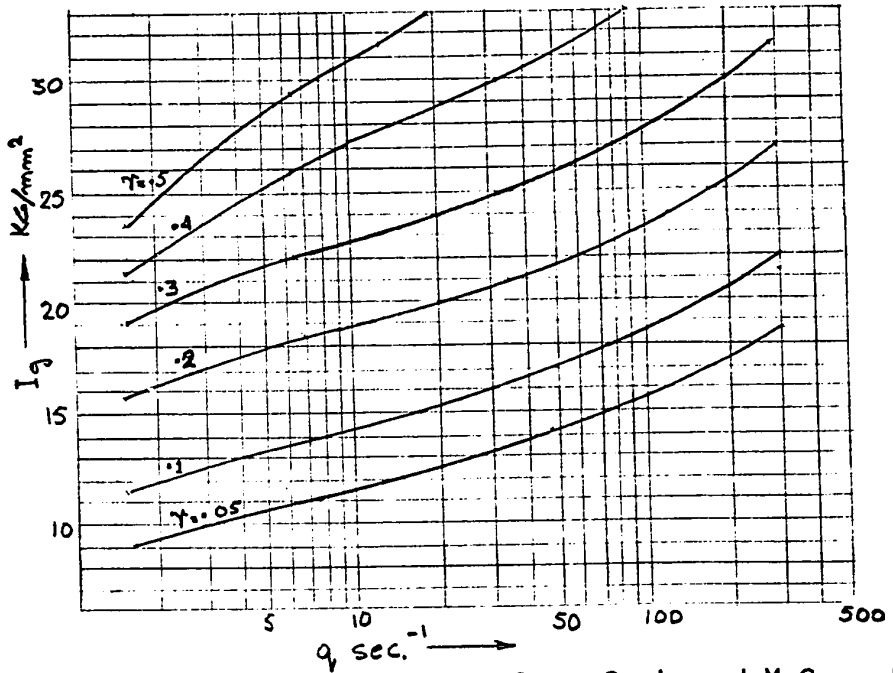

FIGURE 51 : I_g functions from Cook and McCrum for low carbon steel at 1000°C (15)

$$I_g = K_g \sqrt{\frac{1+r}{1-r}} \quad \text{.....3.9-6}$$

Cook and McCrum published a large number of families of curves for graphical computation of C_p, C_g, I_p, I_g, for a wide range of steels and non-ferrous metals.

Figures 48, 49, 50 and 51 show some typical families of curves for the above functions.

3.10 DISCUSSION

The diagrams and formulae provided by Cook and McCrum for determination of roll force and torque in flat rolling, provide the simplest and quickest method for making the basic calculations necessary for the design of flat-products mills. In practical design office practice, there is seldom enough time and capability to carry out design calculations, necessary for the establishment of basic design parameters for mechanical and electrical equipment, by the more classical theories of rolling or by the Orowan theory which, though more sound and closer to the truth than the other theories, is too cumbersome and laborious for application in daily design calculations. Perhaps further studies can be made to adapt the basic Orowan procedure and mathematical formulae for solution by today's high speed computers.

CHAPTER 4

PRACTICAL APPLICATION OF ROLLING THEORY

4.1 SELECTION OF A TECHNIQUE FOR CALCULATING ROLL FORCE & TORQUE

It is evident from the preceding pages that there is a wide diversity of methods and approaches available for the treatment of specific rolling operations. For instance, to consider only the calculation of roll force in hot rolling, we have numerous formulae at our disposal, most of which have been derived from theoretical considerations, tempered by the need for ease of practical calculations and, in some cases, modified by empirically-established correction factors. To name a few of the authors of such formulae, we have:

1. Ekelund (4).
2. Tselikov (39).
3. Golovin and Tiagunov (2).
4. Greleji (51).
5. Siebel (16).
6. Samarin (2).
7. Orowan and Pascoe (2).
8. Cook and McCrum (15).
9. Trinks (5).
10. Stone (46).

It is beyond the physical limitations of this paper to consider and evaluate the merits and demerits of each of these approaches to the evaluation of roll force. Wusatowski and Bala (24) made, in 1954, a comparison of the various formulae available at the time, against data obtained from actual rolling tests. The methods compared were those of Ekelund, Siebel, Trinks, Orowan-Pascoe, Geleji and Tselikov. They concluded that the methods of Ekelund and Siebel gave the closest results for rolling of plates; Ekelund, Siebel and Tselikov for rolling of strip; and Ekelund, Siebel and Orowan-Pascoe for the rolling of shapes.

Since the publication of the Cook and McCrum data, in 1958, for the rolling of flat products, this method has been widely used for the calculation of roll force and torque for hot strip and other flat products mills. This method provides the simplest and quickest way of making what, by the other established formulae, are essentially laborious calculations. The Cook and McCrum method of roll force and torque calculations are based on Sims' theory of hot rolling. As has been mentioned earlier, Sims based his theory on the Von Karman and Orowan theories of rolling, with the additional assumptions of small angles of contact, and sticking friction over the entire arc of contact, and his theory is eminently applicable to hot rolling of wide thin sheets or strip. Sims carried out, among other verifications, a comparison of loads calculated by his theory with those obtained in tests

by the S.K.F. Bearing Co. of Sweden. Figure 52 shows the above comparison in the case of rolling 0-1% carbon steel 5.5, 4.4, 3.3, and 2.2 mm - thick and 85.5 mm. wide, rolled in a four-high mill with work rolls of diameter 205 mm, rotating at a speed of 150 r.p.m. It is seen that the calculated values are grouped quite closely about the SKF curve, with the loads increasing slightly with entry thickness. No correction was made for the elastic distortion of the roll surface although, for 2.2 mm. thick strip, the applied correction would increase the load by 4% at the higher reductions.

To verify his formulae for the angular distribution of roll pressure as given by Equations 3·8-1 and 3·8-2, Sims calculated values of specific roll pressure for the cold rolling of annealed copper, to compare against similar calculations and pressure distribution curve prepared by Cook and Larke based on Orowan's equations. The copper was assumed to be 0.100 inch. initial thickness and was given a 30% cold reduction between 18 inch diameter rolls. Cook and Larke, in their calculations, applied Orowan's criteria for sticking and slipping, while Sims assumed sticking friction throughout the contact arc. Furthermore, Cook and Larke had allowed for separately calculated values of yield stress for each considered point on the contact arc, whereas Sims employed a constant mean yield stress which he deduced from

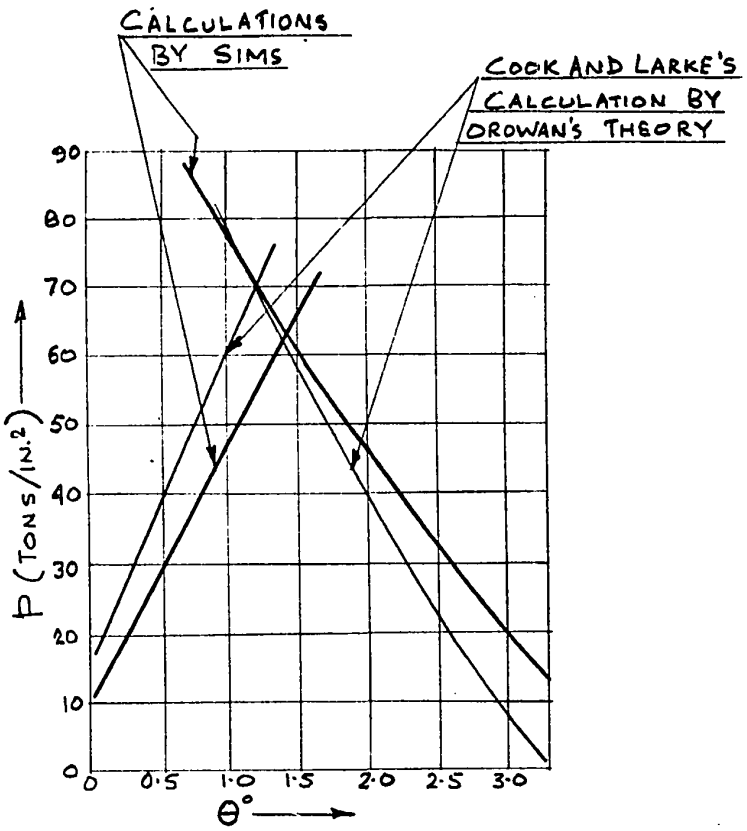

FIGURE 53 : Comparison of roll pressure curves based on Sims's theory and Orowan's theory (11)

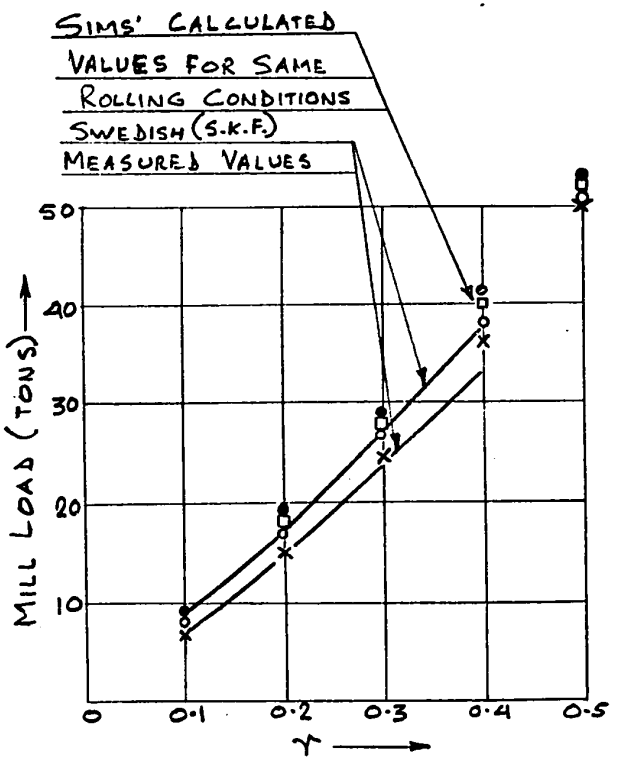

FIGURE 52 : Sims' comparison between calculated load and Swedish measurements (11)

the yield stress variation curve. It was found that the differences between the two values are not great, and the mill loads calculated from them differ by less than 2%, although there is a bigger variation in the calculated specific roll pressure at different points on the arc. Figure 53 shows, comparatively, the roll pressure distributions by the Orowan and Sims methods.

Orowan's theory is generally accepted as the most comprehensive of all the theories of rolling proposed to this day, as it does not make most of the simplifying assumptions present in the other theories. However, the theoretical formulae for roll force and torque proposed by him are very complicated and not suitable, at present, for use in practical design calculations.

It is thus proposed to select the Cook and McCrum method, based on Sims' theory, for the calculation of roll forces in hot flat rolling. In spite of the drawbacks of the yield stress data obtained by Cam plastometer tests with uniaxial, constant strain-rate compression, the calculated values of roll force and torque are generally sufficiently accurate for practical purposes. Furthermore, as discussed earlier, the simplifying assumptions made in Sims' theory do not result in appreciable variations of calculated values from rolling test data, or from calculations based on Orowan's theory.

4.2 CASE STUDY: COMPARISON OF CALCULATED AND MEASURED VALUES OF ROLL FORCE

Measurements were taken, during rolling operations on a 4-high Hot Strip Mill, of the various parameters involved in roll force calculations, viz., strip width, thicknesses before and after reduction in each pass, strip temperature, roll r.p.m., work roll diameter and material specifications. The roll separating force at each pass was also recorded.

4.2 1 DESCRIPTION OF ROLLING SETUP

The measurements and other data were taken during the hot rolling of low-carbon steel strip on a 27" and 49" x 66" 4-High Reversing Hot Strip Mill equipped with a Hydraulic Automatic Gauge Control System which works in conjunction with an X-Ray Thickness Gauge located on the exit side of the mill. Strip temperature, during the reversing rolling operations, is maintained reasonably constant by means of reheat furnaces which enclose the coiling mandrels located on either side of the millstand. The 4-High Mill receives its stock from a combination of a vertical edging mill and a 2-High slabbing mill, which reduce the heated slabs and ingots to a thickness suitable for the final strip rolling operation. The work rolls of the 4-High mill are driven by a 5000 h.p. D.C. motor, through a 1:1 ratio pinion stand.

Pass settings for the work rolls, i.e., the gap between them, are done by remote control from the operator's pulpit and are achieved to within very close tolerances by means of a position transducer which forms part of the Automatic Gauge Control System. Deviations of strip thickness, from the pass settings are monitored by the X-Ray Thickness Gauge, and are generally found to be negligibly small.

The roll separating force during rolling was obtained from the output signals of the two pressure transducers which sense the pressure in the two hydraulic capsules located between the top backup roll chocks and the housing screws. The speed of the motor was obtained from the output signal of a tacho-generator driven from the rotor shaft. The traces of these variables were recorded by means of a Honeywell 906 Visicorder, and are shown in Figures 54 and 55. The temperature of the strip at each pass was also noted from readings of an optical pyrometer mounted on the mill. Figure 56 gives a schematic representation of the rolling tests as described in the preceding lines.

4.2.2 EXPERIMENTAL AND CALCULATED RESULTS

Table 2 shows the measured data as obtained during the tests. The figures for motor speed are scaled off from the visicorder charts and the average values are taken when the motor attains a steady speed after reversal and acceleration. The total roll force is deduced by scaling off and

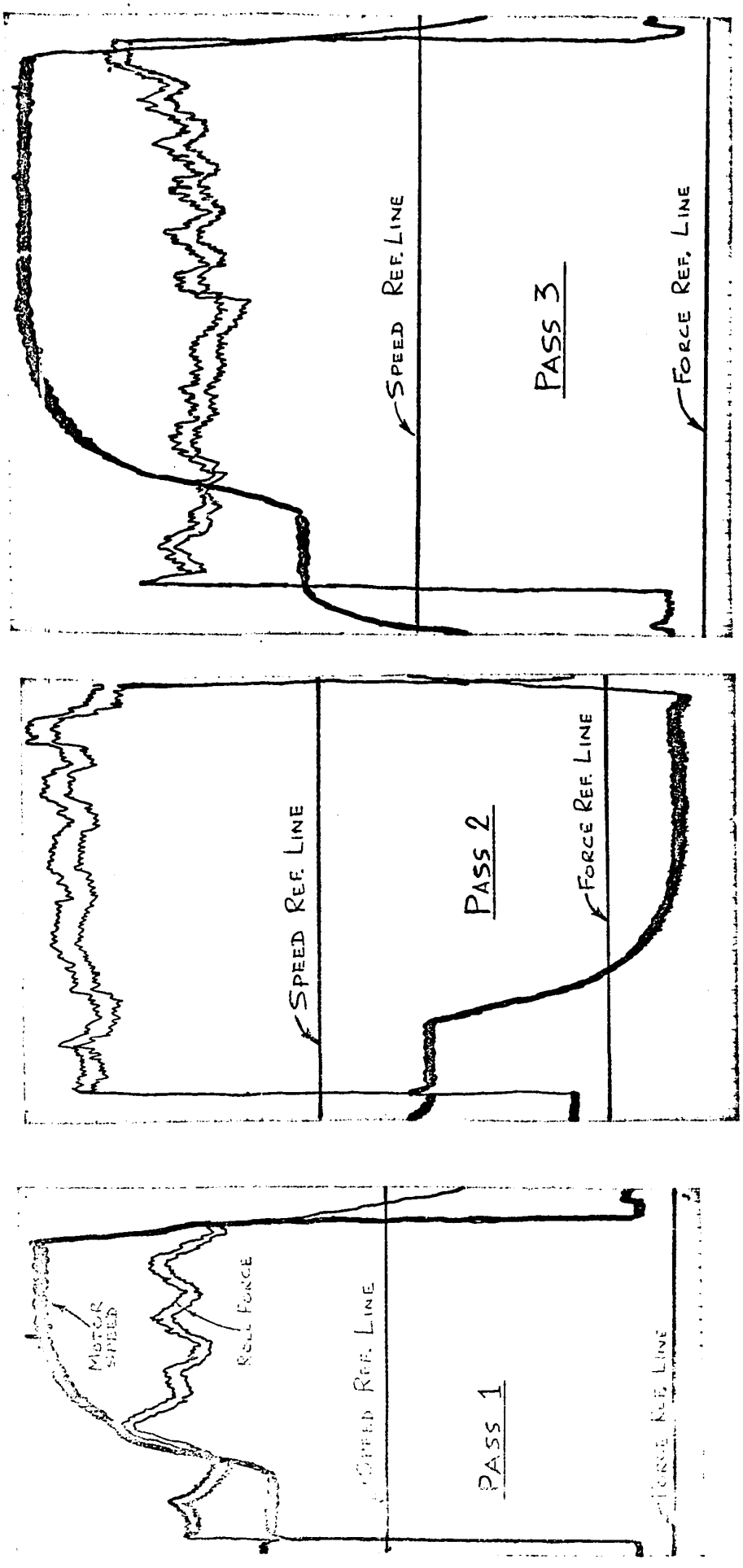

FIGURE 54: Roll force and speed traces from rolling test

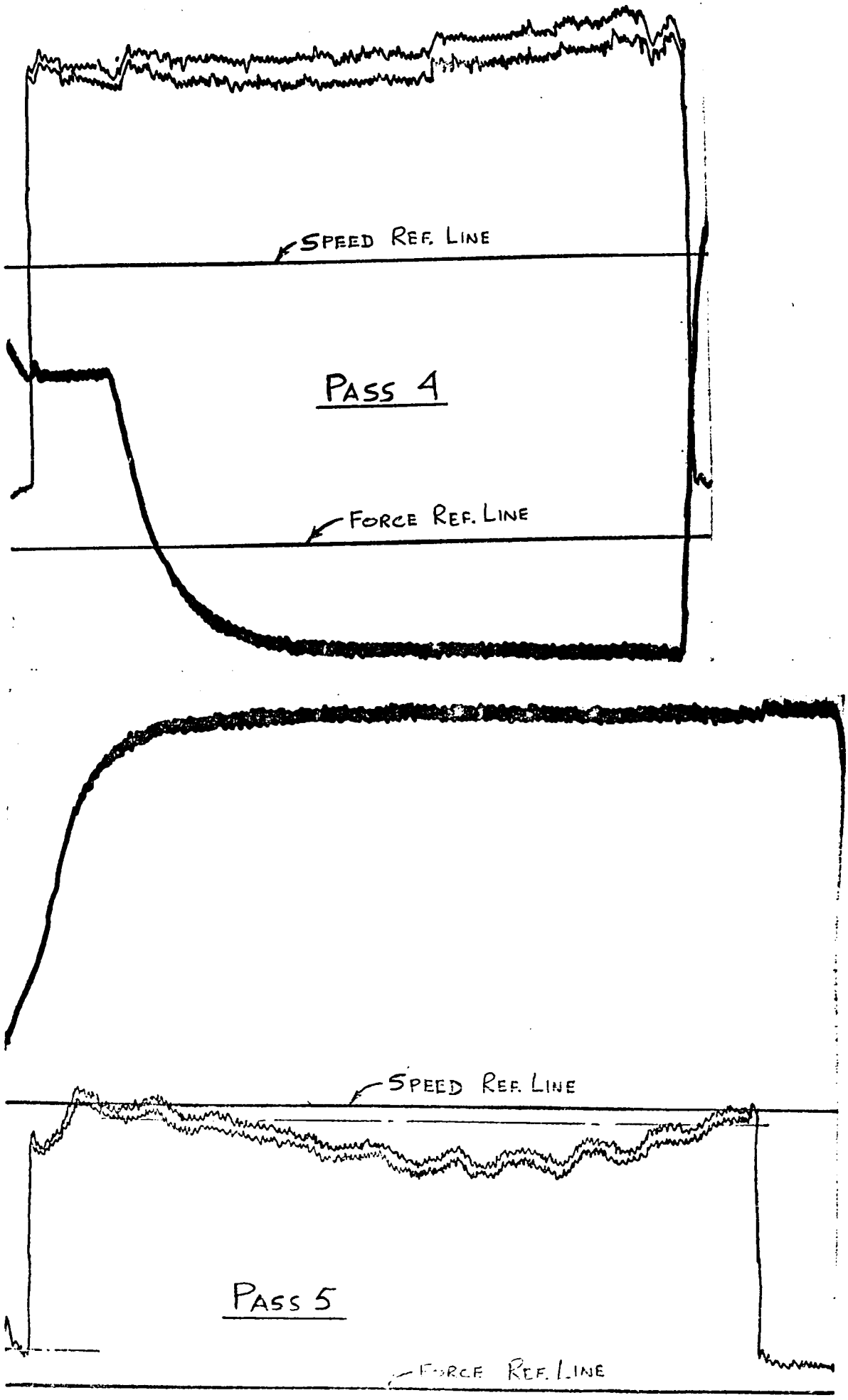

FIGURE 55 : Roll force and speed traces from rolling test

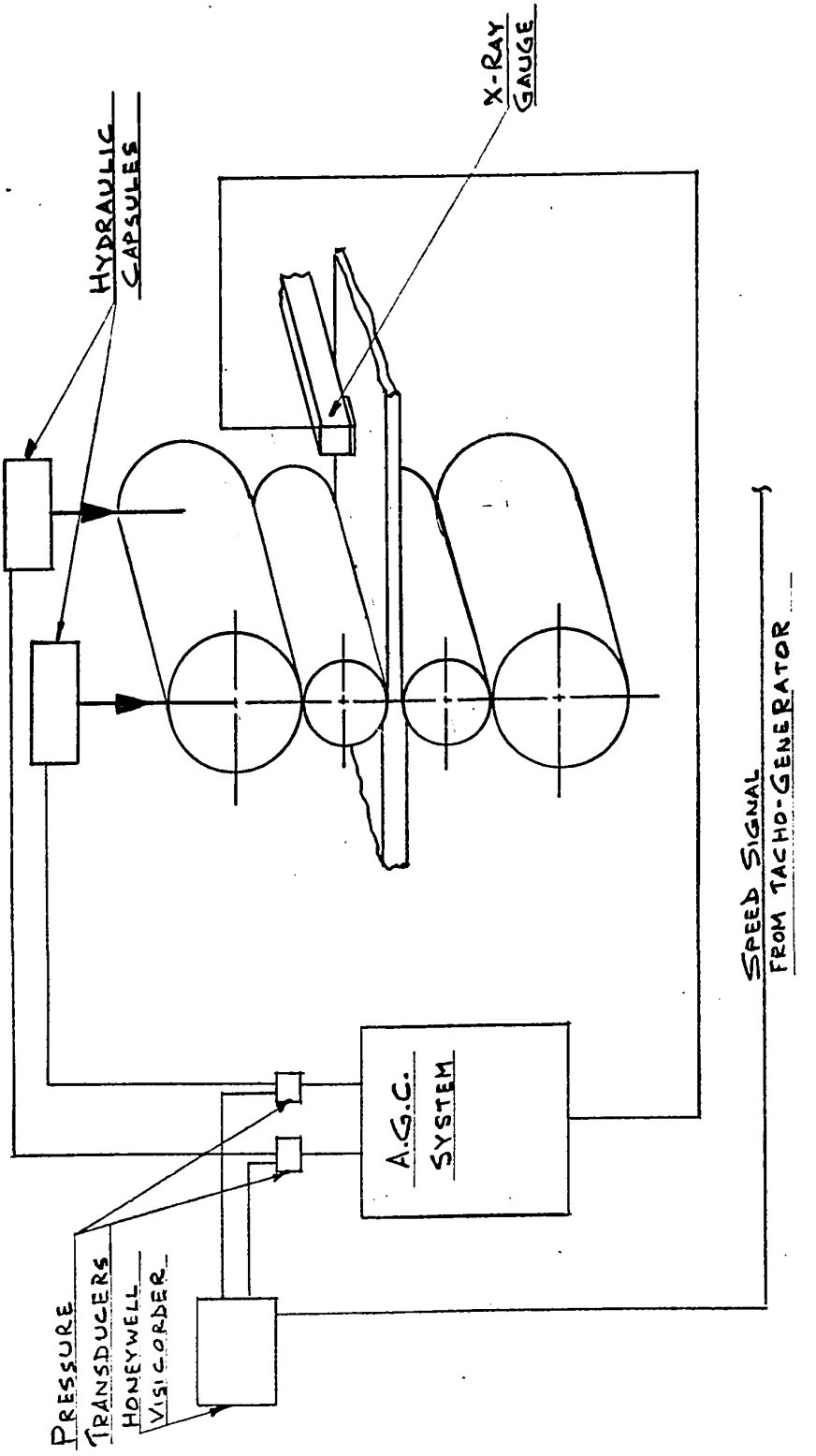

FIGURE 56 : Block diagram representation of rolling setup

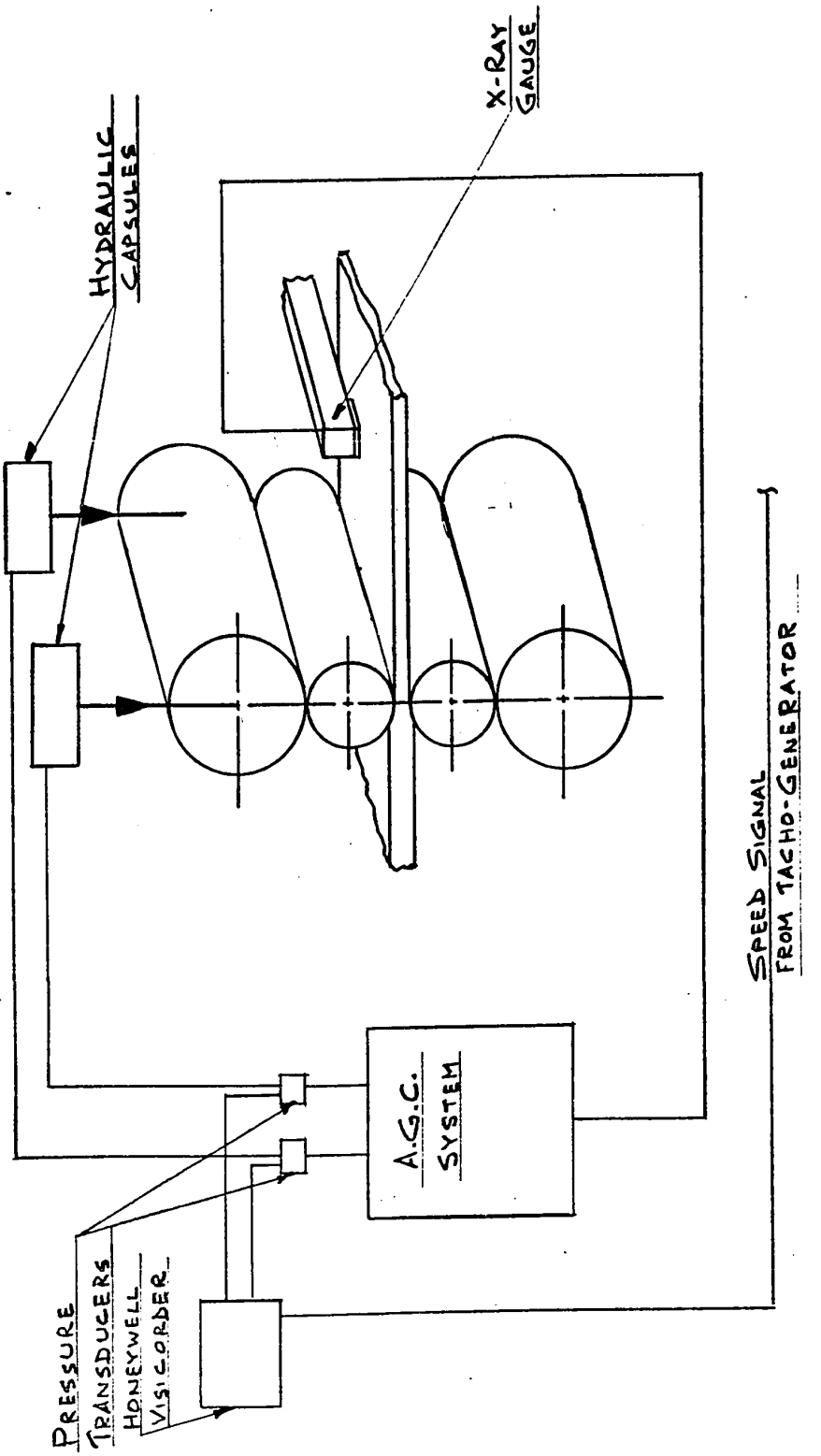

FIGURE 56 : Block diagram representation of rolling setup

TABLE 2

Experimental Results

Pass No.	Strip Thickness "		Strip Width "	Strip Temperature °F	Motor Speed R.P.I.A.	Roll Force (short tons)
	In (h_1)	Out (h_2)				
1	0.670	0.455	46.875	1720	152.3	1580
2	0.455	0.310	46.875	1720	164.5	1810
3	0.310	0.210	46.875	1690	176	1700
4	0.210	0.161	46.875	1690	181	1650
5	0.161	0.131	46.875	1570	184.1	870

Steel Specification: Low Carbon, equivalent to AISI C1006.

Work Roll Diameter : 26.25"

Conversion Factor for Motor Speed trace: 1 inch = 65.75 r.p.m.

Conversion Factor for Roll force trace : 1 inch = 264 short tons.

TABLE 3

Calculated Results

Pass No.	R/h_2	Strain[o] Rate q	r	C_p *	I_p * long tons	Calculated Force P_c short tons	Measured Force P_m short tons	Difference $\frac{P_c - P_m}{P_m}$ %
1	28.8	49.5	.322	.123	19.32	1640	1580	+ 3.8
2	42.3	62.5	.319	.1135	20.5	1605	1810	-11.3
3	62.6	81	.323	.111	22.53	1725	1700	+ 1.47
4	81.4	83.2	.233	.088	19.59	1195	1650	-27.6
5	100	81	.186	.071	16.38	802	870	- 7.83

* From Cook and McCrum (15)

o From Wusatowski (2)

adding the ordinates of the traces obtained from the output signals of the two pressure transducers, one for each hydraulic capsule.

Table 3 shows the values of the roll forces as calculated from the input data, using the Cook and McCrum method. The mean strain rate is calculated from the figures for roll diameter, roll speed, ingoing and outgoing strip thicknesses using curves based on Wusatowski's (50) formula, for mean strain rate under "Sticking" conditions, as given in equation 2.5.3-4. The variation of roll force with each pass, in both measured and calculated values, is shown in Figure 57. Some typical calculations and procedure to arrive at roll force is given below.

4.2.3 TYPICAL CALCULATION OF ROLL FORCE

Detailed calculations are given below for roll force determination in Pass 1, using the Cook and McCrum formulae and graphs for P, Cp and Ip and using Wusatowski's graphs (2) for strain-rate:

We have:

$h_1 = 0.670"$

$h_2 = 0.455"$

$R = 26.25/2 = 13.13"$

Temperature $T = 1720^{\circ}$ F $= 940^{\circ}$C

Hence $\frac{R}{h_2} = 28.8$, $r = .322$

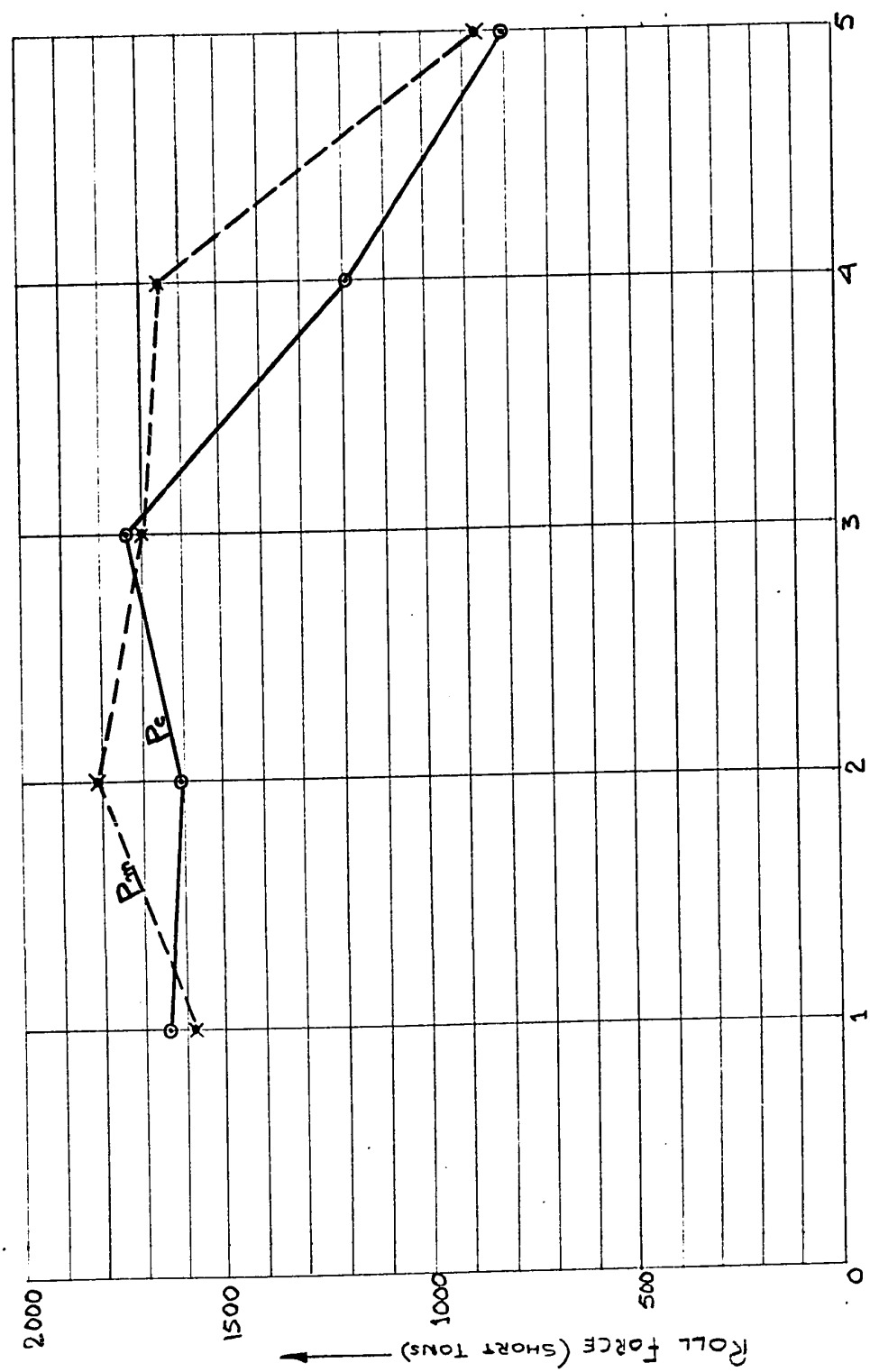

FIGURE 57 : Variation of measured and calculated values of roll force, during rolling schedule

Using Wusatowski's curves,

Strain rate $q = 0.325 \times 152.3 = 49.5 \text{ sec}^{-1}$

From Cook and McCrum's curves,

$Cp = .123$

I_p at $900^\circ C = 20.6$ long tons

I_p at $1000^\circ C = 17.4$ long tons

By extrapolation between these values, we get

I_p at $940^\circ C = 20.6 - (20.6 - 17.4) \times 0.4$

$= 19.32$ long tons

Hence Roll force $P = R.C_p.I_p.b$

$= 13.13 \times .123 \times 19.32 \times 1.12 \times 46.875$

or $P = 1640$ short tons.

Here, the effect of roll flattening is neglected, due to conditions of hot rolling, however, marginally higher accuracy can be obtained by considering this effect.

4.2.4 DISCUSSION OF RESULTS

As is seen from Figure 57, there is reasonably good agreement between experimental and calculated values of roll force in the first, third and fifth passes, while appreciable differences exist in the values for the second and fourth passes. This is partially attributed to inaccurate temperature readings at these two passes, caused by the fact that the measuring optical pyrometer is located on the entry side for passes 1, 3 and 5 whereas for passes 2 and 4 it measures the temperature of the strip on the exit side. The accuracy of the pyrometer reading for Passes 2 and 4 is

affected by the creation of a cloud of powdered scale and steam at the entry of the strip into the roll gap.

We find also that, while the calculated roll forces for passes 1 and 3 are higher than the corresponding measured values, pass 5 shows a calculated value which is lower than that measured. Furthermore, pass 4 shows a larger percentage difference between the calculated and measured values than does pass 2. It is possible to conclude that there is a gradual deterioration in accuracy of calculated values of roll force at higher strain rates, as existing in passes 3, 4 and 5, by the Cook and McCrum method. This has also been observed by Dahl (45) and Weinstein (8), in their experiments by rolling tests and the plane-strain drop test, by which it was found that there was an increasing difference between measured values of I_p as compared to the corresponding Cook and McCrum data, for strain-rates greater than 70 sec^{-1}. This variation between calculated and actual values, with higher strain rates, would create increasingly serious discrepancies in the case of modern, continuous hot strip mills where finishing speeds and strain rates are much higher than those for the reversing mill featured in this case study.

CHAPTER 5

CONCLUSION AND RECOMMENDATION FOR FURTHER WORK

5.1 CONCLUSION

The mechanical forming of metals by rolling is perhaps the most widespread and productive method used in the metals industries for production of finished and semi-finished strip, sheet, plate, merchant bar and structural shapes. Basically comprising of a process by which metal is reduced in cross-section and shaped by passage through a pair of powered cylindrical rolls, rolling mills of today have reached a high degree of sophistication in general design, drive systems, gauge and shape control, roll metallurgy, etc.

In the preceding pages, the author has attempted to present, in a broad spectrum, the diverse and complex nature and influence of the many variables that radically affect the deformation of metals by rolling. As is evident, most of the theoretical work so far has been concentrated on the flat rolling of metals at elevated and ambient temperatures, i.e., under the conditions where the assumption of plane-strain compression can be made with consequent partial simplification of the analysis. When this assumption cannot be made, i.e., in the rolling of structural sections and merchant bars and shapes, the analysis becomes increasingly complex. Much of the formulae and roll pass designs used in this latter case

are based on empirically derived conclusions based on operating experience, and little or no theoretical work is available on the subject. It is easy to appreciate the need and importance of intensive and continuous research into the mechanics of the rolling process, in order to arrive at a sound and practical basis for the economic design and manufacture of machinery which, in spite of the several handicaps in analysis, have reached an advance stage of sophistication in performance and control.

5.2 RECOMMENDATION FOR FURTHER WORK

As stated earlier, theories and formulae on roll force and torque determination, in order to be of any practical use, have to make several simplifications and assumptions which may often lead to major discrepancies. It is generally accepted that Orowan's theory has, to date, provided the soundest theoretical approach towards explaining the rolling process. However, because of the complex and laborious calculations, it has served only as a basis for the development of more simplified theories proposed by later researchers. With the availability, today, of high-speed iterative computation techniques through the use of present-day computers, it is suggested that further work should be undertaken, to arrive at different forms of the Orowan equations suitable for computer solution. Standard computer programs should be developed whereby, by suitable substitution

of initial or intermediate parameters, solutions can be obtained for the widest possible range of rolling conditions.

One of the principal drawbacks of the present status of roll force calculations, is the unavailability of reliable and meaningful data for the yield stress of metal at elevated temperatures, under the rolling conditions. The plane-strain drop test (8) has shown that the possibility exists, of acquiring this information through test apparatus and indenters designed to simulate, as closely as possible, the process of deformation by rolling.

Further work is thus proposed, for investigation and future research, to perform the analysis of rolling problems using Orowan's equations applied to computer solution and yield stress data established by the plane-strain drop test, to supply the same wide extent of information as is presently available through the B.I.S.R.A. publication of Cook and McCrum's data.

BIBLIOGRAPHY

1. A.H. El Waziri : An up-to-date examination of Rolling Theory, Iron and Steel Engineer Yearbook, 1963, P.753.
2. Z. Wusatowski : Fundamentals of Rolling, Pergamon Press.
3. L.R. Underwood : The Rolling of Metals, Chapman and Hall.
4. S. Ekelund : Analysis of factors influencing rolling pressure and consumption in the hot rolling of steel, Steel, Vol. 93, Aug. 1933.
5. W.R. Trinks : Roll pass design, Penton.
6. United Steel Companies, Sheffield : Roll pass design.
7. H.J. McQueen and J.J. Jonas : Hot workability testing techniques, Metal forming, A.I.M.E., 1971.
8. A.S. Weinstein and A. Matsufuji : Initial report on the variable strain-rate effect on the deformation of metals, Iron and Steel Engineer, September 1968, P. 121.
9. A.S. Weinstein : The variable strain-rate effect on the deformation of metals - II- The aspect ratio effect, A.I.S.E.,Publication, 1970.
10. E. Orowan : The calculation of roll pressure in hot and cold flat rolling, Research on the Rolling of Strip, B.I.S.R.A., 1960, P. 10.
11. R.B. Sims : Calculation of roll force and torque in Hot rolling Mills, Research on the Rolling of Strip, B.I.S.R.A., 1960, P. 175.

12. H. Ford : Researches into the deformation of metals by cold rolling, Research on the Rolling of Strip, B.I.S.R.A., 1960, P. 39.

13. E.C. Larke : The rolling of sheet, strip and plate, Chapman and Hall.

14. H. Polakowski : An examination of modern theories of rolling in the light of rolling mill practice, Sheet Metals Industry, Vol. 27, 1950.

15. P.M. Cook and A.W. McCrum : The calculation of load and torque in hot flat rolling.
V B.I.S.R.A., 1958.

16. E. Siebel : Resistance to deformation and the flow of material during rolling, Stahl und Eisen, December 1930.

17. T. von Karman : On the Theory of Rolling, Zeit fur Ang. Mathematic und Mekanik, Vol. 5, 1925, P. 139.

18. A. Nadai : Plasticity - A Mechanics of the Plastic State of Matter, McGraw-Hill, 1931.

19. E Siebel and W. Lueg : Investigations into the Distribution of Pressure at the Surface of The Material in contact with the rolls, Mitt. K.W. Inst. Eisenf., Vol 15, 1933.

20. A. Nadai : The rolling process, American Soc. for Steel Treating, Paper, September 1930.

21. W.L. Roberts : Choice of work roll diameter in Cold Rolling Mill design, Iron and Steel Engineer, December 1969, P. 93.

22. Z. Wusatowski : Draught, elongation and spread in hot rolling, Prace Badaw ze GIMO, 1949, P. 27.

23. Z. Wusatowski and R. Wusatowski : Influence of speed, temperature and type of rolls on spread and elongation in rolling, Prace Badaw ze GIMO, 1950, No.2, P.111.

24. Z. Wusatowski and S. Bala : Comparison of methods of calculation of roll force in hot rolling, Prace IMH, 1954, P. 120.

25. S.K.F. : Roll pressure and power consumption in hot strip rolling.

26. G. Weddige : Hot rolling tests on unalloyed and high alloy steels under different conditions of rolling, Stahl und Eisen, Aug. 1937, P. 913.

27. H. Unckel : A contribution to the Theory of metal flow during rolling, Archiv. Eisenhütte, July 1936, P. 13.

28. N. Metz : Experimental investigations into the flow of material during rolling, Archiv. Eisenh., Sept.1927, P.193.

29. A. Hollenberg : Observations on the rolling of iron, Stahl und Eisen, Vol.3, 1883.

30. A. Pomp and W. Lueg : Experiments on the rolling of carbon and silicon steels at medium temperatures, MITT. K. W. Eisenf, Vol. 15, 1933, P. 81.

31. A. Pomp and W. Lueg : The influence of roll diameter on the cold rolling of strip steel, MITT. K. W. Eisenf, Vol. 17, 1935, P. 219.

32. H. Hencky : On the theory of plastic deformation, Z. Ang. Math. und Mek, Vol. 4, 1924, P. 323.

33. R. Von Mises : Mechanics of solid bodies under conditions of plastic flow, Nachr. d. Gesselsch. d. Wissensch. Zu. Gottingin, Maths-phys. Klasse, 1913.

34. H.W. Swift : Plastic flow in metals, The Metal Industry, Feb. 1940.

35. G. Cook : Some factors affecting the yield point in mild steel, Trans. Inst. of Eng. and Shipbuilders, in Scotland, 1937-8 , P. 371.

36. A. Korolev : Deformation of metals during rolling, Moscow 1953.

37. C.L. Smith, F.H. Scott and W. Sylwestrowicz : Pressure distribution between stock and rolls in hot and cold flat rolling, Journal of the Iron and Steel Institute, 1952, P. 347.

38. E. Siebel : The plastic forming of Metals, Stahleisen, Dusseldorf, 1932.

39. A.I. Tselikov : Effect of external friction and tension on the pressure of the metal on the rolls in rolling, Metallurg, No. 6, 1939, P. 61.

40. W. Tafel : The theory and practice of rolling steel, Penton Publishing Co.

41. W. Trinks : Roll pressure in hot rolling, Blast Furnace and Steel Plant, Vol. 25, 1937, P. 1005.

42. Z. Prandtl : A mechanical analogy for the kinetic theory of solid bodies, Z. ang. Math. und Mek., 1928, P. 85.

43. E. Orowan : The Cam Plastometer, B.I.S.R.A., 1950.

44. J.F. Alder and V.A. Philips : The effect of strain and temperature on the resistance of Aluminum, Copper and Steel to compression, Journal Inst. of Metals, 1954, Vol. 83, P. 80.

45. W. Dahl, E. Wildschutz and J. Langer : Hot rolling tests, Archiv. fur das Eisenhutten Wesen, Apr.1961,P.213.

46. M.D. Stone : Rolling pressure in strip mills, Iron and Steel Engineer, Feb. 1943,

47. M.D. Stone : The rolling of thin strip, Iron and Steel Engineer Yearbooks, 1953, P.115 and 1956, P.981.

48. M. Cook and E.C. Larke : Calculation of loads involved in metal strip rolling, Journal Institute of Metals, 1948-9, Vol. 74, P. 55.

49. G. Wallquist : New investigations of roll force, power consumption, etc., in hot flat rolling, Kugellager, 1950, P. 1-17.

50. Z. Wusatowski : The rate of deformation in rolling, Prace IH, 1958, Vol. 10, P. 120.

51. A. Geleji : Calculation of forces and Power Consumption during metal working, Budapest, 1955, II ed.

52. D.R. Bland and H. Ford : The calculation of roll force and torque in cold strip rolling with strip tensions, Research on the Rolling of Strip, B.I.S.R.A. 1960, P. 68.